Characterisation of Recombinant

Aryl Hydrocarbon Receptor Ligand Binding Domain

By Tao Jiang, B.Sc.

Thesis submitted to the University of Nottingham
for the degree of Doctor of Philosophy

October 2004

To My Parents and Sister

Acknowledgment

I would like to acknowledge my supervisor Dr. David R. Bell, for his scientific guidance, constant encouragement throughout my PhD. My sincere thanks go to him for the critical discussion and the successful completion of this project. His great enthusiasm and scientific endeavor has been and will be extremely influential in all my scientific work.

I would like to thank the previous members of the Bell Laboratory, including Drs. Neill J. Horley, Chris Mee and Helen Sims. I sincerely appreciate their kind and generous helps during the early time of my study. I would like to thank all present members in this group, including Dr. Minqi Fan and Mr. Muhammed, Osama, Abdullah for their friendly and pleasant companion in every day lab work. My big thanks give to our technician Declan who helped me order all stuffs during these three years. There are so many to learn from each of them. I really enjoyed study and work in this environment.

At last I would like to thank my parents who provide me financial and moral support. My special thanks go to my dearest sister, Xin, who is always there when I need support.

Abstract

Aryl hydrocarbon receptor (AhR) is a ligand-activated transcription factor, which mediates the toxicity of dioxin and related compounds, and has an important role in development. However, a structural basis for ligand binding to the AhR remains unclear and the study was hindered by the low abundance and inherited instability of the AhR. Based on a previously defined minimal ligand-binding domain (LBD, residues 230-421), in the present study a series of truncated LBD constructs were created and expressed in insect cells (Sf9) using a baculovirus expression system.

An antibody was produced to analyze the expressed. The antisera can detect as low as 0.3ng of AhR LBD from cytosol of Sf9. An *in vitro* [^{3}H]TCDD binding assay was developed to characterized the expressed LBD. The assay yielded an estimate for the K_D of C57Bl/6 mouse liver binding at 1.4nM.

The present expression system yields soluble AhR LBD protein at ~0.15% of cytosol protein. Supplementation of the Sf9 culture medium with additional glucose resulted in an increase in the amount of soluble AhR, due to an increase in intracellular ATP level. However, cotransfection of LBD with hsp90 interaction protein p23 made no substantial change in the amount of cytosolic AhR. The soluble recombinant LBD retains functionality in the form of specific binding to dioxin, and its thermal stability was indistinguishable from that of mouse liver. However the ligand-binding activity of LBD was molybdate dependent, indicating a weaker association of mouse AhR LBD with Sf9 hsp90. A differential effect of Triton X-100 on the recombinant AhR LBD and native AhR also suggests that the interaction between AhR and Sf9 hsp90 is less stable.

The study refined the minimal LBD to a region of 125 amino acids, which should be amenable for structural studies of the LBD.

Aims of the project (at the end of the Introduction Chapter)

Functional AhR can be expressed simply in reticulocyte lysate (Bell and Poland 2000), but bacterial expression of AhR fails to yield functional protein (Coumailleau, 1995). A baculovirus expression system has been successfully used to produce microliter to milliliter of full-length AhR (Chen et al, 1994). However there is no previous report on recombinant expression of the AhR LBD in insect cells and no functionality characterizations on this protein. Therefore the aims of this study were:

1). To produce an antibody to the AhR LBD for analysis of the expressed LBD.

2). To develop an *in vitro* [^{3}H] TCDD binding assay for evaluating the binding capacity of the recombinant LBD

3). To recombinant express the AhR LBD in insect cells using baculovirus expression system, and optimizing cytosolic AhR recovery from the transfected cells.

4). To characterize the function of a series of truncated recombinant LBD and to refine the minimal LBD.

Future work (at the end of the Discussion Chapter)

A truncated AhR LBD was expressed in insect cells using a baculovirus expression system. The system yields soluble AhR LBD protein at –0.15% of cytosol protein and which retains its ligand binding activity. However the there is a discrepancy between LBD protein levels and ligand-binding capacity in such cultures (Section .) Given that the functionality of the AhR requires chaperone protein hsp90 and a number of cochaperones and the formation of the AhR/hsp90 complexes is an ATP dependent process, it was found that supplementation of the Sf9 culture medium with additional glucose resulted in an increase in the amount of soluble AhR, due to the a increased intracellular ATP level. However it is not clear whether the enhanced soluble AhR production is accompanied by a greater binding capacity of the LBD to dioxin. Furthermore, cotransfection of AhR with cochaperone p23 reduced the amount of AhR in high-speed pellet; through it did not change the level of soluble AhR. It is of interest to investigate the ligand binding capacities of the AhR under further optimized expression conditions. Having established the binding activity of the recombinant LBD, the recombinant protein can also be used to screen other ligands, either exogenous or endogenous, of the AhR.

The aim of the project was to produce large amount of functional AhR LBD for crystallographic study. For this reason, a his-tag has been inserted into the N-terminal of the LBD construct for facilitating the recombinant protein purification on a Ni-NTA column. Therefore purification of the recombinant AhR LBD is necessary and can be performed based on a large-scale expression.

Chapter 1 Introduction

1.1 General background

A wide variety of aromatic hydrocarbons are ubiquitous environmental contaminants. These compounds can be divided into two classes according to their chemical structures. The first class is halogenated aromatic hydrocarbons (HAHs), and the second class is nonhalogenated polycyclic aromatic hydrocarbons (PAHs). These chemicals can be considered together because many of them produce similar a and characteristic pattern of toxic response, and act by a common mechanism (Poland and Knutson 1982).

1.1.1 Dioxin and related compounds

The term 'dioxin' usually refers to a group of compounds, polychlorinated dibenzo-*p*-dioxins (PCDD), of which there are 75 possible congeners. The parent molecule of PCDD consists of two benzene rings linked by two oxygen bridges (Figure 1-1). The physical, chemical and toxic properties of dioxins are determined by the number and position of halogen substituents (Walker 2001). Among them, 2,3,7,8-tetrachlorodibenzo-*p*-dioxin (TCDD or "dioxin") is one of the most toxic synthetic compounds known. Other dioxin congeners are less active by a factor ranging up to several thousands to millions (Poland and Knutson 1982). TCDD is not formed for commercial purposes; rather, it arises as a trace contaminant, in e.g. synthesis of 2,4,5-trichlorophenol, which is used to manufacture 2,4,5-trichlorophenoxyacetic acid derivatives as herbicide and

defoliant (Poland and Knutson 1982). Other dioxin-like chemicals include polychlorinated biphenyls (PCBs), dibenzofurans (PCDFs), and related compounds. Many of them are very stable against chemical and microbiological degradationsand therefore are persistent in the environment. They are fat soluble and this tends tolead to bioaccumulation in tissue lipid and in the food chain. These factors increase their potential hazards to humans and animals. (Poland and Knutson 1982; Walker 2001).

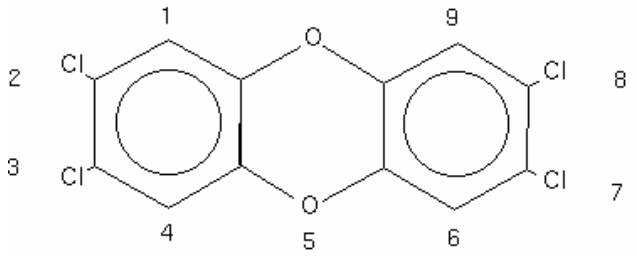

2,3,7,8-Tetrachlorodibenzo-p-Dioxin

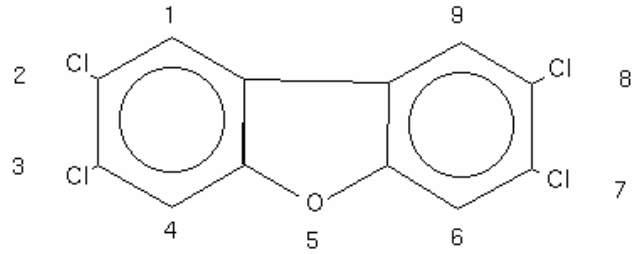

2,3,7,8-Tetrachlorodibenzofuran

Figure 1- 1. Chemical structure of TCDD and TCBF.
2,3,7,8-tetrachlorodibenzo-p-dioxin (TCDD), 2,3,7,8-tetrachlorodibenzofuran (TCBF), and their ring numbering**.**

Another class of chemicals, PAHs, have similar toxic effects, but areless potent than HAHs. They are generated from the incomplete combustion of various carbon sources and are typically found in diesel exhaust, cigarette smoke, and fried foods (Schmidt and Bradfield 1996).

1.1.2 Toxic responses

Exposure to TCDD and related compounds produces a wide spectrum of toxic effects. The toxic response depends on the dose of the toxin, the length of exposure, species, strain, age, and sex of the animals (Poland and Knutson 1982). On the other hand, the different dioxin congeners are differently potent. The acute TCDD toxicity in animal models includes liver necrosis; embryotoxicity/teratogenesis; epithelial hyperplasia and metaplasia; lympoid involution, porphyria; severe wasting syndrome followed ultimately by death, and the induced expression of a battery of genes (Poland and Knutson 1982).

As a characteristic feature of acute toxicity, sensitivity to TCDD exposure can differ both quantitatively and qualitatively in different species. For example, the acute oral LD_{50}s at the two extremes are 1μg/kg for guinea pigs and 5000μg/kg for hamsters (Poland and Knutson 1982). This large variation in TCDD sensitivity between the guinea pig and hamster is not simply the result of difference in the rate of *in vivo* metabolism of TCDD, since the whole body half-life for TCDD only differs by 3-fold between these species. In humans, the most commonly observed effect after a high-level exposure to TCDD is chloracne. However, it was not commonly observed in other laboratory animals after TCDD exposure (Poland and Knutson 1982). One characteristic of TCDD toxicity is that the majority of the toxic effects of dioxins are not observed until weeks following the exposure. It is likely that the adverse effects are the results of gene expression in target cells, which may account for the delayed toxic responses (Denison, Pandini et al. 2002).

In addition to acute toxicity, TCDD has capacity to cause cancer by acting as a tumour promoter. TCDD promotes the growth and transformation of already initiated cancer cells (Pitot, Goldsworthy et al. 1980). TCDD is not a mutagen, because TCDD dose not covalently bind DNA, RNA or protein (Poland and Glover 1979).

1.1.3 Identification of the Ah receptor

It was realised that the toxic responses of dioxin and related compounds were not the result of a direct reaction of the toxin. No evidence has been presented to show the TCDD-induced formation of covalent adducts with proteins, nucleic acids (Poland and Glover 1979; Geiger and Neal 1981); or direct damage to cellular DNA (Shu, Paustenbach et al. 1987). A series of experiments were set out to investigate the mechanism of action. These experiments led to the identification of the Ah receptor, which mediates most, if not all, of the toxic response.

Initially, it was observed that the inducibility of P4501A1 by 3-methylcholanthrene (MC) varied significantly among inbred mouse strains and it failed to induce P4501A1 in some strain of mice (nonresponsive mice) (Poland and Knutson 1982). In contrast, TCDD was able to induce P4501A1 in nonresponsive mice. It was postulated that MC and TCDD evoked the same induction response, but TCDD had a greater potency and more prolonged duration of action. Subsequently, genetic study using cross and back cross between these strains showed that the inducibility of P4501A1 was controlled by multiple alleles at a single locus. The locus was hypothesised to encode a structural gene for a

receptor, which binds to TCDD and triggers the enzyme induction and other activities (Poland & Glover, 1975). It was proposed that the mutation in nonresponsive mice results in a defective recognition or receptor site, and that therefore this strain has diminished affinity for MC. Finally, [^{3}H] TCDD ligand-binding assay directly detected a cytosolic protein that specifically binds to radioligand TCDD. The high-affinity binding of this protein for TCDD is saturable and reversible (Poland and Kende 1976). For a large number of HAHs, there was an excellent correlation between their binding-affinities for the cytosol protein and their protencies of induce P451A1 in vivo. Weak inducers e.g. PAHs have lower binding affinities for the protein, suggesting their potency may be due to rapid metabolism in vivo in contrast to TCDD and other potent congeners (Poland and Knutson 1982). On the other hand, the much lower specific binding for [^{3}H] TCDD in nonresponsive mice was most likely attributable to a binding species with reduced affinity rather than a reduced receptor concentration. Thus the existence of the aryl hydrocarbon receptor or AhR was confirmed.

1.1.4 AhR ligand-binding site modelling

In order to characterise the physical and chemical features of the AhR ligands, as well as to model the AhR ligand-binding site, a large number of HAHs and PAHs were investigated by structure-activity relationship study (Waller et al 1995; Bonati et al, 1996; Fraschini et al, 1996). The results showed that the AhR ligand-binding site is hydrophobic, can accept planar non-polar ligands with maximal dimensions of 14 x 12 x 5 Å. However the toxicity drastically decreases on adding nonlateral chlorines or removing lateral chlorines from this structure. In general

the toxicity of planar PAHs is extremely sensitive to both the number and position of halogen constituents (Safe 1990; Mhin, Choi et al. 2001). High affinity binding appears to be critically dependent upon key thermodynamic and electronic properties of the ligands. The overall picture emerging from these studies highlights the role of electrostatic and dispersion-type interactions in ligand-AhR binding (reviewed by (Denison, Pandini et al. 2002).

Although this model can predict some ligands, it is too simple and strict. Because a wide range of chemicals, that showed their binding properties to the AhR or their ability to induce gene expression in a AhR dependent manner, were structurally distinct from the classic HAH and PAH ligands. Thus an unsolved problem is what is the actual spectrum of chemicals that can bind to the AhR.

1.1.5 Naturally-occurring ligands

In order to identify the existence of endogenous ligands, some investigations were carried out in the absence of exogenous ligands. Under this condition, the activation of AhR signalling pathway was observed (Chang and Puga 1998). Disruption of AhR using antisense resulted in decreased development of mouse blastocysts (Peters and Wiley 1995) and alterations in normal cell cycle progression (Ma and Whitlock 1996), supporting the existence of endogenous ligands. AhR-null animals showed the best evidence of a role of the AhR in normal development. In AhR-null mice, many physiological changes and developmental abnormalities were observed (Schmidt and Bradfield 1996; Lahvis, Lindell et al. 2000; Lin, Ko et al. 2002). These changes are presumed to result

from loss of AhR activation by an endogenous ligand, although the identity of the responsible chemical(s) remains to be identified.

The greatest source of exposure of individuals to AhR ligand comes from diet (Denison, Pandini et al. 2002; Denison and Nagy 2003). Numerous studies have described and characterized a variety of naturally occurring dietary chemicals as agonist and antagonist for AhR. Some flavonoids play an antagonistic or agonistic role for AhR (Ashida 2000). 7-ketocholesterol, for example, antagonises TCDD effects *in vivo* (Savouret, Antenos et al. 2001). 7-ketocholesterol has been suggested to have physiological significance since its physiological plasma concentration was detected in human blood (Savouret, Antenos et al. 2001). Conversion of dietary indoles (including I3C and Trp) in the mammalian digestive tract to significantly more potent AhR agonists was also demonstrated (Perdew and Babbs 1991).

Recently, a number of endogenous ligands have been reported to have a high affinity for AhR (Heath-Pagliuso, Rogers et al. 1998; Wei, Bergander et al. 2000). Most of the chemicals are tryptophan derivatives. Indirubin and indigo isolated from urine were reported to serve as an even more potent ligand of AhR than TCDD in a yeast assay system (Adachi, Mori et al. 2001).

1.1.6 AhR signalling pathway

Studies performed by many laboratories for over the past two decades showed that the AhR acts as a ligand activated transcription factor. In the absence of ligand,

the latent AhR exists in cytosol associated with a dimer of hsp90 (Wilhelmsson, Cuthill et al. 1990), the hsp90-interacting protein p23 (Kazlauskas, Poellinger et al. 1999) and XAP2/AIP/ARA6 (Carver, LaPres et al. 1998; Bell and Poland 2000). This heteromeric complex maintains the AhR in a conformation with high affinity to its ligand, and is located predominantly in the cytoplasmic compartment or evenly distributed in both cytoplasm and cell nucleus (Pollenz, Sattler et al. 1994). The hydrophobic AhR ligands enter the cell by diffusion and are bound by the hsp90-associated AhR. Ligand binding causes a conformational change. As a result, the AhR translocates to the nucleus, where the hsp90 is replaced with Arnt (Ah receptor nuclear translocator) and a transcriptionally active AhR-Arnt complex is formed (Swanson, Tullis et al. 1993). The resultant AhR-Arnt heterodimer binds to dioxin responsive enhancers (DREs), and transactivates a battery of genes encoding xenobiotic-metabolizing enzymes, most notably *CYP1A1, CYP1A2,* and *CYP1B1* (Schmidt and Bradfield, 1996; (Whitlock 1999). Transactivation of target genes has been shown to be mediated through a variety of histone acetyltrannsferases (HATs) and SWI/SNF coactivators (Hankinson 1995). The AhR signal can be down regulated by two mechanisms. One is through agonist-dependent degradation pathway (Gu, Hogenesch et al. 2000), and the other is through AHRR negative feed back loop (Mimura, Ema et al. 1999).

Very recently, an investigation using a protein interaction network (PIN) strategy identified 52 novel and two known AhR modifiers that are required for AhR signal transduction (Yao, Craven et al. 2004). The authors proposed that AhR

signal transduction is regulated at five discrete steps: (1) receptor folding, (2) receptor translocation, (3) receptor transcriptional activation, (4) receptor level, and (5) a previously undescribed signalling event related to the PASB domain (Yao, Craven et al. 2004). The results generated a new insight into our understanding of the AhR signalling pathway.

1.2 Molecular structure of the AhR

1.2.1 BHLH/PAS proteins

The bHLH/PAS protein is found in a wide range of living organisms (Zhulin, Taylor et al. 1997) PAS-containing proteins have been categorised into three functional subgroups: 1) transcription activators, 2) sensor modules of two-component regulatory systems, and 3) ion channels (Zhulin, Taylor et al. 1997). The PAS was named after the first letters of its three founding members, the *Drosophila* **P**eriod clock protein (PER) (Crews, Thomas et al. 1988), the vertebrate **A**ryl hydrocarbon receptror nuclear translocator (ARNT) (Hoffman et al 1991), and *Drosophila* **S**ingle-minded (SIM) protein (Crews, Thomas et al. 1988). These three proteins are involved in regulation of circadian rhythms, activation of the xenobiotic response, and cell fate determination, respectively. They share a homology region called PAS domain. This domain typically encompasses a ~250-300 amino acids region, which includes two direct sequence repeats (PAS-A and PAS-B) of ~ 50 residues each (Gu, Hogenesch et al. 2000).

The PAS domain may have two main functions in different cases. First, it acts as a surface for the protein-protein interactions. For example, PAS-containing proteins such as AhR, Arnt, SIM, and hypoxia-inducible factor (HIF-1) can form homo or heteromeric complexes through their bHLH (basic helix-loop-helix) region and the PAS repeats (Huang, Edery et al. 1993; Hogenesch, Chan et al. 1997; Kay 1997; Kay 1997). Second, the PAS domain can bind small molecule ligand and /or cofactor, as in the case for the AhR and for the heme-binding bacterial O_2-sensing protein FixL (Monson, Weinstein et al. 1992; Coumailleau, Poellinger et al. 1995).

With the exception of PER, all members of the PAS proteins contain a bHLH region immediately N-terminal to their PAS domain(Huang, Edery et al. 1993; McGuire, Coumailleau et al. 1995; Kikuchi, Ohsawa et al. 2003; Chapman-Smith, Lutwyche et al. 2004). This region is known to mediate both DNA binding (basic region) and protein dimerization (HLH) with other bHLH transcription factors. The bHLH/PAS domain is conserved across the species.

Consistent with their activities, most PAS proteins have transcriptionally active domains (TAD) within their C-terminal ends. In contrast to the bHLH/PAS regions, the TAD of most PAS proteins shows little sequence homology. However, it is a glutamine-rich domain(Schmidt and Bradfield 1996; Gu, Hogenesch et al. 2000). Taken together, the PAS domain appears to be a complex structure harbouring a number of distinct functional activities.

Three-dimensional fold of the PAS domain have been proposed for several proteins in this superfamily(Pellequer, Wager-Smith et al. 1998; Denison, Pandini et al. 2002; Procopio, Lahm et al. 2002). Among them, the photoactive yellow protein (PYP) and the bacterial O_2 sensing FixL protein are relevant to the AhR, because both FixL PAS domain and PYP are activated by ligans (Denison, Pandini et al. 2002; Procopio, Lahm et al. 2002). In FixL, oxygen binding at the heme binding PAS domain controls that activity of a histidine kinase domain; and in PYP, a local conformational change occurs once the p-hydroxycinnamoyl cromophore is bound. In Figure 1-2 is showed structures of PYP and FixL PAS domains.

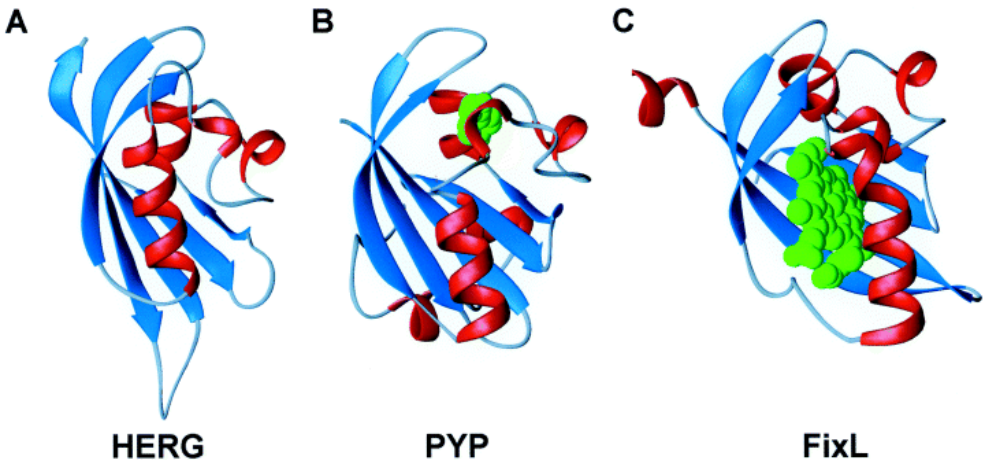

Figure 1- 2. Modeling of PAS proteins
The largest shift amongst the conserved secondary element position occurs in FixL due to the presence of the large heme cofactor. Secondary structure elements are coloured blue (strands) and red (helices), cofactor ligands green (adopted from (Procopio, Lahm et al. 2002)).

1.2.2 The AhR is a PAS protein

Cloning of the four alleles of the murine AhR made it possible to carry out a detailed molecular analysis of the AhR structure (Poland et al. 1994). A similarity search of the translated cDNA sequence of the AhR demonstrated the characteristic multiple domains of the PAS superfamily (Gu, Hogenesch et al. 2000). That is: a consensus bHLH domain, a region with significant identity to the PAS domain, and a glutamine-rich region in the C-terminal portion of the receptor, thereby, confirmed the AhR as a member of the PAS superfamily (Gu, Hogenesch et al. 2000).

It has been recognized that there are four different alleles of AhR among different murine strains, which rendered these strains different sensitivity to TCDD toxicity (Poland and Knutson 1982). In vitro translation/transcription of the cDNAs encoding each of these alleles allowed a detailed dissection of differences between these alleles. An early work revealed the different molecular weights of the AhR between these alleles (Poland and Glover 1990). In consistent with this finding, further work showed that this difference in molecular weight is primarily due to differences in the position of the AhR's translational termination codon, rather than differential splicing or posttranslational modification (Poland, Palen et al. 1994). The ligand binding affinity of Ah^{b-1} Ah^{b-2} and Ah^{d} translated from cDNAs were also investigated by the radioligand 2-[^{125}I]iodo-7-8-dibromodibenzo-*p*-dioxin. Equilibrium dissociation constants for these receptors are shown in Table 1-1. The *Ah*^{d} allele, which has a lower ligand binding affinity, differs from the *Ah*$^{b-2}$ receptor by only two amino acids. The reduced Ah^{d} ligand

affinity was the result of an $Ala_{375} \rightarrow Val_{375}$ polymorphism. This amino acid change is localized to the ligand-binding domain (Poland and Glover 1990).

Alleles	Ah^{b-1}	Ah^{b-2}	Ah^{b-3}	Ah^{d}
Ligand affinity	High	High	High	Low
K_D	6-10pM	6-10pM	ND	37pM
M_r	95kDa	104kDa	105kDa	104kDa
In vivo induction by MC	Responsive	Responsive	Responsive	Responsive
Representative strains	C57BL	C3H,CBA BALB/c	*M.spretus* *M.hortulanus*	DBA/2, SJL129

Table 1- 1. The AhR is polynorphic across mouse species.
The four mouse alleles differ in size and ligand-binding affinity ((Poland, Palen et al. 1994)). K_D, dissociation constant; Mr, relative molecular weifht; MC, 3-methylcholanthrene (an AhR agonist); ND, not done (adopted from (Carver and Bradfield 1999)).

Although the AhR is structurally different from other known transcription factors, shuch as steroid/thyroxin receptors, the mechanism by which it binds to the ligand is similar to that of the steroid/thyroxin receptors (Schmidt and Bradfield 1996; Gu, Hogenesch et al. 2000). The AhR binds to a dimer of the hsp90 (Perdew and Poland 1988). This association was correlated with the cytosolic localization of the AhR and a receptor state with high affinity for the ligand, but not DNA. However as a transcript factor, the AhR is distinct in that it binds to DRE (dioxin responsive element) as part of a heterodimeric complex (Dolwick, Swanson et al. 1993). The formation of the heterodimer with a nuclear partner protein Arnt is prerequisite for the AhR to bind DRE (Pollenz, Sattler et al. 1994). It has been shown that the Arnt protein was required to direct the ligand-activated AhR to enhancer element upstream of genomic targets similar to those found upstream of

the *Cyp1a1* gene (Burbach, Poland et al. 1992). This finding led to a general accepted AhR signalling pathway.

1.2.3 Human AhR

The AhR is abundant in many human tissue and cell lines. In general, the mechanism of action of human AhR is very similar to that of rodent tissues (Josephy 1997). There are some distinct differences, however, between human and mouse AhR. When compared with the responsive mouse, firstly, molybdate is required to stabilise human AhR and mouse AhR^{d}, but it is not important for the stability of AhR^{b-1} (Manchester, Gordon et al. 1987; Poland, Palen et al. 1994). Secondly, the affinity of human AhR for TCDD is much lower than the affinity of mouse AhR^{b-1} for TCDD. The affinity typically ranges from 3 to 5 nM in human samples (Ema, Ohe et al. 1994), compared with a K_D of about 1nM in cytosol from responsive C57BL/6 mouse (Poland and Knutson 1982). Polymorphism may play a role in determining individual susceptibility to TCDD. An Ala_{381} to Val_{381} is partly responsible for the reduced ligand-binding affinity in human. The mutation of Val_{381} to Asp_{381} (equivalent to position of 375 of mouse AhR) completely abolished the ligand binding activity of human AhR (Dolwick, Schmidt et al. 1993; Ema, Ohe et al. 1994; Poland, Palen et al. 1994). Interestingly, in human populations the polymorphisms could involve differences either in the target gene expression or in the enzyme function (Harper, Wong et al. 2002; Mimura and Fujii-Kuriyama 2003).

1.2.4 *Ahr* knockout mice

In order to elucidate the endogenous function of AhR and its role in the toxicity of TCDD, AhR-null mice were generated independently by three groups (Fernandez-Salguero, Pineau et al. 1995; Schmidt, Su et al. 1996; Mimura, Yamashita et al. 1997). The AhR-null mice were viable, however the growth rate the AhR-null mice was significantly retarded as compared with the wild type mice for the first three weeks. The mutant mice were revealed to be defective in development of liver, immune system (Schmidt, Su et al. 1996); abnormal hepatic and kidney vascular structures (Fernandez-Salguero, Pineau et al. 1995; Mimura, Yamashita et al. 1997). Concerning xenobiotic metabolism, the lack of the AhR abolished the inducible expression of *CYP1A1* and *1A2* genes in response to TCDD. These results suggest that the AhR may play an important role in liver growth and immune development, and there may exist a constitutive ligand for AhR.

1.2.5 Domain structure of the AhR

As a PAS protein, the AhR is composed of multiple functional domains as defined in this family. In the very N-terminal end, the AhR contains a bHLH region that involves in DNA binding, dimerizing with its nuclear partner Arnt and with heat shock protein 90 (hsp90) (Schmidt and Bradfield 1996; Gu, Hogenesch et al. 2000). The N-terminal of this region also contains nuclear localisation (NLS) and export (NES) domains (Ikuta, Eguchi et al. 1998; Berg and Pongratz 2001). The bHLH domain is required for heterodimerization, reorganisation and binding of these factors to dioxin response element upstream of the target genes (Landers and

Bunce 1991; Fukunaga, Probst et al. 1995). C-terminal to the bHLH domain is PAS domain, which composes of two imperfect repeats of 50 amino acids, PAS-A and PAS-B (Nambu 1991). The PAS domains are involved in AhR/Arnt dimerization (PAS-A), AhR ligand, hsp90, and several other co-chaperone binding (Gu, Hogenesch et al. 2000; Carlson and Perdew 2002). The ligand-binding domain of AhR is located in the PAS domain, overlapping in part with the PAS-B region (Coumailleau et al. 1995). Hsp90, a molecular chaperone protein, is thought to be important for correct folding of the AhR ligand-binding domain (LBD), and for regulating nuclear localisation of the AhR signalling complex (Carver, Jackiw et al. 1994; Perdew and Bradfield 1996). The very end of the PAS domain is shown to be the AhR repressor (AHRR) binding site (Mimura, Ema et al. 1999). The C-terminal segment of AhR contains a complex transactivation domain, consists of multiple stimulatory and inhibitory subdomains (Figure 1-3) (Jain, Dolwick et al. 1994; Whitelaw, Gustafsson et al. 1994).

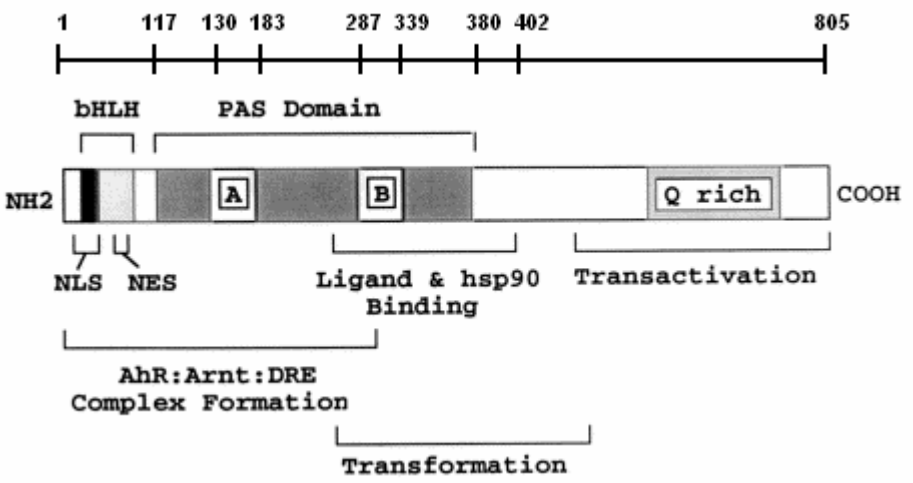

Figure 1- 3. **Functional domains of mouse AhR** [b-1]
The basic region (b), helix-loop-helix (HLH), PAS, and transactivation (TAD) domains are labled. The regions that have been shown to play a role in nuclear localization (NLS)

and export (NES); ligand and hsp90 binding; Arnt:DRE heteromeric formation; and repressor binding are indicated (adopted from Denison, et al 2002). The positions of some residues are labeld by bar on the top of the graph (Poland, Palen et al 1994; Ema, Ohe et al. 1994).

1.2.6 Ligand binding domain

The AhR protein belongs to bHLH/PAS protein superfamily, however it is distinct in harbouring a ligand-binding domain (LBD) in its central PAS-B region (Coumailleau, Poellinger et al. 1995). As a transcription factor, the AhR is activated by ligand binding, which triggers the dioxin-signalling pathway (Gu, et al. 2000). In addition, the LBD has also been postulated to be involved in the repression of a number of receptor activities that map outside the LBD itself (McGuire, Okamoto et al. 2001). These repressed functions include dimerization with Arnt, DNA binding, and transcription activity (McGuire, Okamoto et al. 2001). Since the LBD plays an important role in the AhR functionality, definition of the functional LBD of mouse AhR^{b-1} has been an objective of many investigations over past 10 years.

Initially the ligand binding property of the AhR was identified in a CNBr cleavage fragment, which covalent bound to photoaffinity-labeled ligand. The sequence of this fragment was then confirmed by amino acid sequencing (Burbach, Poland et al. 1992). The fragment covalently bound radioligand was 12kDa, located to amino acids 232 to 334 of mouse AhR^{b-1} (Burbach, Poland et al. 1992). However, it was considered that the amino acid residues distant from these residues might actually involved in the formation of a ligand-binding pocket. Therefore, this tentative assignment was further investigated by deletion analysis. In these

experiments the ability of the deletion constructs to bind the photoaffinity ligand were investigated. The approximate N- and C-terminal boundaries were defined to be between residues 166 to 425, since additional deletions in both N- and C-terminal abolished ligand binding (Dolwick, Swanson et al. 1993). This result was further confirmed by the other work, in which the carboxyl side of the LBD was defined at amino acid 402 by a truncated AhR construct, because further shortening to 377 amino acids eliminated binding. While the N-terminal truncations produced a more graded loss of binding (Poland, Palen et al. 1994).

Several investigations were carried out to delineate the minimal LBD. In consistent with the ligand binding property, the discrete functional LBD was expected to bind both ligand and hsp90. The latter of which is believed to be prerequisite for the proper folding of the AhR and maintaining LBD in a conformation with high affinity for the ligand. A study showed that the AhR construct with deletion of the PAS-A repeat (amino acids 121-182) reduced ligand binding only 30%, while deletion of the PAS-B repeat (amino acids 259-374) completely abolished binding, as did of the complete PAS region (Fukunaga, Probst et al. 1995). Therefore the minimal LBD was mapped between amino acids 230 and 397 (Fukunaga, Probst et al. 1995), the region that encompasses the PAS-B repeat and a high affinity binding polymorphic residue 375 (Fukunaga, Probst et al. 1995).

One other study showed a minimal LBD from the central PAS region, comprising of amino acids 230 to 421. Coincidentally, this region was found to be able to

interact with hsp90 in vitro. Expression of the minimal LBD in wheat germ lysates or bacteria, systems that harbour hsp90 homologs unable to interact with the AhR, resulted in non-ligand binding forms of this minimal 230 to 421 fragment (Coumailleau, Poellinger et al. 1995). Importantly, affinity of the minimal LBD for TCDD was similar to the affinity inherent in the full-length AhR (Coumailleau, Poellinger et al. 1995). The results showed that the ligand binding by the AhR is an independent property of the centrally located LBD. Since it contains all the information necessary for ligand binding, this minimal LBD of the AhR was shown to be transferable, retaining its activity when attached to other proteins (Coumailleau, Poellinger et al. 1995). A summary of the above results is shown in Table 1-2.

	Ligand binding domain residues	References
1	232-334	Burbach et al, 1992
2	166-380	Dowick et al 1993
3	1-402	Poland, et al 1994
4	230-421	Coumailleau et al, 1995
5	230-397	Fukunaga, et al, 1995

Table 1- 2. Definition of the AhR LBD
1, a fragment (a.a. 232-334) covalently bound to photoaffinity ligand (Burbach et al, 1992); 2, deletion constructs with N-terminal deletion of a.a. 165 and C-terminal deletion of a.a. 379 retained ligand binding activity (Dowick et al 1993); 3, C-terminal deletion outside a.a. 402 retained ligand binding activity (Poland, et al 1994); 4, a fragment (a.a. 230-421) retaining full-length ligand binding activity (Coumailleau et al, 1995); 5, deletion of the a.a 230-397 completely abolished ligand binding (Fukunaga, et al, 1995).

Although comparison of the amino acids sequences of this AhR LBD across species reveals a high degree of identity and homology, several naturally occurring mutations within this region alter AhR ligand binding affinity (Ema, Ohe et al. 1994; Poland, Palen et al. 1994). For example, the reduced Ah^d ligand

affinity was the result of an $Ala_{375}\rightarrow Val_{375}$ mutation, a residue locates in the minimal LBD. Mutation of Val_{375} in the DBA/2 mouse (or the equivalent Val_{381} in human AhR) to alanine could partly restore the ligand binding affinity of the nonresponsive DBA/2 mouse and human receptors to that of the responsive mice (Ema, Ohe et al. 1994; Poland, Palen et al. 1994).

Currently there are no X-ray or NMR-determined structure of liganded or unliganded AhR (Denison, et al. 2003). This hinders detailed analysis of the molecular mechanisms controlling the formation of the functional LBD and the mechanisms by which the LBD interacting with the ligands.

1.3 Chaperone proteins of the AhR

At present it is widely accepted that the AhR mediates many, if not all, of the divers biochemical, biological, and TCDD and related compounds (Poland and Knutson 1982; Landers and Bunce 1991). It is well established that the binding affinity is correlated with the activation of the AhR and the subsequent production of a toxic response (Poland and Knutson 1982). The activation of the AhR is regulated by its association with other cellular factors. Among them are hsp90 and hepatitis B virus (HBV) X-associated protein 2 (XAP2 or AIP or APA6) (Bell and Poland 2000). In addition, the formation of the functional AhR requires a series of chaperone and co-chaperone proteins (Yao, Craven et al. 2004).

1.3.1 Composition of the AhR complex

In early observations, the AhR was found to exist in cytosol in association with other proteins (Denis, Gustafsson et al. 1988; Perdew and Poland 1988). Later it was established by chemical cross-linking studies that this heterotertrameric complex composed of the AhR, and three additional components, with molecular weight of approximatly 88-, 96- and 46-kDa (Perdew and Bradfield 1996). The 88- and 96-kDa components were shown to be isoforms of hsp90 (Meyer, 1999), and the low molecular weight protein to bind directly to AhR has been identified (Chen and Perdew 1994).

Specifically, three distinct forms of the receptor have been demonstrated to exist. One is a cytosolic complex. This cytosolic AhR complex has a sedimentation coefficient of 9S and a calculated molecular weight of 270-kDa, representing the AhR bound to a dimer of hsp90 (Perdew 1994). This form has high affinity for ligand. The second form is a 160- to 200-kDa nuclear form with a sedimentation coefficient of 6S and consisting a 100-kDa ligand-bound subunit and a 110-kDa subunit protein Arnt (Gasiewicz, Elferink et al. 1991). This form displays a high affinity for DNA and can be converted from the 9S *in vivo* by adding ligand (Denison, Vella et al. 1986) or *in vitro* by treating the receptor with heat (Kester and Gasiewicz 1987). A third form has a sedimentation coefficient of 4S and Mr of 104-kDa. This form can be detected after prolonged treatment of the 9S form with high salt (Denison, Harper et al. 1986; Denison, Vella et al. 1986). It is clear that salt disrupt the binding of the receptor to hsp90 (Pratt 1997).

1.3.2 Heat shock protein 90 (hsp90)

The association of AhR with a dimeric form of hsp90 is a prerequisite for the receptor to acquire its ligand-binding activity (Ingemar P, 1992). Hsp90's function is assisted and regulated by a number of accessory proteins as chaperone and co-chaperones (reviewed by (Pratt and Toft 2003). Structural determination and functional analysis of hsp90, identification of cochaperones that hsp90 function were landmarks towards understanding of signal transduction pathways (Prodromou, Panaretou et al. 2000; Richter and Buchner 2001; Meyer, Prodromou et al. 2003).

1.3.2.1 General properties of hsp90

The heat shock protein hsp90 is one of the most abundant cytosolic proteins, accounting for 1-2% of the total soluble protein (Richter and Buchner 2001). In eukaryotic cells two genes encode hsp90. The isoproteins of hsp90 are expressed to different degrees. The yeast *HSC82* and human hsp90β genes are, typically, more constitutive and moderately inducible in their expression, whereas yeast *HSP82* and human hsp90α genes are generally expressed at lower basal levels and are strongly inducible under stress conditions (Cox and Miller 2003). Hsp90 proteins are essential for eukaryotic viability (Pearl and Prodromou 2001; Richter and Buchner 2001). Hsp90 acts as classic molecular chaperone by preventing aggregation and maintaining the native conformation of proteins in cells under various stress conditions (reviewed by (Richter and Buchner 2001). However, hsp90 proteins also have direct role in the regulation of intracellular signalling pathways in unstressed cells (reviewed by (Pratt, Galigniana et al. 2004). In the

chaperon process, hsp90 acts as an integral component of the protein heterocomplex. A growing number of the chaperones and co-chaperones, which assist and regulate hsp90, have been identified. Among them are hsp70, hsp40 and the co-chaperones Hop (hsp organization protein), a 23-kDa protein (p23), Aha1 and one of several immunophilins (Sullivan, Stensgard et al. 1997).

1.3.2.2 ATP-ase cycle of hsp90

Structure and biochemical studies showed that hsp90's chaperone activity is absolutely dependent upon binding and hydrolysis of ATP (Grenert, Sullivan et al. 1997; Obermann, Sondermann et al. 1998; Panaretou, Prodromou et al. 1998). In the absence of ATP, the hsp90 dimer is found in an extended conformation, in which the N-termini are not dimerized. In this relaxed state, hsp90 is ready to accept the substrate protein to bind. Upon ATP binding, hsp90 undergoes a big conformational change resulting in a closed state. This conformational change includes N-termini association not only with each other but also with its own middle domain. As a result, ATPase activity is stimulated and it acts as a 'clamp' on the substrate (Chadli, Bouhouche et al. 2000; Prodromou, Panaretou et al. 2000; Meyer 2004). It is believed that association of substrate protein with hsp90 is required for the opening of the hydrophobic ligand-binding cleft of the receptor (Morishima, Kanelakis et al. 2001).

1.3.2.3 A cycle for activation of steroid hormone receptor

hsp90 regulated activation of the client proteins is a complicated process. To date, the best known maturation process driven by hsp90 is the assembly of steroid receptors, glucocorticoid receptor and progesterone receptor (GR and PR) into a high-affinity hormone-binding conformation (Dittmar and Pratt 1997). In the assembly process, three dynamic steps have been observed. The receptor initially associates with molecular chaperone hsp70 (Murphy, Morishima et al. 2003)This association is assisted by hsp40. Then, Hop (also called Stil or p60) binds to hsp70 and promotes its ATPase activity. As a result, an "early complex" is formed (Dittmar and Pratt 1997). This early complex is loaded to hsp90 via Hop and leads to the formation of the "intermediate complex" consisting of hsp70, Hop and hsp90. This three-protein complex is shown to be sufficient to transform steroid hormone receptor from the non-steroid binding form to the steroid binding form in vitro (Dittmar and Pratt 1997). However, to yield the final activated heterocomplex, Hop and hsp70 have to be exchanged against one of the immunophilin protein and p23 to form a mature complex (Dittmar, Banach et al. 1998; Richter and Buchner 2001).

The mechanism of hsp90-mediatied receptor activation is an important aspect not understood. It could be that interaction of hsp90 with the hormone-binding domain of GR opens the hydrophobic binding site for the steroid hormone. p23 binding to the assembled heterocomplex guarantees the prolonged opening of the glucocorticoid binding site and confers stability to the otherwise unstable complex (Morishima, Kanelakis et al. 2001).

The ligand binding domains of the AhR and GR are mechanistically similar in requiring interaction with hsp90 to enable ligand binding. However the distinct sequences seem different for the reconstitution of ligand binding of the AhR (Coumailleau, Billoud et al. 1995). For example, the ligand binding capacity of the mineralocorticoid receptor (MR) could be restored by coincubation of bacterial expressed MR with reticulocyte lysate, which resulted from the reassociation of the hsp90. whereas the dioxin binding state of bacterial expressed and purified AhR LBD failed to be reconstituted using these protocols (Coumailleau, Billoud et al. 1995).

1.3.2.4 Roles of hsp90 in modulating the AhR activities

Hsp90 interacts with two distinct motifs of the AhR, the ligand binding PAS-B domain and the bHLH domain (Antonsson, Whitelaw et al. 1995). The former binding domain of hsp90 spans amino acids 340 to 422 (Denis, Gustafsson et al. 1988; Perdew and Poland 1988; Whitelaw, Gustafsson et al. 1994), and the latter spans amino acids 12 to 41 of the murine AhR (Pollnez 2002). A yeast strain, in which the levels of hsp90 could be regulated, was used to study the role of hsp90 in the AhR signalling. At wild-type hsp90 levels, normal AhR signalling was seen; however, when hsp90 levels were decreased to 5% of wild type, ligand-induced AhR signalling was blocked (Carver, Hogenesch et al. 1994; Whitelaw, Gustafsson et al. 1994). *In vitro* experiment showed that hsp90 could interact with the AhR via the minimal LBD (residues 230-421) (Coumailleau, Billoud et al. 1995). Expression of this fragment in wheat germ lysates or bacteria, systems that harbour hsp90 homologs unable to interact with the AhR, resulted in non-ligand

binding form of this fragment. This means that the fragment was critically dependent upon hsp90 for its ligand binding (Coumailleau, Billoud et al. 1995)

It has been shown that hsp90 plays three main roles in the AhR signalling. Firstly, hsp90 maintains the receptor in a high-affinity ligand binding conformation by proper folding and stabilizing the AhR. Ligand occupation leads to down-regulation of AhR protein levels, both in cultured cells and *in vivo* (Swanson and Perdew 1993; Pollenz, Sattler et al. 1994). This effect is due to destabilization of the hsp90/AhR complex caused by ligand binding. Treatment of cells with antibiotics geldanamycin that binds to the ATP binding site of hsp90 and disrupts the interaction of hsp90 with the AhR, leads to rapid proteolytic turnover of the AhR *in vivo* (Chen, Singh et al. 1997). Dissociation of hsp90 *in vitro* by high salt or heat leads to an inability of the AhR to bind ligand (Grenert, Sullivan et al. 1997). Because increasing of the temperature and the salt concentration cause a significant increase in ATP-hydrolyzing activity of hsp90, which results in the disruption of the hsp90/AhR complex (Grenert, Sullivan et al. 1997). It is also known that molybdate can stabilize the AhR/hsp90 complex (Poland and Glover 1990). This probably arises from its ability to stabilize an ATP-bound conformation of hsp90 after ATP has been hydrolyzed (Grenert, Johnson et al. 1999).

Secondly, binding of hsp90 to AhR represses the ability of the AhR to heterodimerize with Arnt (McGuire, Whitelaw et al. 1994). Thirdly, dynamic assembly of heterocomplex with hsp90 is required for intracellular traffic of the

AhR (Kazlauskas, Sundstrom et al. 2001; Pratt, Galigniana et al. 2004). AhR has a nuclear localisation signal (NLS) in its N-terminus capable of binding to importin-α, which targets the AhR to the nuclear rim (Ikuta, Eguchi et al. 1998). The binding of hsp90 to NLS appears to participate in masking NLS (Pollenz 2002). Binding of the AhR to importin-α is ligand-dependent and inhibited by geldanamycin, also implying a role of hsp90 (Pratt, Galigniana et al. 2004).

1.3.3 The immunophilin-like X-associated Protein 2

Immunophilins are a family of proteins who have peptidylprolyl isomerase (PPIase) activity. These proteins are involved in neural regeneration (Sabatini, Lai et al. 1997), and found as components of many steroid receptor chaperone complexes (Pratt 1997). In its N-terminal half, immunophilin harbours a peptidylprolisomerase domain, which is able to bind to immunosupressive drugs such as FK506 and cyclosorin A (Pratt, Galigniana et al. 2004). In its C-terminal half, immunophilin harbours three tetratricopeptide repeat motifs (TPR) (Pratt, Galigniana et al. 2004). TPR motifs are 34-amino acid residue repeat regions that form a predominantly α-helical structural unit that acts as a protein-protein interaction domain (Pratt, Galigniana et al. 2004). X-Associated Protein 2 (XAP2) is an immunophilin-like protein, containing TPR motifs. However unlike other immunophilins, XAP2 is unable to bind to the FK506. Like other immunophilins, XAP2 is associated with hsp90 complexes but it preferentially associates with the AhR/hsp90 complex and interacts poorly with steroid hormone receptors.

XAP2 was discovered due to its ability to associate with the X-protein of the HBV (Kuzhandaivelu, Cong et al. 1996). Soon afterwards, it was identified as a core component of the mature AhR/hsp90 complex in cytoplasm (Meyer, Pray-Grant et al. 1998). XAP2 is also known as AIP (AhR interacting protein) (Ma and Whitlock 1997) and ARA9 (AhR associated protein 9) (Carver and Bradfield 1997), as it was independently identified by three laboratories. XAP2 is expressed in all tissues that have been examined, and predominantly is present in cytoplasm (Ma and Whitlock 1997; Carver, LaPres et al. 1998). In mammalian cells and in yeast, XAP2 has been found to associate with hsp90 (Ma and Whitlock 1997; Meyer and Perdew 1999). In a reticulocyte lysate system, XAP2 bound to both hsp90 and the AhR; whereas binding to the AhR appeared to be an hsp90-requiring process, which was both ATP-dependent and sensitive to geldanamycin (Bell and Poland 2000). The studies of truncated mutants of XAP2, used to localize domains required for AhR core complex assembly, has demonstrated that the C-terminal half of XAP2 is required for binding to both hsp90 and the AhR (Carver & Bradfield, 1997; (Bell and Poland 2000). Mutation of a conserved basic residue in TPR of XAP2 displayed reduced AhR binding and no observed binding to hsp90 (Bell and Poland 2000). This study suggested that the conserved TPR domain was involved in binding to both AhR and hsp90, with the hsp90 interaction being very sensitive to mutation in this region. The ability of XAP2 to bind to the AhR appeared less sensitive to TPR mutations, however the α-helical C terminus of XAP2 is absolutely necessary for binding to the AhR.

It is clear now that the AhR LBD, together with additional specific motifs within the AhR is required for XAP2 to bind the AhR. XAP2 binds directly to the C-terminus of hsp90 via its TPR domain (Bell and Poland 2000).

Two functional roles of the XAP2 have been established. Firstly, XAP2 enhances the transcriptional activity of the AhR. This has subsequently been shown to be a result of increased AhR stability (LaPres, Glover et al. 2000). The stability effect of XAP2 on the AhR has been shown to be specific, and mediated by direct assembly of XAP2 into the core complex (Meyer, Petrulis et al. 2000). Recent reports have provided evidence that increased AhR levels result from the ability of XAP2 to protect the unliganded AhR from ubiquitination, thus limiting proteosomal degradation of the AhR (Kazlauskas, Poellinger et al. 2000; Ma and Baldwin 2000; Lees and Whitelaw 2002).

Secondly, XAP2 is capable of modulating the subcellular localization of the AhR. The endogenous AhR was found to localize to both cytoplasm and nucleus, but when XAP2 was overexpressed, the AhR is redistributed to the cytoplasm (Meyer et al, 2000; Petrulis et al, 2000; Kazlauskas et al, 2000; LaPres et al, 2000). This redistribution of the AhR to the cytoplasm is inhibited by geldanamycin (Kazlauskas et al, 2000), suggesting that both hsp90 and XAP2 are required for trapping of the AhR in the cytoplasm. This process is inhibited by cytochalasin B, which inhibits polymerize of actin filaments (Berg and Pongratz 2002). Thus it is thought that XAP2 anchors the ligand-free AhR to actin filaments to maintain its cytoplasmic localization (Berg and Pongratz, 2002; Petrulis et al, 2003). The AhR has an NLS in its N-terminus that binds importin, which targets the receptor to the

nuclear rim. Studies focused on binding of AhR to importin-β, and coexpression of XAP2 was found to decrease recovery of importin-β with the receptor (Kazlauskas et al, 2001). The mechanism for this effect has been determined to be due to XAP2 altering the ability of the AhR to be recognized by importin-β (LaPres et al, 2000; Petrulis et al, 2003; Kazlauskas et al, 2001). However, upon the ligand binding, nuclear uptake of the AhR complex is mediated by a conformational change that leads to enhanced importin recognition (Kazlauskas et al, 2001; Petrulis and Perdew, 2002).

1.3.4 Hsp90-associated protein p23

Prior to ligand binding, the AhR is retained in a complex with the molecular chaperone hsp90. Hsp90 may keep the receptor in a mature conformation. The steps leading to the mature of hsp90/AhR complex involve several other factors, including a 23 kDa protein, p23 cochaperone (Pratt and Toft, 1997; Freeman et al, 2000). p23 is a ubiquitous, highly conserved protein, and was first identified in an hsp90-binding protein (Johnson, Chadli et al. 2000). There are three p23 proteins, yeast p23 (sba1p) (Fang, Fliss et al. 1998) and the two human p23 homologs, p23 and tsp23. Sba1p was indistinguishable from human p23 in assays of seven intracellular receptor activities in both animal cells and in yeast; in contrast, certain effects of tsp23 were specific to that homolog (Freeman, Felts et al. 2000).

P23 associates with various steroid receptors, presumably by its interaction with hsp90 (Pratt and Toft, 1997). p23 binds to the N-terminal nucleotide binding

pocket of hsp90 in an ATP-dependent manner (Chadli et al 2000). It has been reported that p23 has three functions in the molecular chaperoning process.

Firstly, the binding of p23 to hsp90 is to physically stabilize the receptor-hsp90 interaction, thereby enhancing the amount of receptor that exists in the high-affinity ligand binding conformation (Pratt and Toft, 1997; Cox and Miller, 2002). Deletion of the *SBA1* gene (yeast p23 homolog) reduced ligand-mediated AhR signalling by approximately 40% and shifted the ED_{50} of the β-napthoflavone ligand by five-fold in a reporter gene assay. The AhR signalling was restored in the sba1 strain by a plasmid-borne *SBA1* gene, confirming that the signalling defect was due to *SBA1*. The data show that p23 enhances the AhR signalling (Cox and Miller, 2002). In a recent report, it was shown that cochaperone p23 is the limiting component of the multiprotein hsp90/hsp70-based chaperone system *in vivo* (Morishima et al, 2003). Coexpression of p23 with the GR increased the proportion of cytosolic receptors that were in stable GR/hsp90 heterocomplexes with steroid binding activity. Moreover, coexpression of p23 eliminated the insoluble GR aggregates (Morishima et al, 2003).

Secondly, p23 couples the ATPase activity of hsp90 to client protein dissociation and thus can function as a substrate release factor for hsp90 (Kazlauskas, Poellinger et al. 1999; Young and Hartl 2000; Kazlauskas, Sundstrom et al. 2001). The nuclear form of the AhR interacts with Arnt and no longer possesses the ability to bind ligand. Dissociation of hsp90 from the AhR is essential for formation of the AhR/Arnt heterodimer (Heid, Pollenz et al. 2000). Therefore,

release of hsp90 form the AhR is a critical step in the activation process of the AhR (Kazlauskas, Poellinger et al. 1999). This process depends on the hsp90 ATPase and is blocked by geldanamycin. The cochaperone p23 greatly stimulated hsp90 substrate release with ATP (Young and Hartl, 2000). However, release of hsp90 from the AhR was not observed upon ligand binding in the absence of Arnt (Kazlauskas et al, 2001).

Thirdly, p23 may also assist more directly in the chaperoning process since it can interact passively with denatured proteins to maintain them in a folding-component stage (Bose, Weikl et al. 1996; Freeman, Toft et al. 1996); Freeman et al, 1996)

Taken together, p23 cooperates with hsp90 to facilitate, for example, ligand binding by the receptor. P23 also can act as a substrate release factor for hsp90.

1.3.5 Other chaperoning proteins of theAhR

Studies in reticulocyte lysate suggested that the AhR complex could associate with Hop and Hip, suggesting that the initial assembly of the AhR/hsp90 complex is similar to what has been described for the progesterone receptor (Nair, Toran et al. 1996). Aha1 (Activators of the Hsp90 ATPase) is a newly identified cochaperon that associates with “mature complex” of hsp90 chaperone machinery (Panaretou, Siligardi et al. 2002; Meyer 2004); (Meyer, Prodromou et al. 2004). In yeast, Aha1 and its homolog, Hch1 stimulate the ATPase activity of hsp90. Aha1 was found to be required for hsp90-dependent activation of an authentic client

protein (Meyer, Prodromou et al, 2004). However its role in the AhR signalling has to be defined.

1.4 Recombinant expression of the AhR

For structural and functional analysis a large quantities of functional AhR is required. However, the endogenous receptors in target cells and tissues are produced in very low amounts (10-100fmol/mg of cytosolic protein), and the AhR is extremely instable in nature (Landers and Bunce, 1991). When try to purify native AhR using traditional purification methods, the AhR tended to aggregate and form a number of distinct species during chromatigraphy (Gasiewicz and Bauman 1987; Bradfield, Glover et al. 1991). Thus there has been a great deal of interest in the overexpression of functional AhR by recombinant technologies. Bacterial expression of the AhR met with little success. The expressed AhR reached high levels in bacteria, but was totally insoluble (Coumailleau et al, 1995; present study). This could be due to lack of proper posttranslational modification or failure to interact with hsp90, leading to improper folding or aggregation of expressed AhR (Coumailleau et al, 1995). Baculovirus expression system has been one of the most popular systems for expressing mammalian receptors, which are mechanically similar to the AhR (Alnemri, Maksymowych et al. 1991; Chan, Chu et al. 1994). The recombinant proteins are often expressed at high levels in insect cells, and are functionally similar to their authentic counterparts (King, Daugulis et al. 1992). In a previous experiment, the full-length AhR was expressed in insect cells in high-levels and a fraction of the proteins are in soluble form (Chan, Chu et al. 1994). Photoaffinity labeling and gel shift assays

demonstrated that the expressed AhR bound ligand, heterocimerized, and recognised their cognate "dioxin response element" in a manner similar to their native counterparts (Chan, Chu et al. 1994).

In baculovirus expression system, expression of the foreign gene is usually driven by the polyhedrin promoter of the *Autographa californica* nuclear polyhedrosis virus (AcNPV). However the formation of the recombinant virus is a significant bottleneck in the process. There are two main ways of generating a recombinant virus. One way is by homologous recombination and the other is by site-specific transposition. Site-specific transposition proved to be an easy and rapid way, in which the donor plasmid containing the target gene was transposed with Tn7 to insert foreign gene into bacmid DNA propagated in *E. coli*. Colonies containing recombinant bacmids were identified. When the resulting composite bacmid was introduced into insect cells recombinant baculovirus was generated. Then the foreign gene could be expressed in insect cells under the control of the baculovirus promoter. With this method, tedious plaque purification is not required and recombinant virus isolation is easy (Luckow 1993).

Compared with bacterial expression, baculovirus expression system is time consuming and costly. However, it yields high-level soluble proteins. Therefore this system should prove valuable for producing AhR in microgram to milligram quantities for structure-function and biochemical studies.

1.5 Aims of the thesis

Functional AhR can be expressed simply in reticulocyte lysate (Bell and Poland 2000), but bacterial expression of AhR fails to yield functional protein (Coumailleau, 1995). A baculovirus expression system has been successfully used to produce microliter to milliliter of full-length AhR (Chen et al, 1994). However there is no previous report on recombinant expression of the AhR LBD in insect cells and no functionality characterizations on this protein. Therefore the aims of this study were:

1). To produce an antibody to the AhR LBD for analysis of the expressed LBD.

2). To develop an *in vitro* [^{3}H] TCDD binding assay for evaluating the binding capacity of the recombinant LBD

3). To recombinant express the AhR LBD in insect cells using baculovirus expression system, and optimizing cytosolic AhR recovery from the transfected cells.

4). To characterize the function of a series of truncated recombinant LBD and to refine the minimal LBD.

Chapter 2 Materials and methods

2.1 Materials

All the reagents were of the highest standard commercially available. Ammonium acetate, bovine serum albumin, phosphoric acid, TEMED, SDS, Tween 20, ethidium bromide, dithiothreitol (DTT), dimethylsulfoxide (DMSO), β-mercaptoethanol, phenylmethylsulfonyl fluride (PMSF), ampicillin (Amp), kanamycin, gentamicin, tetracycline, Bluo-gal and 40μg/ml IPTG, hemin, chloramphenicol (Chl), imidazole, NaCl, cholic acid (sodium), lauric acid, $Na_2MoO_4 \cdot 2H_2O$, and $CaCl_2 \cdot 2H_2O$ were all obtained from Sigma Chemical Co. Phenol, $MgCl_2$, potassium acetate was from Fisher Scientific Equipment. K_2HPO_4, NaCl, NaOH, $NiSO_4$, $CaCl_2$, methanol, glacial acetic acid and chloroform were from Fisher Scientific UK Limited. Tryptone and Yeast Extract were from Difco Laboratories. Glycerol was from Courtin & Warner. KH2PO4, KCl, glycine, EDTA, glucose, bromphenol Blue, ethanol and ammonium sulphate were from BDH. Agarose was from Boehringer Mannheim. Sodium dithionite was from Kodak. 3-[(3-cholamidoprpyl) dimethylammonio]-1-propanesulfonate (Chaps) was obtained from Melford Laboratories (U.K.). [3H]-TCDD (34.7 Ci/mmol) was from Chemsyn Laboratories, and tetrachloroazoxybenzene (TCAOB) was a kind gift from Dr. A.G. Smith, MRC Toxicology Unit, Leicester, UK. 1,4-Dioxane was from Sigma Chemical Co.

NuPAGE Bis-Tris gels with MES or MOPS buffer, and Tricine gels were from Invitrogen. 30% acrylamide/bisarylamide was from Severn Biotech Ltd.

Coomassie Brilliant Blue G was from Aldrich. Hydrochloride acid, Coomassie Brilliant Blue R-250 were obtained from ICN Flow. Tris-base was from Gibco-BRL. PVDF membrane was from Amersham. Marvel was from Premier International Foods (UK) Ltd. Goat Anti-Rabbit secondary antibodies were from Amersham or Bio-Rad. X-ray film was manufactured by Fuji and obtained from Amersham. X-ray film developer and fixer were obtained from Ilford.

PD-10 column was from Amersham Pharmacia Biotech. His.Bind and Ni-NTA His.Bind resin were from Novagen.

1Kb plus DNA ladder were obtained from Gibco-BRL. Low molecular weight protein marker was form Sigma. Oligonucleotides were synthesised by John Keyte of the Biopolymer Synthesis and Analysis Unit, School of Biomedical Sciences, University of Nottingham.

Enzymes:

BamH I, EcoR I, Nhe I, and *Not I;* and T4 ligase and buffer were from New England Biolabs. Shrimp alkaline phosphatase was from USB Corporation. Extensor Hi-Fidelity PCR Master Mix and 1.1x ReddyMix PCR Master Mix (1.5mM MgCl2) were from ABgene. Lysozyme was from Sigma.

Strains and plasmids:

C41(DE3) was gift from John E.Walker (Miroux *et al*., 1996). JM109 were from Stratagene. Plasmids pRSET-c, pFASTBAC-TH, and DH10Bac competent cells were from Invitrogen. Plasmid GEMT-Easy was from Promega. Plasmid pFastBac containing AhR LBD cDNA was a gift from Dr. David R. Bell. The

plasmid pCWori+ containing N-terminally modified 4A1 with six histidine tag at C-terminus was a kind gift from Prof. Paul R. Ortiz de Montellano. The plasmid pRSET-b containing human cytochrome b5 sense cDNA was a gift from Dr. David R. Bell.

Spotoptera frugiperda (Sf9) cells were obtained from TACC. EX-CELL 420 serum free medium was from JRH Biosciences Inc. USA. Grace's insect medium and SF-900II insect medium were from GIBCO. Trypan blue was from Sigma. Low melting agarose was from Bio-Rad. Fatal Calf Serum (heat inactivated) was from Sigma Chemical Co. DH10Bac competent cells and C_{ELL}FECTIN Reagent were from Invitrogen. Recombinant baculovirus-p23 was a kindly gift from Dr. David O. Toft, Department of Biochemistry and Molecular Biology, Mayo Clinic, USA.

Ultra high purity (UHP) grade water (> 13 Mohms/cm3) was produced using a Purite Select Bio system. CE9500 double beam spectrophotometer was purchased from CECIL instrument Ltd. Optima Ultracentrifuge was purchased from Backman, Coulter, USA.

2.2 General molecular biology techniques

2.2.1 Preparation of $CaCl_2$competant *E. coli* cells

A single colony of *E. coli* cells from a freshly streaked LB agar plate was picked and inoculated onto a 5ml LB broth culture. The culture was grown overnight in a shaking incubator at 37˚C. A 100ml culture of LB medium was inoculated with 0.5% (v/v) of the overnight culture of bacteria and grown for about 3.5h. During this time 0.1M $CaCl_2$ was prepared with UHP water and sterilised by filtration. This solution was kept on ice until use. When the cell culture reached an OD_{600} of 0.5-0.6, it was placed on ice for 15 minutes and then centrifuged at 400g for 15 minutes at 4˚C. The supernatant was discarded and the pellet gently resuspended in 10ml of 0.1M $CaCl_2$. Cells were again centrifuged and resuspended as before. Cells were then pelleted once more, the supernatant discarded and the final pellet resuspended in 400µl of 0.1M $CaCl_2$ solution. The cell suspension was then ready for use. Alternatively the cells were resuspended in 400µlof 0.1M $CaCl_2$, 10% glycerol and stored at -80˚C in aliquots of 200µl for later use.

2.2.2 Preparation of electro-competent *E. coli* cells

Bacteria were grown to mid-log phase, chilled, centrifuged as described in Section 2.2.1. After the first centrifugation, the pellet was washed with 50ml of cool UHP water to reduce the ionic strength of the cell suspension. The cells were then pelleted at 400g for 15 minutes at 4˚C, and resuspended in 50ml of cool UHP

water for a further three times. The cell pellet was finally resuspended in 2x volume of cold UHP water. An aliquot of 60µl cell suspension was dispensed into a sterile eppendorf and was then ready for electro-transformation.

2.2.3 Transformation of $CaCl_2$-competent cells

A 100µl aliquot of $CaCl_2$ cells was thawed on ice. 25-50ng of recombinant plasmid DNA was mixed with the cells and incubated on ice for 30 minutes. The cell suspension was then heat shocked at 42˚C for 90 seconds followed by incubation on ice for two minutes. To this a 1ml of LB broth was added and the cells were incubated for 1h at 37˚C. The transferred cells were then plated onto a LB agar plate containing appropriate antibiotic for selection. The plate was incubated at 37˚C overnight.

2.2.4 Transformation of electro-competent cells

Electroporation is a simple but high efficiency method for introducing cloned genes into a wide variety of cells. Electro-competent cells were prepared as described in section 2.2.2. The DNA (10-50ng) or the diluted ligation reaction, in the volume of 10µl was mixed with chilled cell suspension and then transferred to a chilled BioRad Genepulser cuvette. The electroporation was performed with a voltage of 1.8kV using the electroporator. The cells were then resuspended immediately in 1ml of LB broth and incubated at 37˚C for 60 minutes. Transformed cells were then selected by growing the bacteria on LB agar plates containing appropriate antibiotics.

2.2.5 Purification of plasmid DNA by alkaline lysis

1.5ml of overnight bacteria culture was transferred into an eppendorf tube and pelleted at 14000g for 1min. The resulting pellet was resuspended in 100µl of solution I (500mM glucose, 25mM Tris-HCl pH8.0, 10mM EDTA, 100µg/ml RNAse A). To this a 200µl aliquot of freshly made solution II (200mM NaOH, 1% SDS) was added and the tube mixed by gentle inversion for 5-6 times. The tube was set at room temperature for 5min and then 150µl of chilled solution III (5M potassium acetate, 11.5% glacial acetic acid) was added. The tube was immediately mixed by gentle inversion and then placed on ice for 10min to precipitate bacteria genomic DNA. The tube then was centrifuged at 14000g for 10min to remove the precipitated DNA. The resultant supernatant was transferred to a fresh eppendorf tube. This plasmid DNA containing solution is subjected to phenol/chloroform extraction (Section 2.2.6) and ethanol precipitation as described in Section 2.2.7.

2.2.6 Phenol /chloroform extraction of plasmid DNA

The method of phenol chloroform extraction is used to remove protein contamination from DNA samples. Phenol /chloroform (1:1 v/v) in an equal volume was added to the nucleic acid sample and the mixture vortexed. The organic and aqueous phases were separated by centrifugation for 5min at 15000g. The resulting aqueous phase was collected for ethanol precipitation of nucleic acid.

2.2.7 Ethanol or isopropanol precipitation of nucleic acid

These methods were used to concentrate the DNA solution of interest. Two volumes of absolute ethanol or one volume of isopropanol, and 1/4 volume of 3M-sodium acetate (pH5.2) were added to the DNA sample. The solution was mixed and kept on ice for 30min to precipitate the nucleic acids. The mixture was then centrifuged at 14000g for 30min. The pellet was then washed with 500µl of 75% ethanol and plleted again. The resulting DNA pellet was air dried and redissolved in an appropriate buffer at desired concentration.

2.2.8 Purification of plasmid DNA on Qiagen Mini prep columns

A small-scale sequence grade DNA sample was prepared using Qiagen Mini prep columns according to manufacturer's instruction. From 3ml of overnight bacteria culture the cells were pelleted by centrifugation at 14000g for 1min and resuspended with 0.3ml of buffer P1 (50mM Tris-HCl pH8.0, 10mM EDTA, 100µg/ml RNAse A). To this 0.3ml of buffer P2 (200mM NaOH, 1%SDS) was added with gentle mixing by inversion for 5-6 times. This mixture was incubated at room temperature for 5min, followed by addition of 0.3ml of chilled buffer P3 (3M-potassium acetate pH5.5). The tube was placed on ice for 10min and centrifuged at 15000g for 15min. Meanwhile a Qiange-tip 20 was equilibrated with 1ml of buffer QBT (750mM NaCl, 50mM MOPS pH7.0, 15% ethanol, 0.15%Triton X-100). The resulting supernatant was carefully transferred onto the Qiagen column and allowed to pass through. The column was then washed 4

times with 1ml of buffer QC (1.0M NaCl, 50mM MOPS pH7.0, 15% ethanol). The plasmid DNA was then eluted from the column using 0.8ml of buffer QF (1.25M NaCl, 50mM Tris-HCl pH8.5, 15% ethanol), and the flow-through collected in a clean appendorf tube. The elution was precipitated in 0.7 volume of isopropanol and incubated at room temperature for 20min. The solution was centrifuged at 15000g for 30min to pellet the DNA. The DNA pellet was then washed in 0.5ml of 70% ethanol and pelleted again. The resulting DNA pellet was air dried and redissolved in 30µl of appropriate buffer.

2.2.9 Quantitation of DNA

For quantitation the amount of DNA, readings should be taken at wavelengths of 260 and 280nm. A 5µl aliquot of DNA solution was diluted in 1ml of UHP water and transferred into a crystal cuvette. The absorbance of this solution was measured at 260nm in a spectrophotometer A solution containing 50µg of double-stranded DNA has an absorbance of 1 at 260nm, i.e., A_{260}=1=50µg/ml of double-stranded DNA. The ratio between the readings at 260 and 280nm provides an estimate of the purity of the nucleic acid. Pure preparation of DNA has OD_{260}/OD_{280} value of 1.8.

2.2.10 Restriction digest of plasmid DNA

A restriction digest was performed in a 30µl reaction volume, for a typical reaction containing 0.2-1 µg of DNA, at 37˚C for 1h. The reaction system normally contains 1-5µl of DNA sample, 1µl of restriction enzyme, 3µl of the

appropriate 10x restriction enzyme buffer and UHP water making up to 30µl. After incubation at 37˚C for 1h the reaction was terminated by either ethanol precipitation of the digested sample (Section 2.2.7) or addition of 10x loading buffer (30%glycerol, 0.25% bromophenol blue, 0.25% xylene cyanol).

2.2.11 Polymerase chain reaction (PCR)

The polymerase chain reaction (PCR) is used to amplify a segment of DNA that lies between two regions of the known sequence. Two oligonucleotides are used as primers for a series of synthetic reactions that are catalyzed by a DNA polymerase. PCR was performed using 25µl 1.1x ReddyMix ^{TM}PCR Master Mix (1.25 units *Taq* DNA polymerase, 75mM Tris-HCl pH 8.8, 20mM $(NH)_4SO_4$, 1.5mM $MgCl_2$, 0.01%(v/v) Tween 20, 0.2mM each of dATP, dCTP, dGTP and dTTP, precipitant and red dye for electrophoresis), 1µl 5'- primer (~70ng), 1µl 3'- primer (~70ng) and 1µl template DNA. A negative control was set up by using the same materials as above but substituting the DNA template with 1µl of UHP water. The PCR reaction was overlaid with 50-100µl of mineral oil to prevent the reaction from evaporation. PCR was performed in a Perkin Elmer DNA Thermal Cycle 480 for 25 cycles at 45 sec denaturing at 94˚C, 1 min 50 sec annealing at 66˚C and 1 min 50 sec polymerization at 72˚C. The final cycle consisted of an extension cycle of 5 min at 66˚C followed by 10 min at 72˚C. PCR products were then analyzed by agarose (TBE) gel electrophoresis along with standard DNA marker and negative control.

2.2.12 Alkaline phosphate treatment of DNA

Shrimp Alkaline phosphatase (SAP) catalyzes the removal of 5'-phosphates from fragments of DNA to prevent self-ligation. In an eppendorf tube, to 10µl of restriction digested DNA 1µl of shrimp alkaline phosphatese (10,000u/ml) and 9µl of UHP water was added to give a total volume of 20µl. The mixture was incubated at 37˚C for 35 min. To this a 2µl of 10x NE buffer 3 was added and followed by a further incubation of 30 min at 37˚C. The reaction was terminated by heating to 75˚C for 10 min in the presence of 5mM EDTA to inactivate the SAP. The resulting DNA product was subjected to ethanol precipitation (Section 2.2.7) and resolved by running a SYBR Green gel (Section 2.2.13)

2.2.13 Agarose gel electrophoresis

DNA was separated by agarose gel electrophoresis. The electrophoresis was performed using a Pharmacial GNA-100 gel electrophoresis kit. Agarose was dissolved in 10ml of 1x TBE buffer (45mM Tris-HCl, 44mM Boric acid, and 2mM EDTA, pH8.0) to give a gel in the range of 0.7-2% (w/v). For the purpose of the gel excision of DNA, 1x TAE buffer (40mM Tris-HCl, 1mM EDTA and 5.71%glacial acetic acid) was used. The dissolved agarose was melted by heating in a microwave and allowed to cool to about 60˚C. An aliquot of ethidium bromide (10mg/ml in stock) was added into the agarose to give the final concentration of 0.2µg/ml. The gel was immediately poured into the gel casting mould, which containing a well forming comb, and allowed to harden for 30min. When the gel had hardened it was put into the electrophoresis tank containing

appropriate running 1x buffer (TAE/TBE) and the comb removed. An aliquot of DNA sample was mixed with 10x loading buffer (30%glycerol, 0.25% bromophenol blue, 0.25% xylene cyanol FF). Aliquots of standard DAN marker (1Kb plus) and DNA samples to be run were loaded into the wells. The samples were run at 90V for 1h. The DNA bands were visualized under UV light.

2.2.14 DNA purification by QIAEX II Gel Extraction Kit

QIAEX II Gel Extraction Kit was used to extract and purify DNA from any agarose gel in either TAE (Tris-acetae/EDTA) or TBE (Tris-borate/EDTA) buffer. The QIAEX II contains silica particles, to which DNA fragments bind free of contamination. The extraction was performed according to the manufacturer's introduction, i.e., the DNA band of interest was excised from the agarose gel with a clean, sharp scalpel. The gel slice was transferred into a clean eppendorf tube and weighted. The gel slice was then immersed in 3 volume of buffer QX1 (w/v). To each 2-10μg DNA a further aliquot of 30μl of pre-resuspended buffer QIAEX II was added. The tube was then incubated at 50˚C for 10 min to solubilize the agarose and bind the DNA to the silica particles. During the incubation the tube was vortexed every 2 min to keep QIAEX II in suspension. After the incubation the sample was centrifuged for 30 sec at 15000g and the supernatant removed. The resulting pellet was resuspended by vortexing with 500μl of buffer QX1 to remove residual agarose contaminant. The sample was pelleted again and washed twice with 500μl of buffer PE to remove residual salt contaminants. After being washed the sample was centrifuged for 30 sec at 15000g and all traces of supernatant removed. The pellet was air dried for about 30 min. To this a 10μl of

10mM Tirs-HCl, pH8.0 was added and resuspended by vortexing. The sample was incubated at room temperature for 5-10 min to elute the DNA from the silica complex. The tube was then centrifuged for 30 sec at 15000g. The resulting supernatant containing purified DNA was carefully transferred to a clean eppendorf tube and was stored at -20˚C.

2.2.15 Ligation of DNA

Bacteriophage T_4 DNA ligatase catalyzes the formation of phosphodiester bonds between adjacent 3'-hydroxyl and 5'-phosphate termini in DNA. The ratio of vector DNA to insert DNA is important when performing a ligation reaction. Therefore triplicate reactions were prepared as follows: the vector and insert DNA are in a 1:1, 1:2 and 2:1 ratio. The reaction took place in a total of 10µl volume in an eppendorf tube. In the case of 1:1 ratio, 2µl of vector DNA, 2µl of insert DNA, 2µl of ligatse, 1µl of 10x T_4 buffer (250mM Tris-HCl pH7.6, 50mM ATP, 5mM DTT, 25%(w/v) PGE-8000) and 3µl of UHP water were mixed and spun down for 10 sec. The tube was then incubated overnight at room temperature. This product was used directly for transformation into competent cells.

2.3 Protein methodologies

2.3.1 Bradford protein assay

Bradford assay was used to determine the quantity of the protein ranging from 0-30µg. Bradford reagent is comprised of 100mg Serva blue G dissolved in 100 ml

of 85% phosphoric acid and 50ml of 95% ethanol, made up to 1 litre. Bovine serum albumin (BSA) was usually used as a standard. 50µl of serially diluted BSA standard solution (0µg, 5µg, 10µg, 15µg, 20µg and 30µg) was added to 50µl of 1M NaOH. To this 1000µl of Bradford reagent was added. The assay solution was incubated at room temperature for 5 minutes. Absorbance was read at 590nm in a polystyrene cuvette. UHP water with 50µl of 1M NaOH and Bradford reagent was used as a reference. Standards were in triplicate and means determined. Based on the resultant linear plot, a linear regression was carried out on a spreadsheet. Linear regression was used on the sample readings so that unknown protein sample concentrations could be calculated. Only standard curves that gave rise to R^2>0.95 were used.

2.3.2 Tricine SDS-PAGE

Precast Novex Tricine gel (Invitrogen™) was used for peptides and low molecular weight proteins. Tricine SDS-PAGE was performed according to manufacturer's instruction. That is: the precast Tricine gel was assembled into a Bio-Rad Mini-cell electrophoresis kit. The appropriate amount of Tricine running buffer (Tris Base 12.1g, Tricine 17.9g SDS 1g, distilled water to 1 litre) was filled into the buffer chambers. Protein samples were diluted 1:1 using 2X Sample buffer (900mM Tris-HCl (pH8.45), 24% glycerol (w/v), 8%SDS (w/v), 0.015% Coomassie blue G (w/v), 0.005% phenol red (w/v), and 2% DTT (w/v) was added prior to use). Samples were then heated at 85˚C for 2 minutes to denature the proteins. 10-30µg of proteins were loaded into the wells. The gel was run at 125V for 1.5h or until the blue dye had reached the bottom of the gel. When the run was

complete, the gel cassette was separated with the gel knife and the gel removed. The gel may be fixed, stained with Coomassie blue stain solution.

2.3.3 Silver staining

Silver staining is 30-50 fold more sensitive than Coomassie Blue staining and will detect nanogram quantities of protein. The basic mechanism occurring in the silver staining of macromolecular is the reduction of ionic to metallic silver. Protein bands imagined in the gel due to differences in oxidation/reduction potentials between sites in gels occupied by protein and adjacent sites not occupied by protein. Silver stain was performed using Silver Stain Plus Kit according to manufacturer's instruction. That is, after gel electrophoresis (Section 2.3.2), the gel was fixed in the Fixative Enhancer Solution (reagent grade methanol 50%, reagent grade acetic aced 10%, fixative enhancer concentrated 10% and deionized distilled water 30%) for 20 minutes. The gel was then rinsed with distilled water twice followed by staining in the freshly prepared staining solution. The gel was left to soak in the stain for 15 to 20min until the clear bands were seen. The staining was stopped by replacing the staining solution with the stop solution (5% acetic acid in deionized water) for a minimum of 15min. After stopping the reaction the gel was rinsed in high purity water for 5min. The gel was then ready to be dried or photographed.

2.3.4 Western blotting

Western blot is used to detect specifically trace proteins on an immobilizing membrane and therefore enables further characterization.

The protein was separated by SDS-PAGE (Section 2.3.2), and the gel was transferred onto two pieces of 3MM Whatman blotting paper pre-soaked in transfer buffer (25mM Tris-HCl, 192mM glycine, 20% methanol (v/v) and 0.1%SDS (w/v)). A piece of PVDF filter pre-soaked with 100% methanol was layered over the gel, avoiding any air bubbles trapped between the gel and the PVDF filter sheet. Two more pieces of Whatman paper were placed over the top of the PVDF filter sheet and the resulting 'sandwich' was encased in an Electro-transfer cassette. The cassette was placed into the transfer tank filled with transfer buffer and the transfer was performed at 4˚C and at 90V for 1 hour. When transfer was completed, the PVDF filter was blocked in blocking solution (10% marvel (w/v) in Tris buffered saline (TTBS: 20mM Tris pH7.5, 500mM NaCl and 0.1% Tween) with gentle shaking for 1 hour or overnight. The blot washed three times for 5 minutes per wash in TTBS, and then incubated in primary antibody solution in marvel-TTBS for 1 hour with gentle rocking. To remove the excess antibody, the blot was washed three times for 5 minutes per wash in TTBS. The blot was incubated in Anti-Rabbit secondary antibodies solution diluted in marvel-TTBS for 1 hour with gentle rocking followed by three times wash for 5 minutes per wash TTBS. The blot was developed using the ECL Western Blotting Detection Reagents for 1 min. and then removed from the solution and wrapped in cling film. The blot was put into a film case and brought to the dark room. A sheet of Kodak film (Kodak Bio Max Film) was overlaid on the blot. The film was

exposed for different lengths of time (6, 10, and 15 minutes) and then developed and fixed.

2.3.5 Protein desalting by PD-10 columns

Size exclusive PD-10 column was used to remove low molecular weight substances (Mr<1000) from high molecular ones and to exchange buffers. According to manufacturer's instruction, 2.5 ml of sample was loaded onto PD-10 column pre-equilibrated with 25ml of appropriate equilibrium buffer. When the sample had run into the column, high molecular components (Mr>5000) were eluted with 3.5 ml of equilibrium buffer and eluate collected and assayed.

2.3.6 Chromatography on Ni-NTA His-Bind Resin

Nickel affinity chromatography was performed according to manufacturer's instruction. Ni-NTA His·Bind resin was pre-equilibrated by mixing one volume of the resin with four volumes of bind buffer, and allowed to settle by gravity. The supernatant was removed. Prior to application the protein extract to the resin, the sample was subjected to desalting and buffer exchange using a size exclusive PD-10 column (Section 2.3.5). The protein extract was then mixed with the resin by gentle agitating on ice for 1 hour. The protein-Ni-NTA Resin mixture was then loaded on to a column. The column was washed with 10-bed volume of wash buffer followed by elution with elute buffer. The eluate was collected and analysed by spectrophotomery and SDS-PAGE for protein purity.

2.3.7 Ion exchange chromatography on Uno Q1 column

Prior to application of the protein extract to an Uno Q1 column, the sample was concentrated and desalted in an Amicon stirring cell using YM membrane at 30-40 psi of pressure. The chromatography was performed according to manufacturer's description. The Uno Q1 column was pre-equilibrated with start buffer for 20 minutes at a flow rate of 1ml/minute. The sample was then loaded to the column at the same flow rate. From this point, the column flow-through was collected in 1ml batches and aliquot analysed by SDS-PAGE. The column was washed with start buffer for 20 minutes. The bound protein was then eluted with linear gradient of 100% start buffer to 100% elute buffer (start buffer plus 0.4 M NaCl) in 15 minutes at the same flow rate. Fractions containing purified protein confirmed by spectrophotometry and SDS-PAGE were pooled for further assay.

2.4 Expression of cytochrome b5 in *E.coli*

2.4.1 The structure of plasmid

The plasmid pRSET-b was used to express the recombinant cytochrome b5. The human cytochrome b5 cDNA, which encodes 134 amino acids, was previously subcloned in the *EcoR I* site of pRSET-b in our laboratory (Minqi Fan). The N-terminal fusion peptide in the pRSET-b contains 44 amino acids including a six-histidine tag. Therefore the whole cytochrome b5 fusion protein contained 178 amino acids with a molecular mass of 20,196 Da. The map of pRSET-b b5 is shown in Figure 2-1.

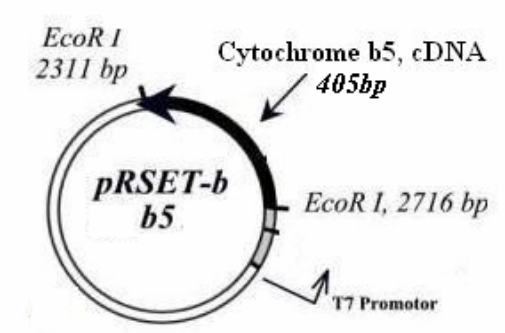

Figure 2- 1. Diagram of plasmid pRSET-b·b5.
Cytochrome b5 cDNA (black filled part) was inserted in the *EcoR I* site of pRSET-b plasmid. The arrow showed the orientation of cytochrome b5. The N-terminal fusion peptide including a six-histidine tag in plasmid pRSET-b (grey filled part) is positioned upstream of cytochrome b5.

2.4.2 Expression of cytochrome b5

Bacteria C41(DE3) was used to produce b5. pRSET-b5 was transformed into C41(DE3) (Section 2.2.3). Transformants were selected by ampicillin resistance. Growth and protein production conditions were optimised to give the highest level of cytochrome b5 expression. In a typical induction, a single colony of C41(DE3)/pRSET-b5 was grown overnight in 2ml LB medium containing 100μg/ml ampicillin and 100μg/ml δ-ALA. The culture, at 0.5% (v/v), was inoculated into 100ml TB medium in the presence of 100 μg/ml ampicillin and 100μg /ml δ-ALA. The inoculum was cultured at 28°C with a 120rpm shaking speed for 6-8 hours to an OD_{600} of between 0.6-0.8. At this point, IPTG was added to induce expression of b5. Induction was for 24 hours. The shaking speed was kept at 120rpm.

2.4.3 Recovery of microsomes

The cells were harvested by centrifugation at 10,000 g for 15 minutes at 4°C. The cell pellet was weighed and resuspended at 70mg/ml of pre-chilled Buffer A (100mM Tris acetate pH7.6, 50mM sucrose and 0.5mM EDTA). The cell suspension was kept on ice for 20-30 minutes and an equal volume of ice-cold water with 0.1mg lysozyme/ml was added. This mixture was incubated on ice for 30 minutes with occasional agitation followed by centrifugation at 10,000 g for 10 minutes at 4°C. The resultant spheroplast pellet was resuspended with 5 ml of ice cold Buffer B (10%w/v glycerol, 20mM Tris-HCl pH8.0, 50mM NaCl and 1mM DTT) supplemented with a protease inhibitor tablet. The bacteria were then sonicated on ice (pulse on 30 seconds, off 30 seconds) 8 times using a Bandelin Eletronic Sonicator at 35% maximum power. Immediately after sonication, an aliquot of hemin (0.7mM/100 ml culture) was added to the suspension to reconstitute the expressed apo-b5. This mixture was centrifuged at 10,000 g for 15min. to remove cell debris. The resulting supernatant was collected and recentrifuged at 110,000 g for 25 minutes at 4°C in a Backman Ultracentrifuge to pellet the microsomes.

The recovered microsomes were resuspended with Buffer C (20mM Tris-HCl pH8.0, 20% glycerol, 10mM NaCl) and solubilized with CHAPS (final concentration of 1%). The solubilized b5 solution was centrifuged at 110,000 g for 25 minuets to remove insoluble debris. The resulting supernatant was collected and b5 content measured.

2.4.4 Measurement of b5

The content of b5 was measured by spectrophotometry (Holmans, Shet et al. 1994). An aliquot of b5 fraction was diluted in 2ml of 0.1M potassium phosphate (pH 7.5). The diluted suspension was divided equally into two cuvettes. The cuvettes were placed in the cell compartment of a CECIL CE9500 spectrophotometer connected to an IBM computer. The baseline was recorded by scanning samples from 400nm to 600nm. A few grains of sodium dithionite were then added to the content of the sample cuvette to reduce b5. The difference spectrum between two cuvettes was scanned again from 400nm to 600nm and recorded. To calculate the content of b5 in solution, a millimolar extinction coefficient of 118 was applied for the absorbance difference at 423.5 and 490 nm(Holmans, Shet et al. 1994).

2.4.5 Purification of b5

The solubilized b5 was purified using nickel affinity chromatography followed by ion exchange chromatography on Uno Q1 column. All chromatography steps were carried out at 4ºC. The chromatography on nickel affinity resin was performed as described in Section 2.3.6. The resultant eluate containing b5 were pooled for further purification.

The chromatography on Uno Q1 column was performed as described in Section 2.3.7. The resultant fractions containing b5 were confirmed by 15% SDS-PAGE, and were pooled and concentrated using an YM-10 Amicon filter. The concentrated sample was diluted fourfold with buffer D (20mM $NaPO_4$, 1mM

EDTA, 0.4% Na deoxycholare) and concentrated again to remove any salt in the sample. The purified cytochrome b5 was stored at –80ºC for further use.

2.5 Expression of AhR LBD in *E. coli.*

A mouse AhR LBD construct, 5g (mAhR residues 285-416) was cloned into the plasmid pRSET-c (a gift from Dr. David R. Bell), and expressed in BL21 (DE3)pLysS.

2.5.1 The structure of plasmid

The structure of plasmid pRSET-5g was shown in Figure 2-2. The 5g cDNA was inserted in the *BamH I* site of pRSET-c, downstream of the T7 promoter. The AhR DNA was jointed to the leader sequence in the pRSET plasmid at 5'-terminus (Figure 2-2), and this then encoded for a 19,267 Da protein (pI=7.69)

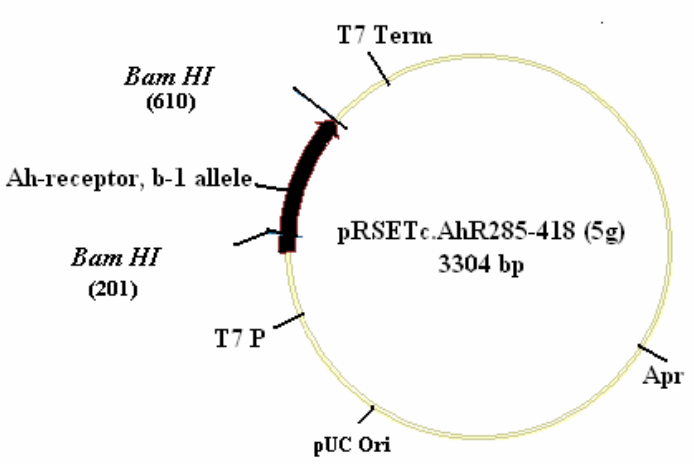

Figure 2- 2. Diagram of pRSETc-AhR286 (5g)
The AhR285 cDNA fragment (filed black) was inserted in the *BamH I* site. T7 promoter and terminator are labelled. The Amp resistance gene and Ori gene from pUC are labelled. The orientation of the AhR is shown with the arrow.

2.5.2 Expression of 5g in *E. coli*

The plasmid 5g was transformed into BL21(DE3)pLysS as described in Section 2.2.4. Transformants were selected by ampicillin resistance. Bacteria containing plasmid 5g were streaked to purity, and then cultured at 37ºC in LB containing 100μg/ml ampicillin and 34μg/ml chloramphenicol for 5-7 hours with vigorous shaking. The culture was diluted 50-fold in LB containing 100μg/ml ampicillin and 34μg/ml chloramphenicol. The bacteria were then grown at 37ºC in the shaking incubator to an OD_{600nm} of between 0.4-0.8. At this point, 1mM IPTG was added to induce expression. Induction was for 2 hours at 37ºC, and the shaking speed was kept at 220rpm.

2.5.3 Purification of 5g

The cells were harvested by centrifugation at 4,000 g for 20 minutes at 4ºC. the cell pellet were resuspended in 20ml of Buffer A (0.1mM Tris.HCl, pH 7.5, 0.5 mM EDTA, pH 8.0, 20% glycerol (v/v), 100μM PMSF, 0.1mM DTT and 10μg/ml apotinin). Lysozyme was added to 0.5mg/ml final concentration and incubated on ice for 1 hour. The solution was then centrifuged at 4,000 g for 30 minutes, and the pellet was resuspended in 10ml of sonication buffer (10mM Tris.HCl, 0.1 mM EDTA, pH8.0, 10% glycerol, 100μM PMSF, and 10μg/ml apotinin). The bacteria were then sonicated on ice (pulse on 30 seconds, off 30 seconds) 8 times using a Bandelin Eletronic Sonicator at 35% maximum power. The sonicated cells were centrifuged at 12,000 g for 20 minutes. The supernatant containing soluble protein

was stored at -80ºC for later examination. The pellet containing inclusion body was resuspended in 10ml of denaturing bind buffer (6M guanidine-HCl, 0.1M NaN_2PO_4, 0.01M Tris.HCl, pH8.0). The solution containing solubilized protein was centrifuged at 12,000 g for 20 minutes to remove the debris. The supernatant was collected and diluted by an equal volume of ice-cold water.

The recombinant protein was purified by nickel affinity chromatography as described in Section 2.3.6. The purity of the eluate was analysed by SDS-PAGE.

The purified 5g protein was used to generate the AhR specific polyclonal antibody from a rabbit. The antisera was produced and the titration determined.

2.6 Baculovirus methodologies

The recombinant protein was expressed in *Spotoptera frugiperda* (Sf9) cells infected with a recombinant baculovirus.

2.6.1 *Spotoptera frugiperda* (Sf9) cell culture

2.6.1.1 Setting up a monolayer culture

Cryopreserved Sf9 cells in a cryovial were removed from liquid nitrogen and thawed rapidly at 37˚C. The cells were transferred to a "T"-flask (25-cm^2) containing 4 ml pre-warmed SF-900 II Serum-Free medium. A minimal viable cell density of $5x10^5$ cells/ml was inoculated. The cells were cultured at 27˚C±1˚C in a cell culture incubator for 1h, and allowed to adhere to the plastic. The culture medium was then removed and exchanged with fresh medium to reduce the

DMSO present in cryopereservation medium. The culture was then returned to the cell culture incubator allowing cells to grow for 3-4 days. When the cells reached 80%-90% confluence, subculture was performed. Cells were seeded at the density between $5x10^5$ to $10x10^5$ cells/ml for two subcultures after recovery, and then returned to the normal maintenance schedule.

To maintain a monolayer culture, the cells from an 80% to 90% confluent monolayer were detached with a sterile cell culture scraper. The detached cells were counted for their viability (Section 2.6.1.3). To each 25-cm^2 flask, 4ml of cell suspension at the density of $3x10^5$ –$5x10^5$ cells/ml was seeded. The culture was incubated at 27˚C with a loose cap to allow gas exchange. The cells were subcultured when the monolayer reached 80% to 90% confluence, approximately 3 to 5 days post-planting.

2.6.1.2 Cryopreserving cells

Cryopreserving, or cell banking, is the freezing and storing of culture cell stocks. This makes it possible to maintain culture resources over a period of time.

When cells reached exponential growth and more than 98% were viable, the cells were harvest by centrifugation at 1,000g, for 5 minutes. The supernatant was discarded and the cell pellet resuspended with ice-cold cryopreservation medium (7.5% DMSO, 10% BSA in SFM 900 II medium) at the cell density of $1x10^7$ to $2x\ 10^7$viable cells/ml. An aliquot of cell suspension was dispensed into cryovials and kept on ice for 30min and -20˚C for 1 h and placed at -80˚C overnight. The cryovials containing cryopreserved cells were then transferred into a liquid nitrogen storage tank.

2.6.1.3 Viable cell count determination

The viable cells were determined by using a haemocytometer in conjunction with a vital stain (e.g. 0.4% Trypan blue). The haemocytometer and coverslip were thoroughly cleaned and wiped both with 70% alcohol before use. The coverslip was moistened and placed centrally over the counting area and across the grooves. An aliquot of the cell suspension was transferred into an eppendorf and diluted 1:1 in trypan blue (0.4% Trypan blue in PBS). The mixed cell solution was added into the junction between chamber and the coverslip. The viable and nonviable cells in the same 1mm^2 area were counted under a light microscope at low magnitude. The number of viable cells/ml was calculated using the following equation:

Viable cells/ml =(Total number of viable cells counted/ number of 1 mm^2 areas counted) x 2 x 10^4

2.6.1.4 Adapting cells to a new medium

During the adaptation of insect cells to a new medium, insect cells tend to stick together and aggregate, this can make obtaining accurate cell counts nearly impossible and lead to inconsistent cell growth and protein expression. The method used can shorten the adapting process.

An appropriate amount of medium, that is 25% new medium (NM) and 75% old medium (OM), was prepared. The cells were split into this medium at a density of 6 x 10^5 cells/ml. The cells were allowed to grown to the usual high density (5 x 10^6/ml) and growth parameters monitored (Section 2.6.1.6). The cells were

continuously cultured under this condition until the growth parameters were within an acceptable range. The cells were then split into a medium with 50% NM plus 50% OM, and proceed as before. This process was continued by gradually reducing the component of OM in the culture, until cells have stabilized in the new medium.

2.6.1.5 Maintaining suspension culture

The cells were seeded at approximately $5x10^5$ viable cells/ml in serum-free growth medium in a 125ml disposable Erlenmeyer flask. To aerate the cultures the cap was loosed about 1/4 to 1/2 of a turn. Cells were incubated at 28±0.5ºC with a stirring rate of 120 rpm and subcultured when the viable cell count reaches $3x10^6$ to $5x10^6$ cells/ml (4 to 5 days post-plating). Once every 3 weeks, the cell suspension was gently centrifuge at 100x g for 5 min., and the cell pellet was resuspended in fresh medium to reduce the accumulation of cell debris and metabolic by-products.

2.6.1.6 Determinations of cell growth data

To collect information on the log phase growth characteristics of a cell line, cells must be subcultured at regular intervals and when the culture is in the log phase of the growth. To do this Sf9 cells from a 2-day old suspension culture were subcultured at a density of 5.5×10^5 cells/ml in fresh medium in a sterile Erlenmeyer flask. The cells were cultured in an incubator at 28±0.5ºC with a stirring rate of 120 rpm. Cell counts were performed every 24h post-planting by

dye exclusion (Section 2.6.1.3). By keeping accurate cell count records, cell growth curve can be generated, and population doubling level and population doubling time can be calculated as follows.

Population doubling level (PDL): the number of generations the cell line has undergone, is the number of population doublings (n).

$2^n = N_H/N_I$ or: $n \log 2 = \log(N_H/N_I) = \log N_H - \log N_I$

so $n = 3.32(\log N_H - \log N_I)$

Where N_H is the number of the cells harvested at the end of the growth period, and N_I is the number of the cells inoculated.

Multiplication rate and population doubling time: multiplication rate (r) is the number of generations that occur per unit. Population doubling time (PDT) is the time taken for the number of cells to double, and is the reciprocal of the multiplication rate (i.e. 1/r). Therefore,

$r = 3.32(\log N_H - \log N_I)/(t_2 - t_1)$ (generations per hour)

PDT= 1/r (hours per doubling)

In practice PDT is used as an estimate of cell cycle time and to determine the length of the phase of the cell cycle.

2.6.2 Expression of AhR LBD in insect cells

2.6.2.1 Structure of donor plasmid pFASTBAC HT-AhR LBD

The plasmid pFASTBAC was used as a donor plasmid for trasposition of the AhR construct into bacmid DNA. Four truncated constructs of the b-1 allele of the mouse Ah receptor, AhR228 (residuals 228-416), AhR265 (residuals 265-416), AhR286 (residuals 286-416), and AhR410 (residuals 286-410) were previously cloned in the *BamHI* site of either pFASTBAC HT b or c vector. As a representative, Figure 2-3 shows the structure of pFASTBAC-AhR228.

The presence of the AhR constructs in pFASTBAC could be revealed by restriction digest with *BamHI* as described in Section 2.2.10.

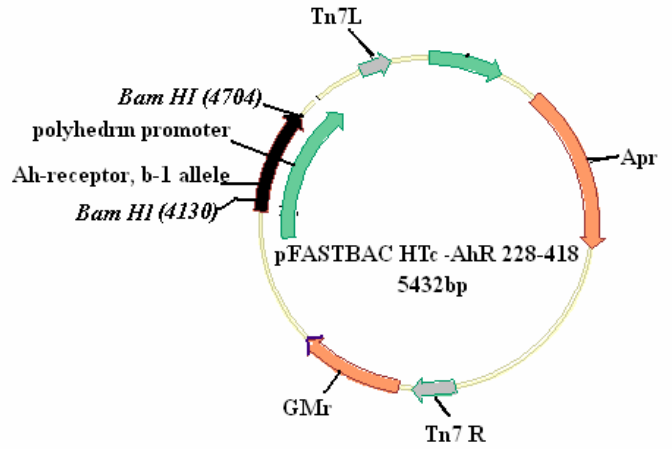

Figure 2- 3. Diagram of pFASTBAC HTc-AhR228.
Mouse Ah-receptor b-1 allele was inserted into pFASTBAC HTc vector down stream of virus polyhedrin promoter. The black filled arrow shows the orientation of the AhR228 flanked by site-specific transposition element Tn7L and Tn7R (gray filled part). The positions of ampicillin resistance (Apr), Gentamicin resistance (GMr) in pFASTBAC HTc were labeled. The positions of *BamHI* site in pFASTBAC HTc and in AhR228 were labeled. The fragments of digestion with *BamHI* for sense is 574bp

2.6.2.2 Generation of recombinant bacmid

When the orientation of the inserted constructs have been determined to be correct, the DNA was transformed into DH10Bac cells for transposition into the bacmid. Transposition was performed according to manufacturer's protocol, i.e., DH10Bac frozen competent cells were thawed on ice and 60µl aliquot of the cells dispensed into a 1.5ml eppendorf pre-chilled on ice. To this 1µl of diluted (1:10) recombinant pFASTBAC donor plasmid DNA was added and gently mixed. This mixture was incubated on ice for 30 min, followed by heat shock at 42ºC for 45 sec. The tubes were chilled on ice for 2 min and 940µl aliquot of S.O.C. medium was added into each tube. The resulting cell suspension was incubated at 37°C for 3 hours, and the cell cultures were spread on LB agar plates (containing 50µg/ml kanamycin, 7µg/ml gentamicin, 10µg/ml tetracycline, 100µg/ml Bluo-gal and 40µg/ml IPTG). The plates were incubated for 48 h at 37°C. The recombinant bacmid colonies were selected by antibiotics and blue white screening. White colonies containing recombinant bacmid were distinguished from the wild blue ones.

2.6.2.3 Isolation of recombinant bacmid DNA

A single isolated recombinant bacterial colony was picked up and inoculated into 2 ml LB medium supplemented with 50µg/ml kanamycin, 7µg/ml getamicin, 10µg/ml tetracycline. The cells were grown at 37°C for 24 hours with shaking at

250rpm. 1.5 ml of cultured cells was transferred into a clean eppendorf tube and the cells were pelleted by centrifugation. The resulting cell pellet was resuspended in 0.3 ml of solution I (15mM Tris-HCl pH8.0, 10mM EDTA, 100μg/ml Rnase A). To this 0.3 ml of solution II (0.2N NaOH, 1% SDS) was added with gentle mixing. The tube was incubated at room temperature for 5 min followed by slow addition of 0.3ml of potassium acetate (3M, pH5.5). The mixture was placed on ice for 5 to 10 min. The sample was then centrifuged for 15min at 14,000g and the resulting supernatant was transferred to another tube containing 0.8 ml isopropanol. This tube was gently inverted a few times to mix and placed on ice for 5 to 10 min, followed by centrifugation for 15 min at 14,000g. After centrifugation the supernatant was removed and the DNA pellet was washed with 0.5ml of 70% ethanol. The DNA was then pelleted again by centrifugation for 5 min at 14,000g. The resulting pellet was air dried at room temperature for 5-10min. The DNA was dissolved in 40μl TE (pH8.0). The DNA solutions were stored at -20°C. However, repeated freeze-thaw cycles should be avoided to avoid a drastic reduction in transfection efficiency.

2.6.2.4 PCR analysis of recombinant Bacmid DNA

The bacmid DNA is over 135 kb. Verification of the insertion of DNA of interest is difficult using classical restriction endonuclease digest analysis. Therefore, the bacmid containing AhR were confirmed by PCR analysis (Section 2.2.11). The oligonucleotide sequences used for amplifying the AhR insert were as follows:

OL292: GGTTGTGATGCCAAAGGGCAGC;

OL400: CAACACCTCTCCGGTAGC;

OL282: AAAACTTCATCTTCAGGATCCAACACAAGCTA-GAC;

OL410: AGAAAGGGCTGGGATCCCCTACAACACAGCCTCT.

2.6.2.5 Generation of recombinant baculovirus

Recombinant bacmid DNA was trasfected into insect cells using liposome reagent, C_{ELL}FECTIN Reagent according to manufacturer's protocol. That is: monolayer Sf9 cells were grown exponentially in EX-CELL 420 serum free medium. The cells were harvested and diluted to a viable density of 9 x 10^5 cells/ml. In a 6-well tissue culture plate, 2ml cell suspension per well was seeded. In two sterile eppendorf tubes, solutions A and B were prepared for each transfection. Solution A contained 3-5µg recombinant bacmid DNA diluted in 100µl medium. Solution B contained 3-4µl C_{ELL}FECTIN Reagent diluted in 100µl medium. The solution A was then added to the tube containing solution B with gentle mixing. The resultant mixture was incubated at room temperature for 15-45 minute, followed by addition of 0.8ml of EX-CELL 420 with gentle mixing. The medium in each well of a 6-well plate was exchanged with diluted lipid/DNA complex and the cells were incubated in this lipid/DNA complex for 5 hours at 27ºC. At the end of the incubation, the transfection mixture was removed and replaced with 2ml of EX-CELL 420 medium. The plate was incubated at 27ºC in a humid box. On day 5-10 post-transfection the cells were evaluated under the microscope. When an obvious cytopathic effect was observed (about 7-10 days), the virus containing cell culture medium was harvested centrifugation of the medium at 500x g for 5 minutes. The clarified supernatant was transferred into

another sterile tube and stored at 4ºC, protecting from light. The titre of the virus was determined by plaque assay.

2.6.2.6 Virus plaque assay

Plaque assay can be used to plaque purifying virus or to determine viral titre in plaque-forming units per ml (pfu/ml).

Monolayer Sf9 cells were grown exponentially and harvested. The cells were seeded at a viable density of $1x10^6$ cells/well in a 6-well tissue culture plate. The plate was incubated at 27ºC for at least 1 hour, to allow the cells to attach. Meanwhile the virus to be titred was diluted in 1 ml aliquots to serial dilutions of 10^{-4}, 10^{-5}, 10^{-6}, $10^{-7,}$ and 10^{-8}. After the cells had attached well to the plates, the medium was removed from the dish and replaced with 0.5 ml of virus dilution to each appropriate well. The plate was incubated at room temperature for 3-4 hours with gentle rocking.

During this time the plaque agarose was prepared. The low melting agarose was dissolved in UHP water to give a final equivalent to 3% (w/v), and sterilized by autoclaving. The melting agarose was placed in water bath at 70˚C. The plaquing overlay was prepared before the end of the cell incubation by mixing (1:1 v/v) of 3% low melting agarose with pre-warmed 2x Grace's medium supplemented with 20% Fatal Calf Serum (heat inactivated) in a sterile hood. The plaque overlay was mixed thoroughly and the bottle of plaquing overlay returned to a 37˚C water bath until use. When the incubation of the cells with virus dilutions was finished, the medium in each well was aspirated off and a 2 ml of plaquing overlay was quickly

added. The gel was allowed to harden for 20 min. The plates were then transferred to a humidified storage box and incubated in an incubator at 27˚C for 4-5 days.

At day 5 post-infection, plaques were stained by adding 1 ml neutral red/PBS solution to each well (1 part 0.4% neutral red in distilled water was diluted with 19 parts 1 x PBS). The plate was incubated at 28˚C in the dark for 2 h and then the staining liquid aspirated. The dish was inverted overnight at room temperature. On the sixth day post-infection, plaques were counted and the titre determined. The titre was calculated by the following formula:

pfu/ml =

(1/ml of inoculum/well) x (mean value of infected cells and / or foci in each well) x (dilution factor).

2.6.2.7 Optimisation of virus stock production

Prior to virus amplification, it is necessary to optimise the conditions for producing high quality and high titre master or working virus stock. Sf9 cells were seeded into a 6-well tissue culture plate at viable density of $2x10^6$ cells/well. The plate was incubated at 27ºC for at least 1 hour to allow the cells to attach. Triplicate wells were infected at each of the following multiplicity of infections (MOIs, i.e., ratio of infectious virus particles to cells): 0.05, 0.1, 0.3 and 0.5. One of the well was maintained as uninfected growth control. The virus inocula required at each MOI were determined as follows:

$$\text{Inoculum required (ml)} = \frac{\text{(desired MOI (pfu/cell) x (total number of cells)}}{}$$

titre of viral inoculum (pfu/ml)

Cell viability was determined and virus-containing medium collected at 24, 48, 72 and 96 hours post-infection. The virus titer of each sample was determined by a plaque assay. The optimal MOI and the harvest time that produce the highest combination of virus titre and culture viability >80% was selected for virus stock production.

2.6.2.8 Amplification of virus stock

With predetermined optimal MOI and the harvest time, the recombinant baculovirus can be amplified. The expanding or amplifying virus stocks can be performed with monolayer culture or scaled-up in suspension culture. To do this, Sf9 cells grown for 2-3 days were diluted to a viable density of $1x10^6$ cells/ml. The cells were infected with virus suspension of early generation at optimal MOI. Total and viable cell counts were performed ever 24 hours post infection to confirm the progress of infection. The virus can be harvested when the viable cells reduced to 70%-80%, usually at day 3 post-infection. In a sterile hood, the growth medium containing virus from the amplification culture was transferred into sterile tubes and centrifuged at 1,500 x g for 10 minutes to remove cells and large debris. The virus-containing supernatant was transferred into a sterile universal tube and stored working virus at 4ºC and master virus at -80ºC protected from light. For long-term storage, BSA was added to the virus stock at a final concentration of 0.1% to 1%.

2.6.2.9 Optimization of protein expression condition

The optimal MOI used for protein expression varies by cell line and the relative infection kinetics of the virus isolate. Therefore a MOI response should be investigated. Sf9 cells grown for 2-3 days at the density of $1x10^6$ to $3x10^6$cells/ml were inoculated with baculovirus at the MOI of 1, 3, 5 and 10. The infected cells were assayed every 12 hours post infection for their viabilities and densities against noninfected controls to confirm progress of infection. At the same time, 1ml aliquot of culture was harvested, protein extract prepared (Section 2.7.1.2) and assayed (Section 2.3.4). An optimal MOI and harvest time that produce the highest protein production was selected.

2.6.2.10 Expression of AhR LBD

Sf9 cells were grown in Ex-Cell 420 serum free medium for 2-3 days in a 75-cm^2 tissue culture flask or a 125ml disposable Erlenmeyer flask. Cells were then harvested and seeded at a density of 2 x 10^6 cell/ml in fresh medium and infected with baculovirus harbouring AhR construct at a MOI of 3. The infected cells were harvested at 48-50 hours post-infection by centrifuge at 800 g for 10 minutes at 4˚C. After harvest the cells were washed with ice-cold PBS and stored at -80˚C until further assay.

2.6.3 Expression of CYP 4X4 and CYP 4Z1 in insect cells

2.6.4 Construction of donor plasmid pFASTBAC

The mouse CYP 4x4 cDNA was subcloned from pGEM-T Easy to baculovirus donor plasmid pPASTBAC HT. The plasmid pGEM-T·CYP 4x4 (a gift from Dr. David R. Bell) and pFASTBAC THc were digested with *Not I* at 37ºC for 1 hour as described in Section 2.2.10. The resultant digest mixture from pGEM-T·CYP 4x4 was further digested with *Nhe I*, whereas the resultant digestion mixture from pFASTBAC THc was further digested with *SpeI* at 37ºC overnight. The resultant digestion mixtures were ethanol-precipitated (Section 2.2.7) and separated by electophoresis on 0.8% TAE SYBR gels (Section 2.2.13). The fragments of the CYP 4x4 cDNA (593bp) and linearised pFASTBAC HTc were excised from the gel and purified (Section 2.2.14). The purified CYP 4x4 cDNA fragment and the plasmid pFASTBAC HTc were ligated by T4 Ligase (Section 2.2.15). The ligation product was then transformed directly into competent JM109 cells (Section 2.2.2) and selected by ampcillin resistance. The orientation of AhR insertion was examined by *BamH I* digestion (Section 2.2.10). Construction of vector pFASTBAC THc·CYP 4x4 is show in Figure 2-4.

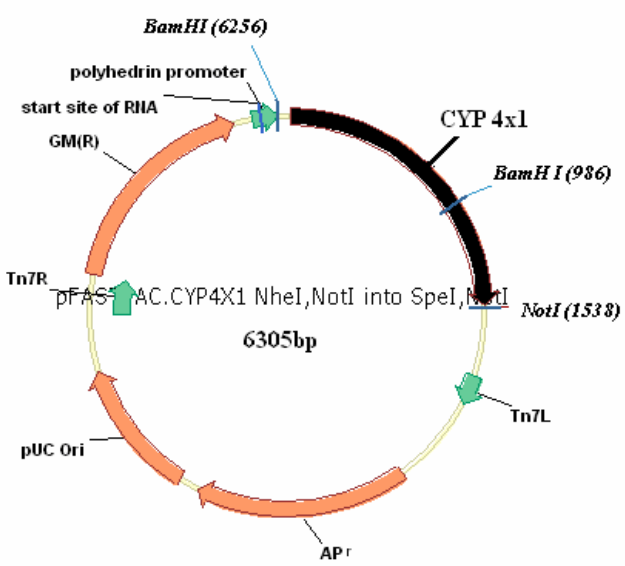

Figure 2-4. Diagram of pFASTBAC·CYP 4X.
The CYP 4x1 cDNA (black filled part) was inserted in the *Spe I* and *Not I* sites of the pFASTBAC. The arrows show the orientation of genes. The positions of ampicillin resistance (Apr), Gentamicin resistance (GMr) in pFASTBAC HTc were labeled. The positions of *BamHI* site in pFASTBAC HTc and in CYP 4x1 were labeled. The fragments of digestion with *BamHI* for sense were 1031bp and 5270bp.

2.6.4.1 Expression of CYP 4x4 and CYP 4z

The donor plasmids harboring CYP 4x4 and CYP 4z constructs were used to transpose *E. coli* strain of DH10Bac cells (Section 2.6.2.2). The recombinant cells were selected by antibiotics and colour screening, and the bacmid DNA was isolated as described in Section 2.3.2.3. The bacmid DNA was used to infect Sf9 cells and recombinant baculovirus generated as described in Section 2.3.2.5.

The baculovirus were used to induce CYP 4x4 and CYP 4z by infecting Sf9 cells at a MOI of 2.

Hemin is required for reconstitute of the expressed CYP450. Therefore, hemin at 2mg/ml (in 50% ethanol and 0.2M NaOH) was added to the culture at 24 hours

post-infection at the final concentration of4μg/ml of culture. Cells were harvested after incubation for an additional 48 hours at 27˚C, and microsomes were recovered as described in Section 2.7.3

2.7 Assay for recombinant protein production and activity

2.7.1 [^{3}H] TCDD ligand binding assay

The functionality of AhR LBD can be determined and quantified by using a in vitro radioligand binding assay. Since Ah receptor is thermo sensitive, the following procedures were carried out on ice or at 4˚C.

2.7.1.1 Preparation of mouse liver cytosol

As a positive control of AhR ligand binding assay, mouse liver cytosol was used. The mouse was killed by cervical dislocation and the liver was perfused *in situ* via the portal vein with 20ml of ice-cold buffer (150mM KCl pH 7.4) to remove the blood. The liver was then removed to a dish placed on ice, and all further work was carried out at 2-4˚C. The liver was finely minced with scissors in 3-fold (w/v) of lyses buffer (MENG buffer (25mM MOPS, pH 7.5, 1 mM EDTA, 0.02% sodium azide, and 10% glycerol) containing 10 mM sodium molybdate, 2mM DTT and 1mM PMSF). The mince was homogenized in a Potter-Elvehjem glass homogenizer with a Teflon drill. The homogenate was centrifuged at 10,000g for 15 minutes in a Backman centrifuge. The supernatant was carefully collected

avoiding disturbing the turbid lipid layer on the surface. The supernatant was re-centrifuged at 100,000g in an ultracentrifuge for 1 hour. The clear supernatant, referred as cytosol, was collected and protein concentration determined using a Bradford protein assay (Section 2.3.1). Aliquots of cytosol were dispensed into eppendorfs and stored at –80˚C for further assay.

2.7.1.2 Preparation of insect cell cytosol

Sf9 cells infected with baculovirus/AhR LBD were harvested at 48-50 hours post-infection by centrifugation at 1000g for 5 minutes. The cell pellet was resuspended at a concentration of 1x 10^8 cells/ml in ice-cold lyses buffer (MENG buffer (25mM MOPS, pH 7.5, 0.02% sodium azide, and 10% glycerol) containing 2mM DTT, 100µl/ml proteases inhibitor cocktail, 1mM PMSF, and 10 mM sodium molybdate). The cells were broken with 50 strokes from a Potter-Elehjen homogeniser, and the lysate was centrifuged at 10,000g for 10 min at 4˚C to remove cell debris. The supernatant from this spin was further centrifuged at 130,000g for 30 min at 4˚C in a Backman ultracentrifuge to remove microsomes. The resultant supernatant, cytosol, was collected and protein concentration determined by the method of Bradford (Section 2.3.1). Aliquots of 200µl cytosol may be stored at -80˚C until use or subjected to ligand binding assay immediately.

2.7.1.3 Preparation of receptor dilution

Sf9 cell cytosol was diluted into 1.0 to 0.1mg of cytosol protein/ml with ice-cold lyses buffer (MENG buffer (25mM MOPS, pH 7.5, 0.02%sodium azide, and 10%glycerol) containing 2 mM DTT, 100µl/ml proteases inhibitor cocktail, 1mM PMSF, and 10 mM sodium molybdate). The receptor dilutions were supplemented with 4mg BSA /ml in lyses buffer to serve as a pool of soluble, low affinity, binding sites that reduce nonspecific adsorption of the radioligand to the recombinant AhR. As a positive control, mouse or rat liver cytosol was diluted to a concentration of 5 mg of cytosol protein /ml. The receptor preparations were kept on ice in a universal tube and gentle stir-mix until it was needed.

2.7.1.4 Preparation of ligand

An aliquot of radioligand, [^{3}H]TCDD with an initial specific activity of 34.7Ci/mmol, 0.929mCi/ml, was diluted with *p*-Dioxane to 535 nanomolar, which served as a master stock stored at -20˚C. In each binding experiment, a further dilution of the master stock in *p*-Dioxane at a concentration of 200 nM was freshly prepared. A non-radioligand, TCAOB, was prepared as a master stock of 3mM in *p*-Dioxane and store at room temperature. Prior to each binding experiment, it was further diluted to 40 µM in *p*-Dioxane.

2.7.1.5 Setting up the binding reaction

A 200µl aliquot of the receptor preparation (Section 2.7.1.3) was dispensed into the assay eppendorf tube. Samples were in triplicate. To this a 1µl aliquot of [^{3}H]

TCDD (at final concentration of 1nM), 1µl of solvent (*p*-Dioxane) was added. A parallel triplicate sample was set up at the same time for determination of non-specific binding. To test non-specific binding, a 1µl aliquot of [^{3}H] TCDD plus a 200-fold excess of TCAOB, non-radioactive competitor, was added. After [^{3}H] TCDD, and solvent or competitor was added, the samples were mixed thoroughly by vortex followed by a brief spin down. The samples were then incubated for 16 hours at 4˚C.

2.7.1.6 Dextran-coated charcoal treatment

After incubation, samples were vortex-mixed and brief spun. A 30µl aliquot of the incubation was transferred from each sample to a scintillation vial containing 5ml of scintillation fluid and the samples subjected to analysis by liquid scintillation counting. This is to determine the total radioligand in solution. The remaining sample in each tube was treated with dextran-coated charcoal to remove unbound and loosely bound ligands. To do this, 30µl of dextran-coated charcoal (33mg charcoal/ml in MDENG buffer (25mM MOPS, pH 7.5, 0.02% sodium azide, 1mM EDTA, 2mM DTT and 10% glycerol) was added to each sample, which gives an optimal concentration of 0.2mg charcoal/mg protein. The sample was mixed by vortex, and incubated on ice for 10 minutes. The charcoal/dextran was pelleted by centrifugation for 10 min at 14,000g at 4˚C. A 150µl of supernatant (equivalent to 127.5µl of original incubation) was transferred from each sample into a scintillation vial containing 5 ml scintillation fluid. The sample was mixed vigorously with scintillation fluid before counting.

2.7.1.7 Measurement of the bound and free ligand concentrations

Radioactivity of [^{3}H]TCDD was determined by liquid scintillation counting using a Packard Tri-carb Model 2100TR Liquid Scintillation Analyser. Quenching was corrected by automatic external standardization. Total radioligand was defined as the concentration of radioligand in solution after the 16 hours' incubation. Total radioligand bound was defined as the radioligand in solution after charcoal adsorption. Non-specific binding was defined as the amount of radioligand bound in the presence of a 200-fold excess of [^{3}H] TCDD. Specific binding was defined as the difference between total and non-specific binding. The unbound (free) ligand was defined as the difference between total radioligand and the total bound radioligand.

The measurement of bound and free ligand (d.p.m.) was converted to molar concentration as follows (Hulme and Birdsall 1993):

$RL^* = B/(V \cdot SA \cdot 2220)$ nM

Where B is the radioligand bound (d.p.m.) corrected for counter background, V is the volume of radioligand assayed (ml), SA is the specific activity of the radioligand (Curies/mmole), and 2220 is the conversion factor from d.p.m. to nanocuries.

2.7.2 Competitive binding assay

Many drug candidates are ligands for the AhR, but differ widely in their binding affinities. To measure the affinities of these ligands, a competitive binding assay was carried out. In this experiment, an exponential dilution method was used (Hulme and Birdsall 1993).

2.7.2.1 Standard assay protocol

Mouse liver cytosol was prepared as described in Section 2.7.1.1. To 20ml of this protein preparation in a universal tube, an aliquot of radioligand [^{3}H] TCDD stork solution was added to give a final concentration of 1nM. The bulk protein-[^{3}H]TCDD mixture was stirring gently on a magnetic stirrer to ensure that the mixture remains uniform. From this mixture, a 3.136ml aliquot was removed to a small tube, containing a magnetic stirring bar. To this, sufficient unknown competitor (competing ligand) was added to yield the highest concentration to be studied in the competitive binding assay. This protein-[^{3}H]TCDD-competitor mixture was stirred sufficiently to maintain a uniform suspension. From this tube, a 1.5ml aliquot was removed into an eppendorf, and the same amount of bulk protein-[^{3}H]TCDD mixture was added into this tube. This step was repeated until the desired competing ligand concentration range had been reached. Six steps reduced the competitor concentration 10-fold.

From each of the above steps, triplicate samples, each containing 0.5ml assay solution with serial diluted competing ligand was generated. Another triplicate sample was set up at the same time for determination of non-specific binding. To test non-specific binding, a 200-fold excess of TCAOB (a known competitor) was

added to a 1.5ml aliquot of bulk protein-[^{3}H]TCDD mixture. The tubes were then incubated at 4˚C for 16 hours.

The assay was terminated by addition of charcoal-dextran (Section 2.7.1.6), and radioactiveties in each fraction was determined (Section 2.7.1.7).

2.7.2.2 Data analysis

Nonspecifc binding was defined as the amount of radioligand bound in the presence of 200-fold excess of known competitor. The total radioligand bound at each concentration of competing ligand minus the nonspecific binding was defined as the specific binding: B_0 = specific binding in the absence of competing ligand and B_x = specific binding at "x" concentration of competing ligand.

To generate a standard curve, the response parameter, B_x/B_0, i.e., the ratio of specific binding at each concentration of competing ligand relative to the specific binding in the absence of competing ligand, was plotted versus the log of the concentration of competing ligand (Bradfield and Poland 1988). The non-linear reration analysis was performed using GraphPad Prism version 4.00 for Windows (GraphPad Software, San Diego California USA)

2.7.3 CYP 450 assay

Sf9 cells infected with baculovirus/CYP450 were harvested 72h post-infection (Section 2.6.3.2). The cell pellet was resuspended with phosphate buffer (0.1M potassium phosphate pH7.4, 20% glycerol (v/v), 0.1mM EDTA), at a ratio of 40ml culture to a 1ml of buffer. The cells were then sonicated on ice (pulse on 5

seconds, off 10 seconds) 3 times at 35% maximum power using a Bandelin Eletronic Sonicator. The microsomes were recovered as described in Section 2.4.3. The recovered microsomes were resuspended in phosphate buffer and subjected to CYP450 assay. The fractions were analysed by SDS-PAGE (Section 2.3.2) and Western blot (Section 2.3.4).

The content of P450 was determined by using Omura and Sato's method (Omura and Sato, 1964). The sample was diluted to 2ml with 20mM potassium phosphate buffer (pH 7.5), 20% glycerol. A few milligrams of sodium dithionite were added to the solution to reduce the iron in P450. The sample was incubated at room temperature for 1 minute to permit the reaction to finish. Then the solution was divided into equal amounts, the sample and reference. The baseline was recorded by scanning samples from 400nm to 500nm. The sample cuvette was taken out and the sample solution was gently aerated with carbon monoxide (CO) for one minute. The P450-CO compound was scanned again from 400nm to 500nm. The concentration of P450 was calculated from the different absorbance between the trough and the peak, by using extinction coefficient of $91mM^{-1} \cdot cm^{-1}$ (Omura and Sato 1964).

2.7.4 Chloramphenicol acetyl transferase assay

Chloramphenicol acetyl transferase (CAT) assay is used as an internal control to determine the transfection efficiency. The assay is based on the enzymatic butyrylation of radiolabeled chloramphenicol as detailed by Seed and Sheen (Seed and Sheen 1988).

In a 6-wll tissue culture plate, infected Sf9 cells were harvested 48h post-transfection and washed once with PBS. The plate was put on ice and to each

well, 1ml of lysis buffer (0.1mM Tris-HCl, pH8.0, and 0.1% Triton X-100) was added. The plate was frozen at –80˚C for 2h and thawed at 37˚C. The plate was then chilled on ice. The cell lysate in the well was transferred to an eppendorf and centrifuged at 10,000g for 5min to remove cell debris. The supernatant was transferred to a second eppendorf and heated at 65˚C for 10 minutes to inactivate deacetylases and other inhibitors of the CAT reaction. This was centrifuged at 10,000g for 3 min. and transferred the cell extract to a third eppendorf. Protein concentration of each sample was determined by the modified Bradford method (Section 2.3.1). 25µg protein sample of cell extract, positive control (50milliunits of CAT) and negative control (cell extract from uninfected cells) were each mixed with 0.1M Tris-HCl, pH6.8 to give a final volume of 50µl. This protein mixture was added to a solution of substrates constituted to give a final volume of 100µl, compromising 10µl of 0.1M Tris-HCl, pH6.8, 25µl of 0.33 mM chloramphenicol, 5µl of 58mCi/mmol [^{14}C] chloramphenicol and 10µl of 2.5mM butyryl-coenzyme A. The sample was then incubated at 37˚C for between 5-24 hours. The reaction was terminated by addition of 2 volumes (200µl) of a 2:1 mixture of 2,6,10, 14-tetramethyl-phentadecane: mixed xylenes and mixing vigorously. After centrifugation for 3 minutes at 10,000g, 90% of the organic phase was removed to a scintillation vial containing 3ml of scintillation fluid and radioactivity determined for 1 minute on a ^{14}C program using a 1900 TR liquid scintillation analyser. Each sample was in triplicate and a mean determined.

Chapter 3. Results

3.1 Expression of cytochrome b5 in *E. coli*

3.1.1 IPTG concentration

Cytochrome b5 was expressed in C41(DE3) cells grown in TB medium. b5 was induced by IPTG at concentrations of 5μM, 10μM 100μM and 1000μM. After 24 hours' induction at 28˚C, the content of b5 in intact cells was measured. The results in Figure 3-1 show that at lower IPTG concentrations, i.e. 5μM and 10μM, the production of b5 stayed steady at 2.5nmol/ml of culture. When IPTG concentration was increased to 100μM, the b5 content reached 3.5nmol/ml of culture. By contrast, 1000μM IPTG failed to induce higher b5 production. Therefore IPTG concentration at 100μM was chosen to induce a high level of b5 expression.

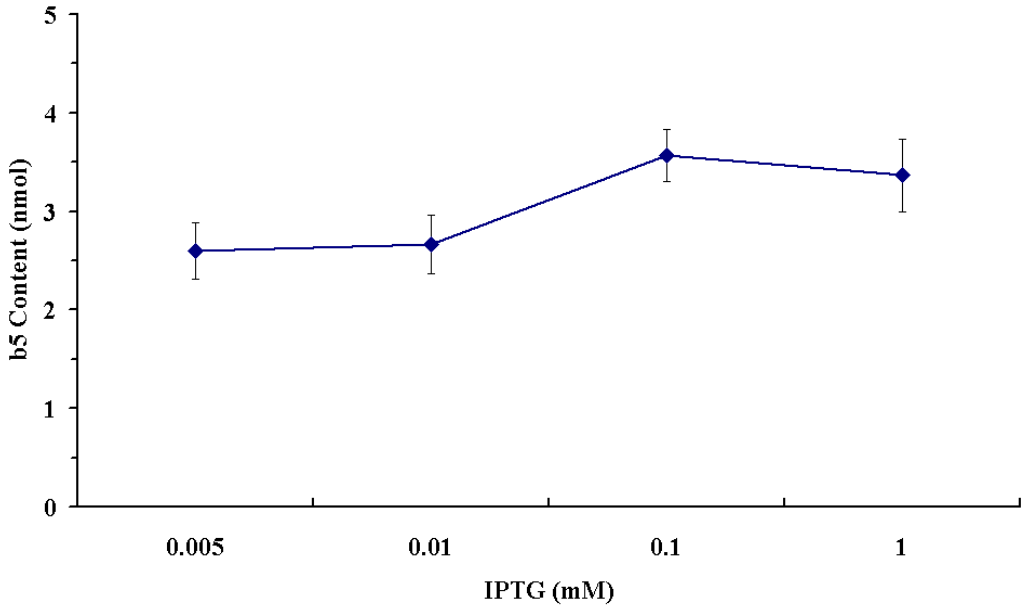

Figure 3- 1. Effect of IPTG on cytochrome b5 production

Cytochrome b5 was expressed in C41(DE3) cells. Bacteria were cultured in TB medium. b5 was induced at 28˚C by IPTG at indicated concentrations (Section 2.4.2). After 24 hours induction, the contents of b5 in intact cells from 1ml aliquot of culture were measured by deference spectrum as described in Section 2.4.4. Each point represented the mean±SD of triplicate samples.

3.1.2 Induction temperature

C41(DE3) cells containing pRSET·b5 were cultured in TB medium. Cytochrome b5 was expressed at temperatures of 26˚C, 28˚C, 30˚C and 32˚C. The content of b5 in intact cells was measured using a spectrophotometer (Section 2.4.4). The results showed that the expression of b5 increased with the increasing of temperature from 26˚C to 28˚C. However, when the temperature was increased to 30˚C and 32˚C, the level of expressed b5 decreased constantly. The highest expression level of spectrally detectable b5 was at 28˚C (Figure 3-2.).

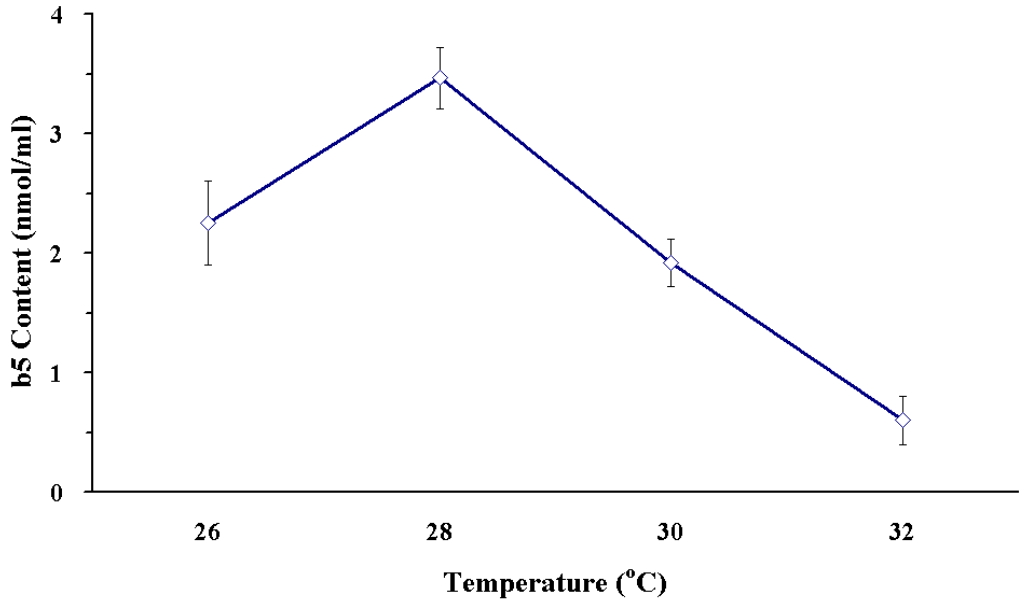

Figure 3- 2. Effect of temperature on b5 production.
Cytochrome b5 was expressed in C41(DE3) cells. Bacteria were cultured in TB medium. At indicated temperatures b5 was induced by 100μM IPTG for 24 hours (Section 2.4.2). The contents of b5 in intact cells from 1ml aliquot of culture were measured by deference spectrum (Section 2.4.4). Each point represented the mean±SD of triplicate samples.

Consistent with the above data, it was also observed that the cultures induced at 28˚C the cells showed a visibly more intense colour, suggesting a greater incorporation of haem by cytochrome b5. In contrast when the induction temperature was increased to 30˚C or 32˚C, a faint hint of red colour in the cell pellet was observed, indicating the majority of the fusion protein being expressed in the apo form. This is most likely that a mixture of apo and holo protein is produced, since at higher temperature haem synthesis and incorporation cannot be maintained at comparable levels to the cell growth and protein expression.

3.1.3 Recovery of cytochrome b5

Using C41(DE3) transformed with pRSET-b5 the location and molecular weight of the expressed cytochrome b5 was analysed by SDS-PAGE. It was confirmed that the expressed protein of approximately 20 kDa is consistent with the expected molecular mass of the b5 fusion, and this protein is associated with the membrane of *E.coli* C41(DE3) cells (Figure 3-3), since it was recovered mostly in microsomes. In the absence of the plasmid, there is no expressed band demonstrating that this fusion protein is not an endogenous product of the bacterial cell but a product of the plasmid pRSET-b5.

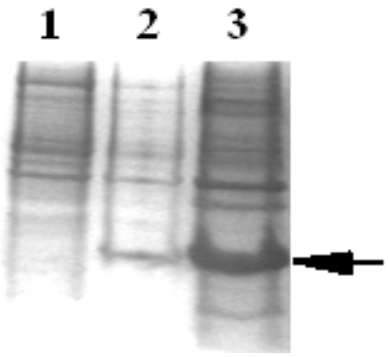

Figure 3- 3. SDS-PAGE of cell fractions
Whole cell extracts and microsomes were prepared from C41(DE3) cells and cells transformed with pRSET·b5 (Section 2.4.3). Proteins were separated on 15% SDS-PAGE and staining with Coomassie blue. The position of b5 was indicated by an arrow. *Lane 1*, whole cell extract from C41(DE3) cells; *lane 2*, whole cell extract from C41(DE3)-pREST·b5 cells; *lane 3*, microsomes isolated from C41(DE3)-pREST·b5 cells.

To recover cytochrome b5, cells were initially lysed and osmotic sensitive spheroplasts were prepared with the aid of lysozyme and EDTA. The spheroplast fraction was then ruptured by sonication to prepare microsomes (Section 2.4.3). Given that the membrane-binding domain of b5 would be easily damaged during preparing of microsomes, therefore the condition for recovering full-length b5 was optimised.

The spheroplasts were resuspended in buffer C (10%w/v glycerol, 20mM Tris-HCl pH8.0, 50mM NaCl and 1mM DTT) supplemented with a protease inhibitor tablet. The suspension was thoroughly mixed with a Potter-Elvehjem homogeniser. Aliquots of this suspension were sonicated for 5 x 20 seconds at either 80%, 40% and 30% powers, followed by centrifugation fractionations. The contents of b5 in each fraction were measured.

Fraction	Sonication power		
	80%	40%	30%
Spheroplast suspension	100	100	100
10,000 g supernatant	78	63	52
110,000 g pellet (microsomes)	23	31	28

Table 3- 1. Recovery of microsomes by sonication at different powers.
Cytochrome b5 was recovered from spheroplasts in 10,000 g centrifugation supernatant. The membrane-bound b5 was recovered in microsomes. Cytochrome b5 in each step was

measured by the spectrophotometer and presented as fractional recovery of b5 in spheroplast suspension. b5 content in spheroplast suspension was defined as 100%.

The results in Table 3-1 showed the effect of sonication strength on the recovery rate of cytochrome b5. A higher sonication power could help to release b5 into extraction solution, however it led to a lower recovery of membrane-bound b5 from microsomes. This was presumably due to the cleavage of the catalytic domain from the membrane-binding domain of b5 by the high power sonication. As a result, there was a high level of b5 in 10,000 g supernatant, whereas a low level of membrane-bound b5 in 110,000 g pellet. When sonication power reduced to 40%-30%, the recovery rate of membrane-bound b5 was increased. Therefore this power range was chosen to recover b5-containign microsomes from bacteria.

3.1.4 Reconstitution of apo-cytochrome b5

The majority of b5 expressed in C41(DE3) was apoprotein. This was confirmed by the dropwise addition of exogenous hemin. This resulted in an intense absorbance at 412 nm (Figure 3-4), the characteristic spectrum of the oxidised state of cytochrome b5.

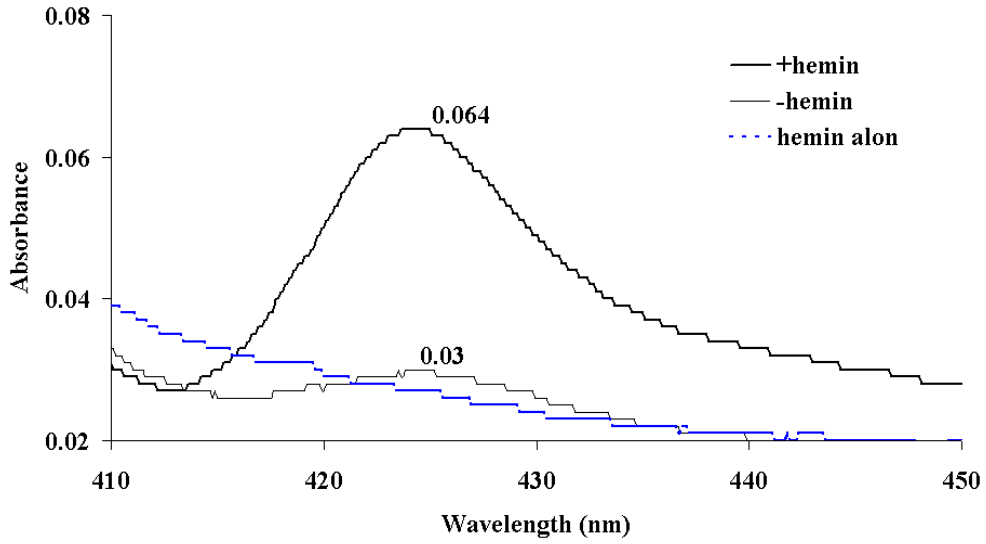

Figure 3- 4. Reconstitution of apo-cytochrome b5.
The increase in absorbance at 412 nm was observed following the addition of hemin to solubilised b5 protein. The profiles indicated the ability of the over expressed b5 protein to bind exogenous hemin. Free hemin was indicated with a dashed line on the bottom. In comparison, cytochrome b5 containing hemin has a narrow absorption spectrum, which peaks at 424nm.

3.1.5 Protein purification

Initially, it was expected in the present study to use a one-step chromatography on His-Bind Resin for b5 purification. However, SDS-PAGE analysis showed that the b5 produced from His-Bind chromatography (Section 2.3.6) was contaminated with other proteins (Figure 3-5). Therefore, the pooled samples from His-Bind chromatography were further fractionated on Uno Q column as described in Section 2.3.7. The chromatography on Uno Q column was shown in Figure 3-6. Fractions in 1ml aliquots were collected and analysed by SDS-PAGE. The fractions corresponding to 1600sec to 1900sec (or 27min to 34min on the SDS-PAGE) at the second peak were identified as b5 (Figure 3-7). The purified b5 were pooled and desalted using an YM-10 membrane as described in Section 2.4.5. The final purified b5 migrated on 15% SDS-PAGE with an apparent

molecular weight of 21 kDa, which corresponds to the expected weight of 20,196Da. The protein was free of detectable contaminations (Figure 3-8). The purified b5 showed the specific absorption spectra of the protein (Figure 3-9), indicating its spectral functionality. The purification scheme is show on Table 3-2.

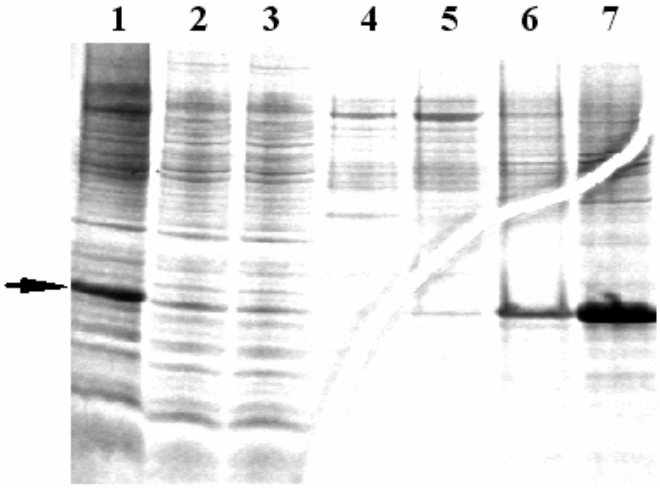

Figure 3- 5. SDS-PAGE of cytochrome b5 samples during His-Bind chromatography.
Samples were separated on 15% SDS-PAGE and stained with Coomassie blue. *Lane 1*, Chaps solubilized b5 before purification; *lane 2-3*, column follow-through after bind to His-Bind column; *lane 4-5*, wash flow-through; *lane* 6-7, purified b5.

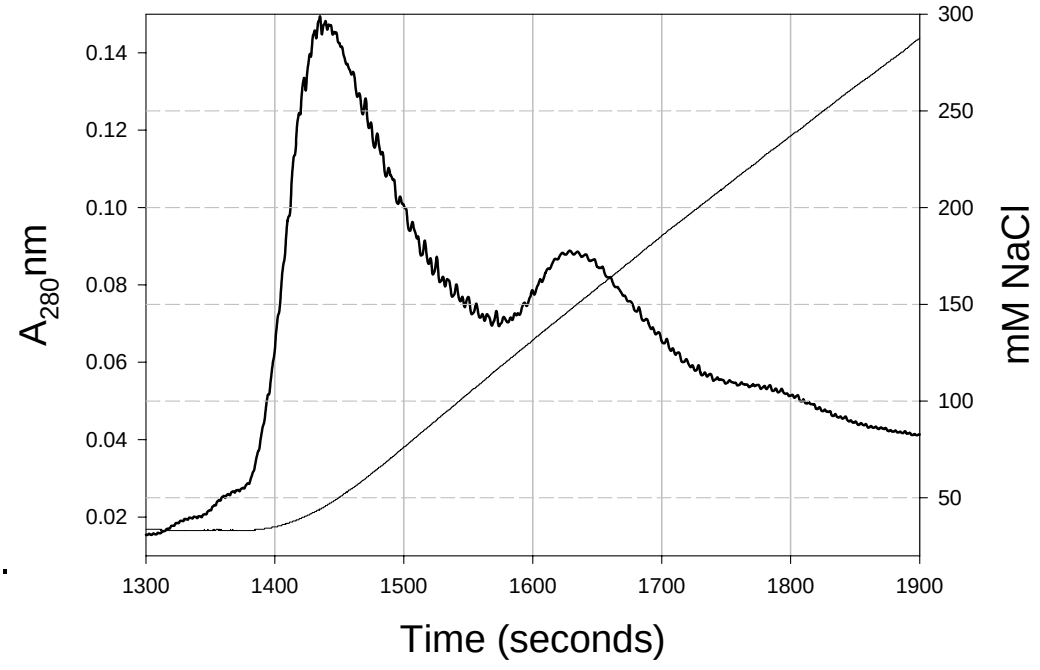

Figure 3- 6. Uno Q1 chromatography of cytochrome b5
Pooled fractions from His-Bind chromatography (lane 6-7 in Figure 3-20) were loaded onto Uno Q column. The absorbance at 280nm of the elute is shown as a solid black line, salt gradient elution is shown by a dotted line. 1 ml fractions were collected and assayed.

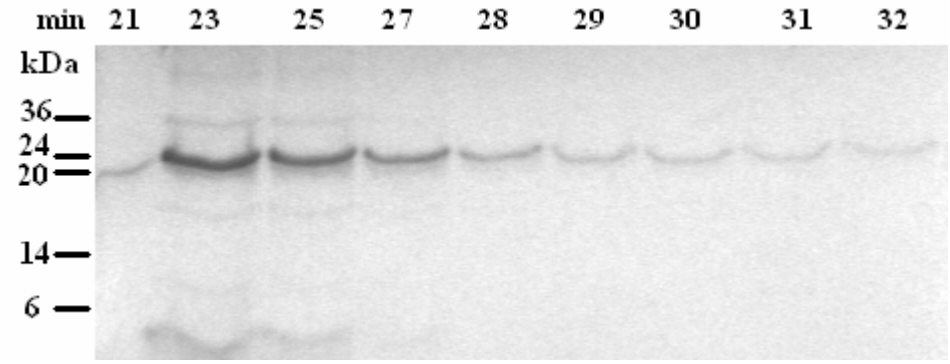

Figure 3- 7. SDS-PAGE analysis of fractions collected at 23-32 minutes
Collection numbers (in minutes) were shown at the top of the gel, and molecular marker (unit=kDa) shown on the left. The second peak, corresponding to 17-32 min, was identified as purified cytochrome b5.

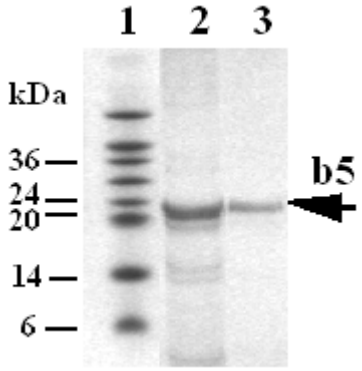

Figure 3- 8. SDS-PAGE analysis of final purified cytochrome b5 on Uno Q1 column.
Samples were separated on 15% SDS-PAGE and stained with Coomassie blue. *lane 1,* molecular standard (unit=kDa) were labelled; *lane 2,* pooled fractions containing b5 form His-Bind chromatography (5μg); *lane 3,* b5 purified on Uno Q1(3μg); The position of cytochrome b5 was indicated by an arrow.

Fraction	Total cyt b5 (nmol)*	Yield (%)
Whole cell	2000	100
After Sonication	869	44.3
After Solubilization.	898	45.6
His-Bind Resin	557	28.2
Uno Q1 column	384	19.2

Table 3- 2. Purification of the membrane-bound form of cytochrome b5
Microsomes were recovered by sonication and solubilized with CHAPS. Chromatography of solubilized b5 was performed on His-Bind metal affinity column followed by on Uno Q1 iron exchange column with recovery rate of 19.2%.
*From a 500ml culture.

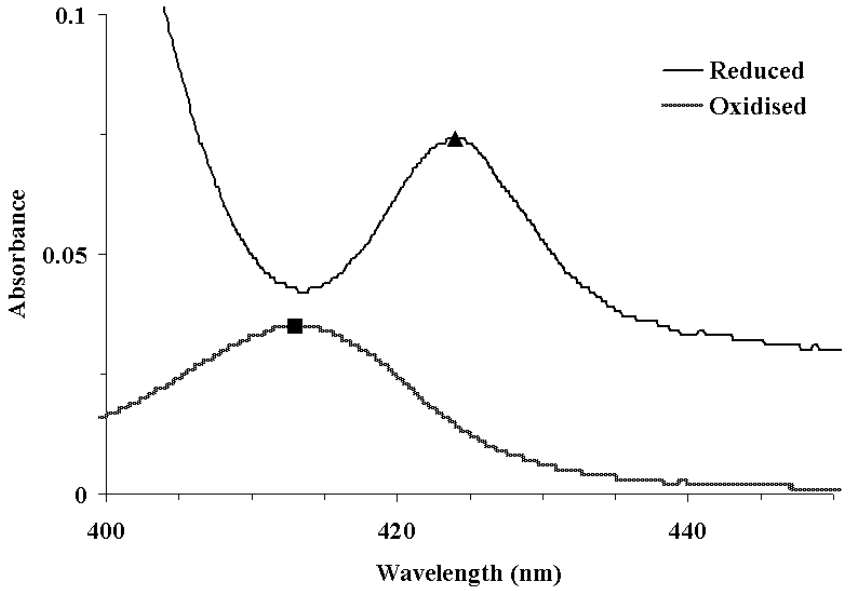

Figure 3- 9. The absorbance spectra of oxidized and reduced cytochrome b5
Purified cytochrome b5 was diluted in 0.1M KPi, pH7.5, and the absorbance spectrum of the oxidized hemoprotein recorded (■). A few crystals of sodium dithionite were added and the spectrum of the reduced hemoprotein recorded (▲). The absorbance of the oxidized b5 peaked at 413nm and reduced b5 peaked at 424nm.

In conclusion, the expression and purification of human cytochrome b5 has been achieved by using a bacterial expression system. The expression level averaged at 80 mg/liter (4000nmol/liter) of culture. The spectrally functional cytochrome b5

was purified to homogeneity by two-step chromatography with a total recovery of 19.2%.

3.2 Expression of AhR285 in *E. coli*

The concentration of the native AhR extracted from biological tissues is too low to permit detection by Coomassie blue staining on SDS-PAGE and thus quantification relies on Western blot analysis. Therefore, it is necessary to produce an AhR specific antibody recognising the AhR LBD. A fragment of the murine AhR b-1 allele (residues 285-416) named as 5g for simplicity was expressed in *E. coli* using T7 system (Section 2.5.1). The plasmid pRSET-c·5g contains the T7 promoter followed by a six-histidine tag at the N-terminus. The whole fusion protein contains 168 amino acids (Figure 3-10), the calculated molecular weight of which is 19,267 Da.

```
1    MRGSHHHHHHGMASMTGGQQMGRDLYDDDDKDRWIQHKLDFTPIGCDAKG
51   QLILGYTEVELCTRGSGYQFIHAADILHCAESHIRMIKTGESGMTVFRLL
101  AKHSRWRWVQSNARLIYRNGRPDYIIATQRPLTDEEGREHLQKRSTSLPF
151  MFATGEAVLYEISSPFSP
```

Figure 3- 10. Amino acid sequences of 5g fusion protein.
Amino acid sequence of LBD of mouse Ah b-1 allele (residues 285-416) was inseted into plasmid pRSET-c for expression in *E. coli*. The leader peptide from plasmid pRSET-c is shown in bold. A six-histidine tag is underlined.

Expression and purification of 5g was described in Section 2.5.2 and Section 2.5.3. The process of purification was examined using a 15% polyacrylamide gel (Figure 3-11). After induction, a thick new band at the position of 19kDa was detected on SDS-PAGE, consistent with the predicted value. However this protein band was not seen in either induced bacteria containing plasmid pRSET-c or

uninduced bacteria containing pRSET-c·5g. Therefore, this protein band was dependent on the presence of the AhR cDNA sequence, and the presence of inducing agent, and is therefore, identified as the recombinant AhR285.

The 19kDa protein band appeared in the 12,000g pellets after sonication and centrifugation (Figure 3-11), showing that the majority of recombinant protein was in inclusion bodies. The inclusion bodies were solubilized in 6M guanidine-HCl and the recombinant protein was purified to homogeneity by Ni-NTA His-Bind resin as described in Section 2.5.3. The purified AhR protein was used for the preparation of antiserum. A Coomassie blue staining gel further confirmed that antigen 5g purified from bacterial expression migrated on the gel with a mass of 19kDa (Figure 3-12A).

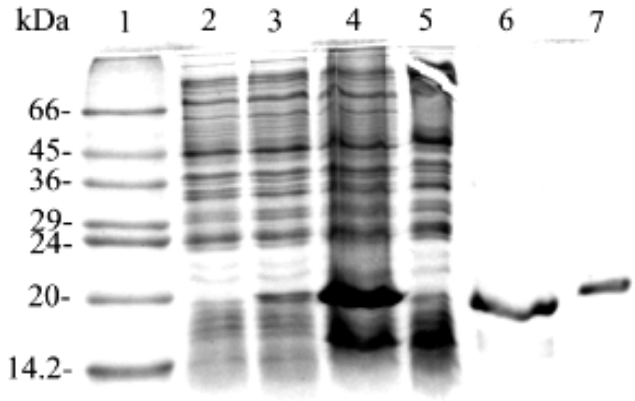

Figure 3- 11. Expression and purification of recombinant AhR285
Protein samples were separated on 15% SDS-PAGE and detected by Coomassie blue. *Lane 1*, proetin marker (unit=kDa); *lane 2*, induced bacteria containing pRSETc; *lane 3*, uninduced bacteria containing plasmid pRSETc-5g; *lane 4*, induced bacteria containing plasmid pRSETc-AhR285; *lane 5*, soluble protein in the supernatant after cintrifugation at 12,000g; *lane 6*, inclusion body in the pellet after centrifugation at 12,000g; and *lane 7*, purified AhR285.

3.2.1 Specificity of the anti-Ah receptor antibody

The antibody was generated by using the 5g peptide expressed in and purified from *E. coli* as described in Section 3.2. The specificity of the antibody to AhR LBD was analysed by Western blot. The AhR antigen 5g (5ng), cytosol protein prepared from uninfected Sf9 cells, cells infected with irrelevant baculovirus and baculovirus-AhR228 was separated on SDS-PAGE. The protein blot was immunodetected by using the AhR antibody as described in Section 2.3.4. The antigen was also used as a positive control for Western blotting. The results in Figure 3-12B show that the specific bands in both AhR marker and in cytosol from baculovirus-AhR228 infected cells were detected by using this antibody. However, this protein band was not seen in cytosol from either uninfected cells or cells infected with irrelevant baculovirus, showing that this antibody specifically detected the AhR protein but not other proteins in Sf9 cells. Therefore, the specificity of the antibody was justified.

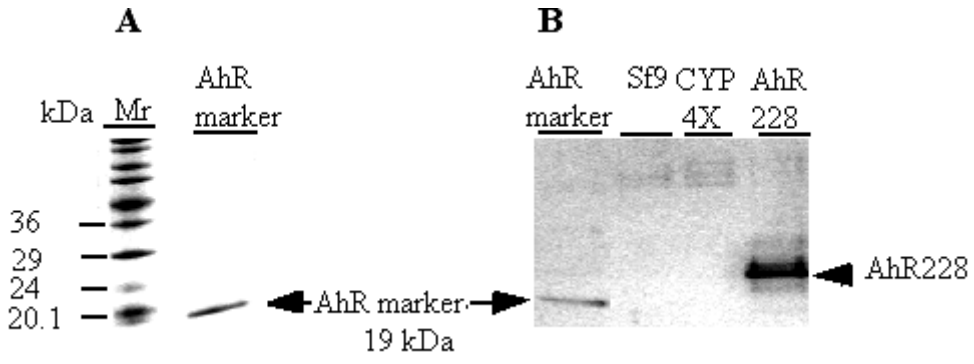

Figure 3- 12. Specificity of the AhR antibody
A, Coomassie brilliant blue staining of the AhR marker (AhR285, 19 kDa, 3µg/lane). Standard molecular marker (Mr, unit=kDa) was indicated. **B**, a typical Western bolt of the cytosol extract. Cytosols were prepared from baculovirus-AhR228-, -CYP 4X infected cells and uninfected Sf9 cells as described. Cytosol proteins (12µg/lane) and AhR antigen purified from bacteria (5ng/lane) were separated by 16% SDS-PAGE. Western blotting

was performed by using an antibody against the AhR. The position of AhR228 was indicated by an arrowhead, and that of a purified AhR285, as a marker, was indicated by an arrow on each side of the blot.

3.3 Expression of AhR LBD in insect cells

3.3.1 Insect cell growth parameters

Growth parameter determination is important for two reasons. It helps firstly to evaluate cell state when optimizing amplification and expression, and secondly, to track the *in vitro* age of the cell line. As a result, one may then restrict studies of a given experimental series to cultures within a selected age range. Cell growth curve was determined as described in Section 2.6.1.6 and shown in Figure 3-13. Under current culture condition the doubling time of Sf9 cell was between 23 to 25 hours, and the cells underwent 2.9 to 3.5 generations over three days during Log Phase replication. The maximum density to which the cells would grow was 6 x 10^6cells/ml. The low density split tolerance was 3 x 10^5 cells/ml and cells could recover within 12h. Healthy cells remain a constant size of 16-19μm in diameter.

Figure 3- 13. Growth curve for normal Sf9 cells

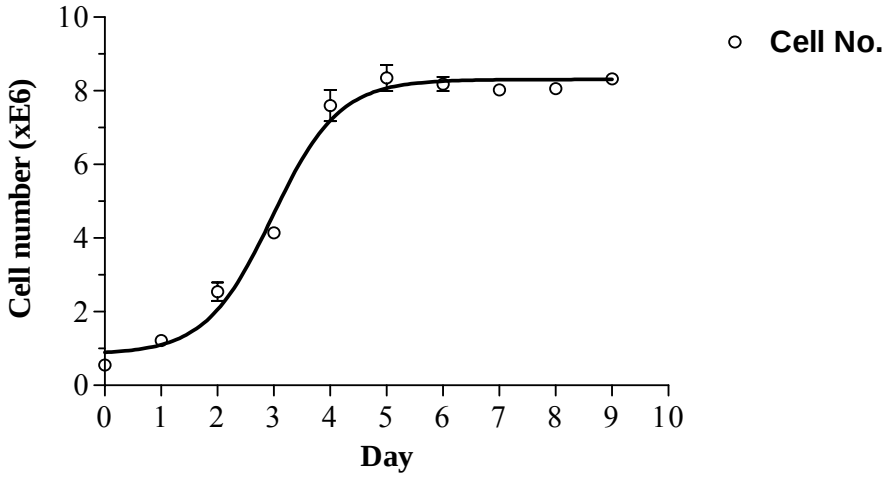

Sf9 cells growing in suspension were seeded at density of 5 x10^5 cells/ml in Ex-cell 420™ serum free medium and cultured at 27˚C±0.5˚C with a stirring rate of 110 rpm. Viable cells were counted very day over a period of 9 days as described. Nonlinear regression (curve fit) was performed using GraphPad Prism version 4.00 (GraphPad Software, San Diego California USA). Each point shows the mean±SD of triplicate determinations.

3.3.2 The AhR LBD constructs

Four truncated constructs of mAhR b-1 allele were designed to evaluate the minimum LBD. These four constructs, AhR228 (residues 228-416), AhR265 (residues 265-416), AhR286 (residues 286-416), and AhR410 (residues 286-410) were previously cloned in the *Bam HI* site of either pFASTBAC HT b or c vector. The AhR LBD construct AhR228 cDNA contains 190 amino acids. The N-terminal fusion peptide from pFASTBAC HTc contains 26 amino acids including a six-histidine tag. Therefore the whole AhR228 fusion protein contains 216 amino acids with a molecular mass of 24,723Da. Likewise, the cDNA of constructs 265, 285 and 410 contains 152, 133 and 125 amino acids, respectively. The fusion proteins of these constructs are179, 161, and 152 amino acids and the corresponding molecular mass are 20,762Da, 18,564Da and 17,557Da respectively. The protein sequences of the constructs are shown in Figure 3-14.

Figure 3- 14. Amino acid sequence alignment of AhR LBD constructs
Protein sequence alignment of AhR410, AhR285 AhR265 and AhR228 was done using Vector, NTI. Dashes indicated deletions in sequence alignment. The amino acids sequences of AhR LBD are show in bold and the six-histidine tag in the N-terminal fusion peptide is underlined.

3.3.3 Restriction digest analysis of the AhR constructs

The presence of AhR LBD construct in pFASTBAC HT could be revealed by restriction digest with *BamH I*. According to the nucleotide sequence of AhR LBD and pFASTBAC HT, the *BamH I* digestion would produce 465bp, 415bp, 381bp and 574bp fragment for AhR265, AhR285, AhR410, and AhR228 construct, respectively. Restriction digest was carried out as in Section 2.2.10 and the expected insert fragments were detected on 0.8% agarose gel. Four AhR LBD constructs in pFASTBAC HT vectors were verified (Figure 3-15). Plasmids were further verified by double strained sequencing.

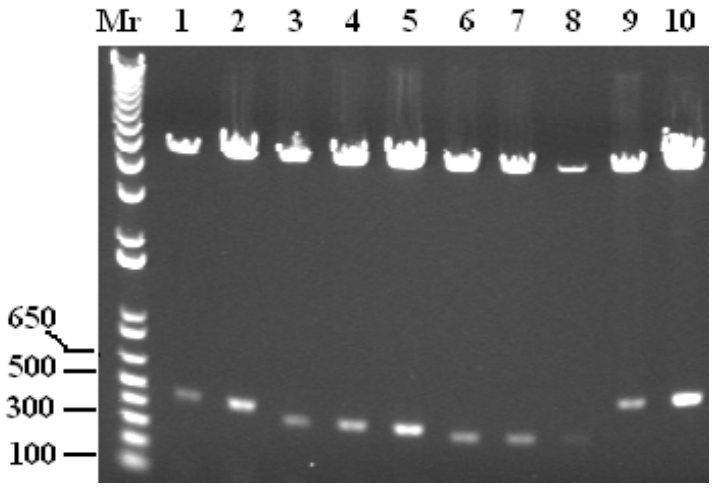

Figure 3- 15. Restriction digest analysis of AhR constructs on pFASTBAC HT vectors
The plasmids were digested with *BamHI* as described. DNA was separated on 0.8% agarose gel and stained by ethidium bromide. Mr, 1Kb plus DNA ladder, the position of 100, 300 500 and 650bp were indicated; lane 1-2, construct 265 (465bp); lane 3-5, construct 285 (415bp); lane 6-8, construct 410 (387bp), and lane 9-10, construct 228 (574bp).

3.3.4 Generation of recombinant bacmid

The minTn7 element on the pFASTBAC plasmid can transpose to the mini-*att*Tn7 target site on the bacmid in the presence of transposition proteins provided by the helper plasmid. The transposition was performed according to manufacture's instruction. The resultant colonies were analyzed by PCR to confirm that the AhR has transposed to the bacmid (Section 2.2.11).

The PCR products were separated on an agarose gel (Figure 3-16). DNA fragments of 354bp (on the left gel) were corresponding to the prediction for AhR285 and AhR410 construct, whilst fragments of 413bp (on the right gel) were for AhR228 and AhR265. The recombinant bacmid, each containing specific AhR LBD constructs were therefore verified.

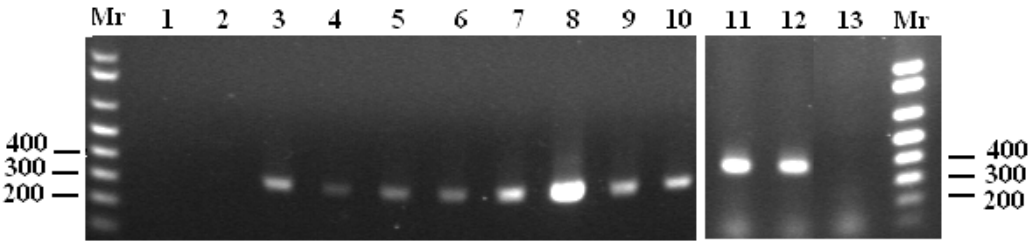

Figure 3- 16. PCR analysis of AhR constructs on recombinant bacmid DNA.
Recombinant bacmid DNA containing AhR LBD was confirmed by PCR analysis using primers OL292, and OL400 (reverse) for constructs AhR285 and AhR410; OL282 and OL410 (reverse) for constructs AhR228 and AhR265, as in Section 2.6.2.4. PCR was performed and products seperated on a 0.7% agarose gel stained by ethidium bromide (Section 2.2.11). Mr, 1Kb plus DNA ladder and the position of 200, 300 and 400bp were indicated in both gels; lane 1 negative control; lane 2, DH10 bacmid DNA without insert; lane 3-6, construct 285; lane 7-10, construct 410; lane11 construct 228; lane 12, construct 265 and lane 13, negative control.

3.3.5 Optimization of insect cell transfection condition

In the present study, bacmid DNA was transfected into Sf9 cells using cationic liposome-mediated transfection. To optimize the conditions for transfection, a recombinant bacmid containing chloramphenicol acetyl transerase (CAT) was used as an internal control to determine the transfection efficiency. Concentration effects of both Cell-Fectin Reagent and bacmid-CAT DNA were tested. It could bee seen (Figure 3-17A) that in the presence of bacmid-CAT DNA (3μg/well) the level of CAT activity detected was transfection reagent dependent. In the absence of transfection reagent, the cells could not be transfected by bacmid-CAT DNA, therefore the CAT activity in these cells was very low (0.08 units/well). The CAT activity in transfected cells increased with the increasing concentration of the transfection reagent, from 0.15 to 3.5μl/well.

Figure 3-17B showed that treatment of cells with transfection reagent in the absence of bacmid DNA had no effect. However, in the presence of the bacmid-CAT DNA, the CAT activity increased drastically. This shows that the significant increases of CAT activity detected are the results of transfection of CAT DNA. The results shown in Figure 3-17 indicate that the amount of reagent used for transfection was a critical factor. The optimal concentration was about 3.5μl/well, whereas a wide range of DNA concentration, from 4μg to 8μg/well, could be used for transfection with over 73% of maximum transfection efficiency (Figure 3-17B).

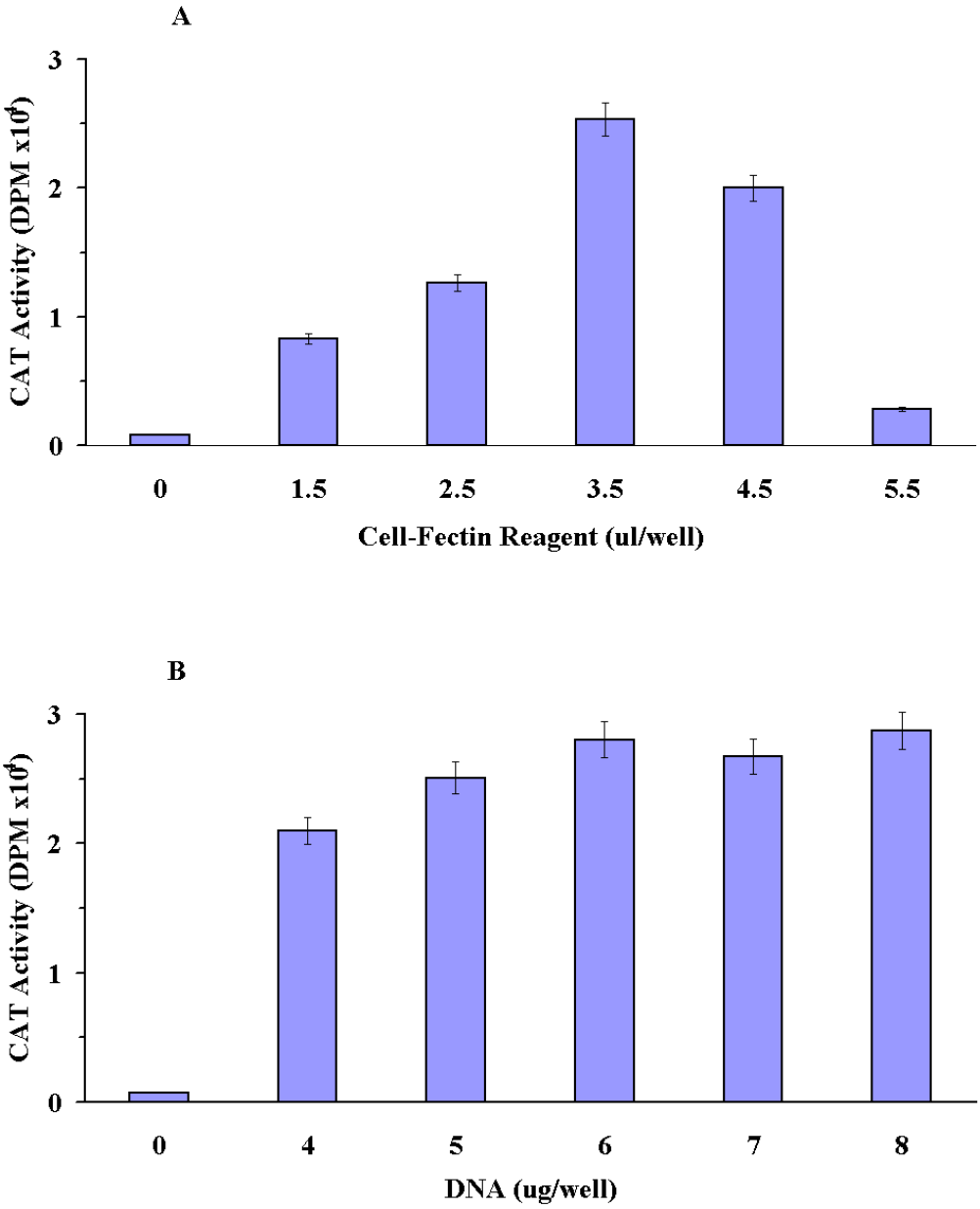

Figure 3- 17. Optimization of bacmid DNA transfection
A, Effect of Cell-Fectin concentration on trasfection. Sf9 cells cultured in 6-well plates were transfected with bacmid-CAT DNA at 3µg/well using different concentrations of Cell-Fectin™ Reagent (0-5.5µl/well). The infected cells were harvested at 48 hours post-infection. Cell extracts were made and assayed for CAT activity as described in Section 2.7.4. The results of CAT assay were expressed as DPM x 10^4. **B**, effect of bacmid-CAT DNA concentration on transfection. Cells were transfected as above using 3.5µl/well of reagent with different concentrations of bacmid-CAT DNA (0-8µg/well). CAT activity was assayed and results expressed in DPM x 10^4. Each bar showed the average ± SD of triplicate samples.

3.3.6 Time course of virus amplification

Bacmid DNA containing AhR LBD constructs were transfected into Sf9 cells to

produce baculovirus using optimal transfection parameters defined in Section 3.2.5. In order to produce high-quality, high-titer master or working virus stock, virus amplification condition was optimized as described in Section 2.6.2.7. The results in Figure 3-18 showed a typical time course for baculovirus amplification. At first day post-infection, cells looked healthy and viable cell counts remained the same as when they were infected. At second day post-infection, the viable cell counts fell down to 80%-85% (Figure 3-18A). In contrast, the virus titer remained as low as the initial titer during the first two days. At day three post-infection, the viral titer increased drastically (Figure 3-18B). Based on this investigation, the optimal MOI and the harvest time that produce the highest virus titer and culture viability >80% was selected. That is: cells infected with MOI of 0.1-0.3 and virus harvest at day three post-infection. Under this condition, virus can be readily amplified by 100- to 1000-fold of original titer through one amplification.

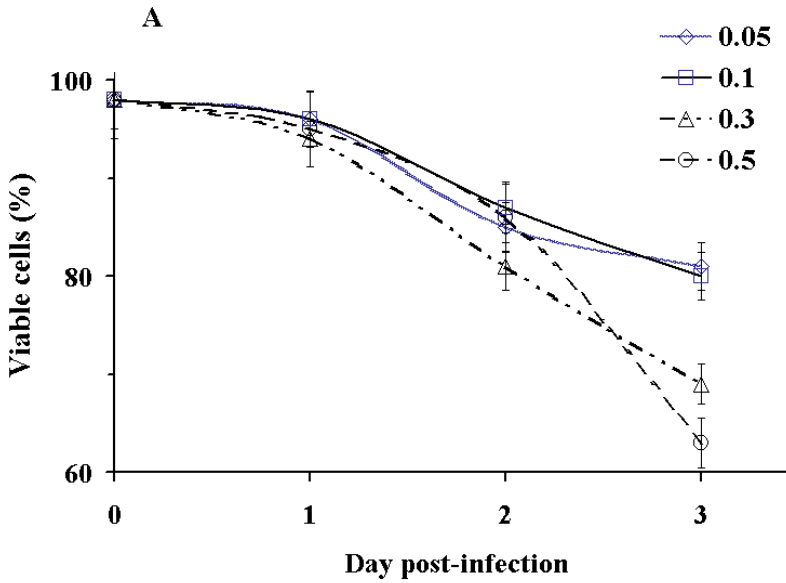

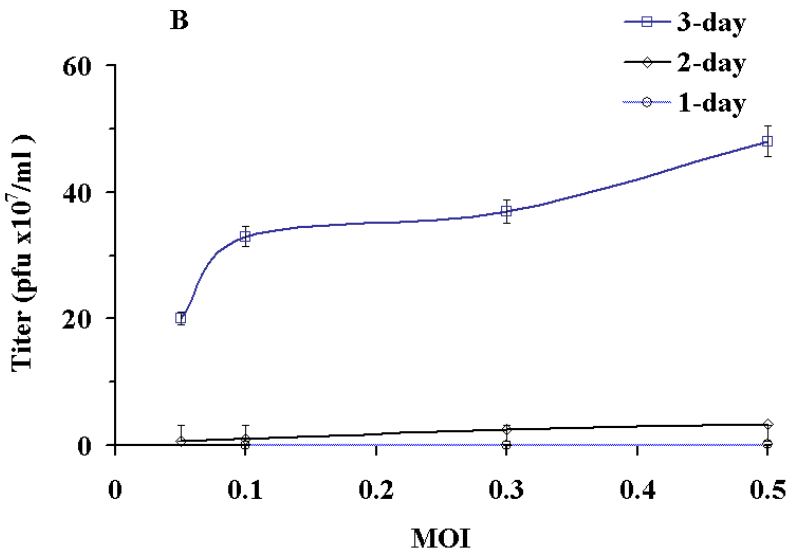

Figure 3- 18. Time course of baculovirus amplification
Sf9 cells growing in monolayer in 6-well plates at a density of $2x10^6$ cells/well were infected with baculovirus-AhR at varying MOI from 0.05 to 0.5 (plaque-forming units/cell), and samples taken over a period of 3 days. Cell viability was determined and virus titer (plaque-forming units/ml) analyzed using a virus plaque assay (Section 2.6.2.6). **A**, viability of Sf9 cells infected with baculovirus of varying MOIs (◊, 0.05; □, 0.1; Δ, 0.5 and ○, 0.1). **B**, virus titer at respective conditions (□, 3-day; ◊, 2-day and ○, 1-day post-infection). Each point shows the mean ± SD of triplicate samples.

3.3.7 Optimization of the AhR expression

High levels of protein expression vary by cell line and the relative infection kinetics of the virus isolate (instruction manual, GIBCO). Therefore MOI responses were tested for each virus containing different AhR construct. The expression condition was optimized in both monolayer and suspension culture at a small scale.

3.3.7.1 Expression in monolayer culture

As a starting point of the optimization, the MOI of 5 and 10 were used to infect Sf9 cells in monolayer culture. Sf9 cells were seeded in 6-well plates at density of $3x10^6$cells/well, and infected with baculovirus-AhR228 and -AhR410 at an MOI

of 5 and 10 for each. The infectivity analysis showed that the addition of baculovirus at both the MOI of 5 and 10 caused synchronous infection of all the cells, and it stopped cell growth immediately (Figure 3-19). The infected cells underwent a similar profile of decline for both MOI of 5 and 10.

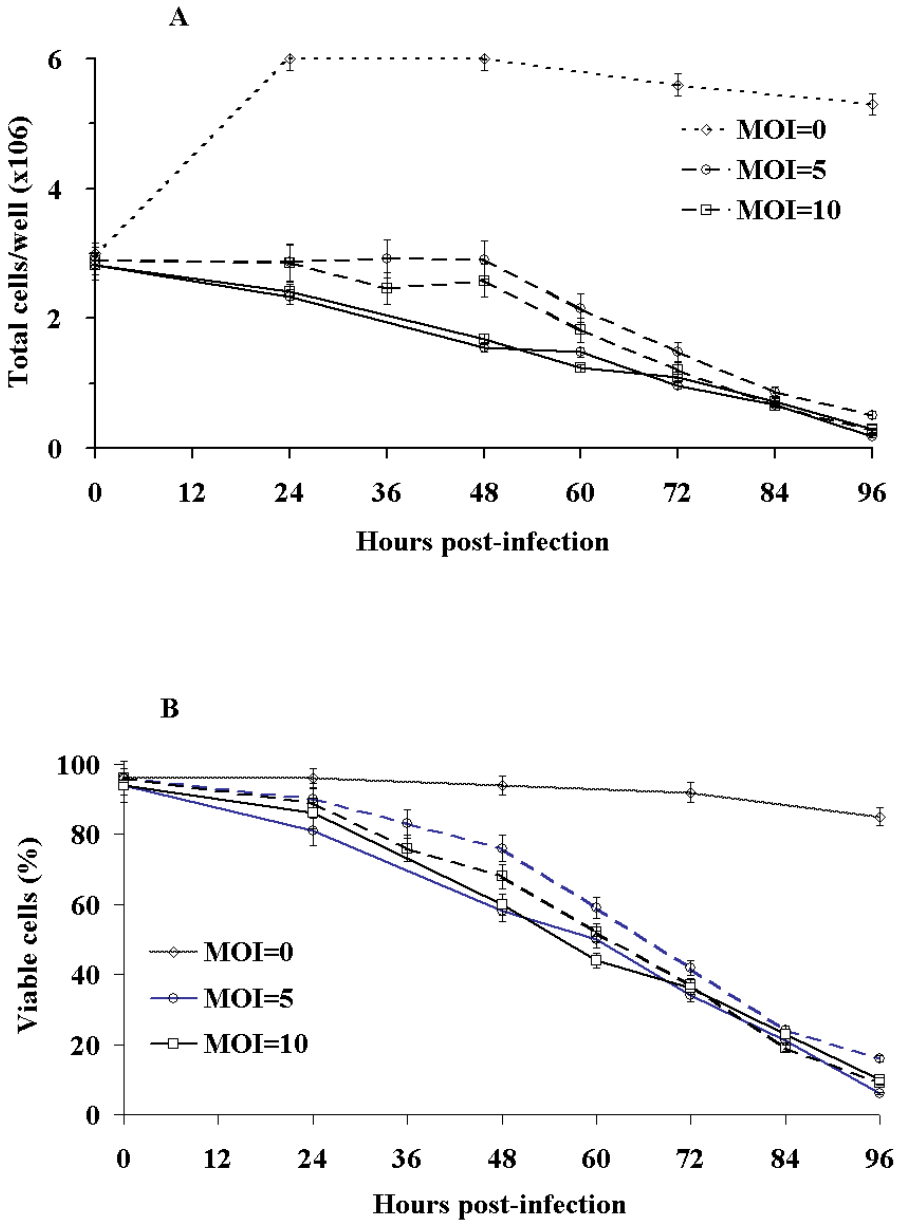

Figure 3- 19. Time course of baculovirus infection in monolayer culture.
Infectivity analysis of baculovirus-AhR228 and -AhR410 infected cells at the indicated number of hours post-infection (dashed line, clone 410; solid line, clone 228). Culture condition for uninfected cells was defined as MOI=0 (dotted line). A, total number of

cells against days post-infection. B, viable cell counts against days post-infection. ◊: MOI=0; ○: MOI=5; and □: MOI=10. Each point represented an average of duplicate determinants and error bar was standard error about the mean.

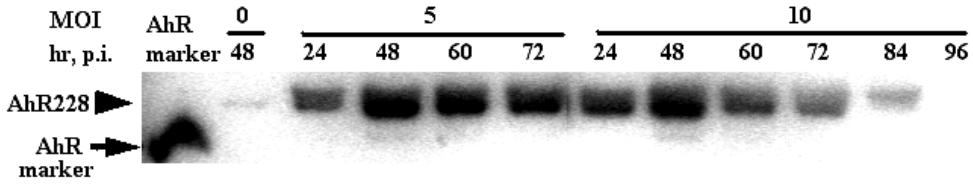

Figure 3- 20. Time course of AhR expression in Sf9 cells in monolayer.
Under the same condition as the legend to Figure 3-10, the infected Sf9 cells were sampled and protein products assayed by Western blot. A typical Western blot analysis of the cytosol extract (7μg protein/lane) prepared from cells infected by baculovirus-AhR228 at an MOI of 5 and 10. Culture condition for uninfected Sf9 cells was defined as MOI of 0. The position of a purified AhR LBD marker (10ng), as defined in the legend to Figure 3-3, was indicated by an arrow and the position of AhR228 was indicated by an arrowhead on the left side of the gel.

From the same samples, the expressed AhR protein was assayed by Western blot by using an AhR LBD specific antibody, which binds specifically to the recombinant LBD (Section 3.1.1). Analysis of the cytosol by Western blot indicated that expressed AhR protein increased within 48h p.i., and slowly decreasing after. Little AhR could be detected at 96h p.i. This was true for inoculated MOI at both 5 and 10 (Figure 3-20). Additionally, in the blot, a very faint band could be seen for the uninfected cells. This might be caused by a spill from the track to the right (Figure 3-20), and could not be reproduced in subsequent experiment.

3.3.7.2 Expression in suspension culture

Suspension culture is the most common way to produce protein in the baculovirus system. Therefore, the expression conditions were further optimized in suspension culture. In this experiment the observation was focused on 24-60h p.i. and

inoculum of virus was down to MOI of 1 and 3. The infectivity was investigated every 12 hours after 24 hours p.i.

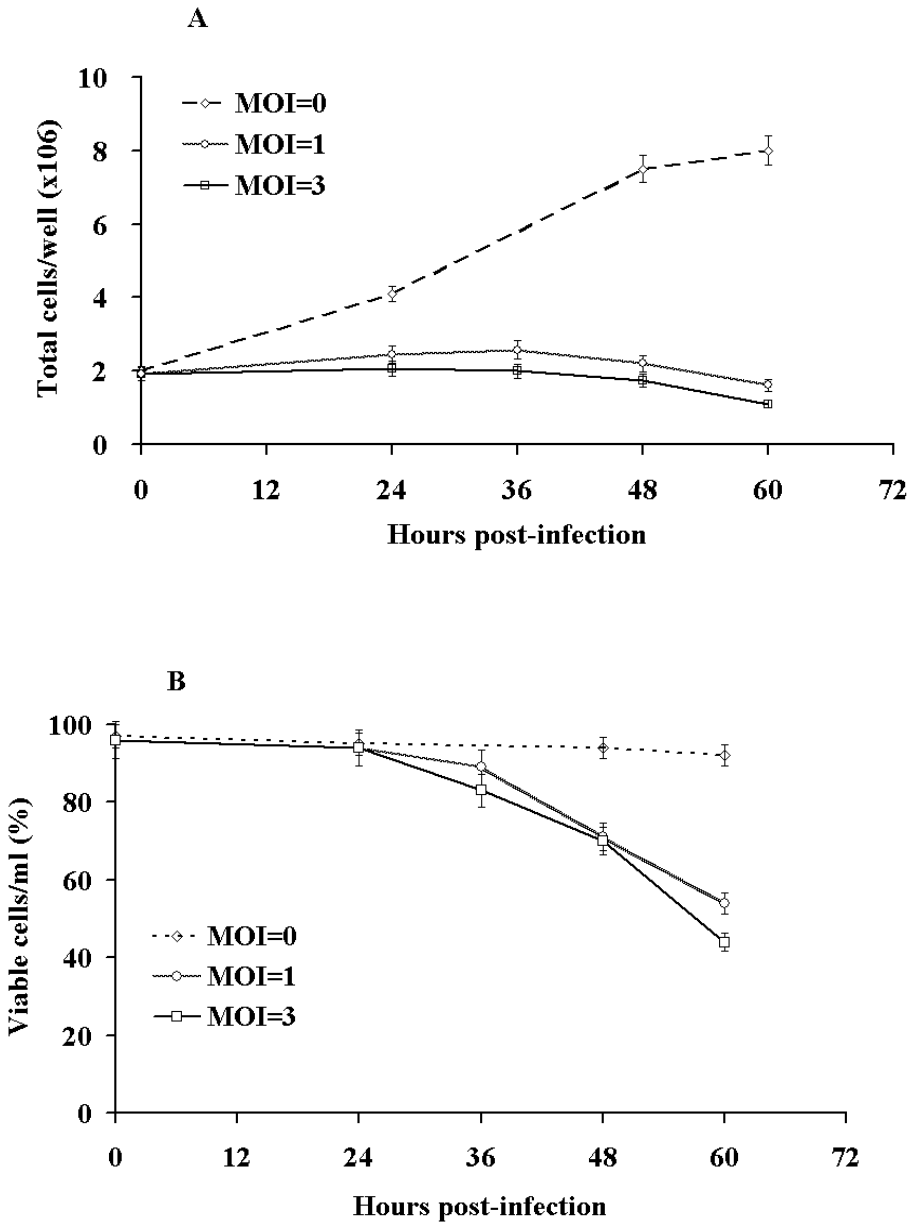

Figure 3- 21. Time course of baculovirus infection in suspension culture.
Suspension Sf9cells cultured at $2x10^6$ cells/ml were infected with baculovirus-AhR228 at an MOI of 1 and 3 (dashed line for MOI of 1, and solid line for MOI of 3). Culture condition for uninfected cells was defined as MOI=0 (dotted line). At the indicated number of hours post-infection, cells were sampled as described in the legend to figure 10. A, viable cell counts at different hours p.i.. B, total number of cells at different hours p.i.. ◊: MOI=0; ○: MOI=1; and □: MOI=3. Each point presented an average of duplicate

determinants and error bar was the standard error about the mean.

The results in Figure 3-21 show that inoculum of virus at MOI of 1 or 3 completely arrested cell growth in suspension culture. Under this condition the progress of cell infection could be precisely controlled.

Aliquots of samples collected at identical time points as above were assayed for the protein production. Crude cell homogenates and cytosol were prepared and proteins separated in SDS-PAGE (Section 2.3.2). Coomassie brilliant blue staining showed that the AhR265 protein in the crude extract, at the molecular size of 20 kDa (Figure 3-22A), began to accumulate at 48h post-infection and continued to increase with time tested. By contrast, in the cytosol preparation this protein band could not be visualized by Coomassie brilliant blue staining (Figure 3-22B). However, Western blot analysis of the cytosol sample showed the presence of the soluble form of the AhR265 (Figure 3-22C). It also shows in Figure 3-22C that the AhR concentration in cytosol was the highest at 48h p.i. when MOI=1. These conditions were therefore chosen for the production of soluble AhR using Sf9 cells in suspension culture.

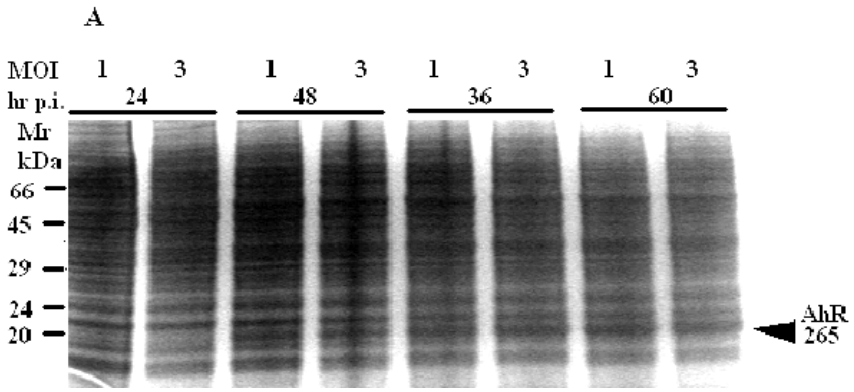

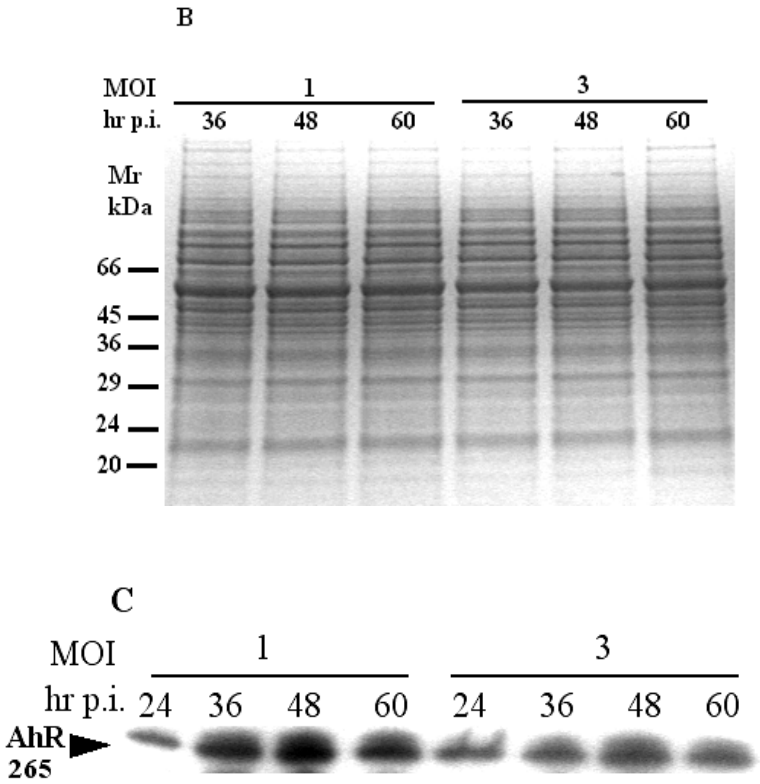

Figure 3- 22. Time course of AhR expression in suspension Sf9 cells.
Coomassie blue staining and Western blot analysis of the time course of AhR expression (24-60 hours p.i.). **A**, Coomassie blue staining of total protein in crude extract (20µg protein/lane). Protein marker (Mr, unit=kDa) was labeled. **B**, Coomassie blue staining of cytosol protein (20µg protein/lane). **C**, Western blot of the AhR228 in cytosol (7µg protein/lane). The position of the AhR was indicated by an arrowhead.

3.3.7.3 Expression of AhR LBD constructs

One of the objectives of the project was to produce high levels of soluble form of AhR LBD. Once high titer baculovirus was obtained and the expression conditions optimized, the attention was turned to scale up the expression of the four AhR LBD constructs. As a negative control baculovirus-CYP 4X was also used to infect Sf9 cells. Cells were infected with baculovirus containing different construct and harvested at 48h and 60h post-infection. Crude cell extracts and cytosol were prepared as described. Crude cell homogenate was analyzed by

Coomassie blue staining. It shows that the putative AhR peptide migrated on SDS-PAGE with an apparent molecular weight corresponding to the expected weight of 24.7, 20.8, 18.6 and 17.6kDa (Figure 3-23A), suggesting that the constructs are expressing the correct peptide. However, the soluble form of AhR in cytosol could not be visualized using Coomassie blue (Figure 3-23B), indicating that the majority of the induced proteins were in an insoluble form. The soluble form of the proteins in cytosol could only be detected by Western blot, each showing a corresponding molecular size as expected (Figure 3-23C). As a negative control, baculovirus-CYP 4X infected cell extract did not show any of these specific bands on the blot. Therefore, these protein bands were identified as the recombinant AhR.

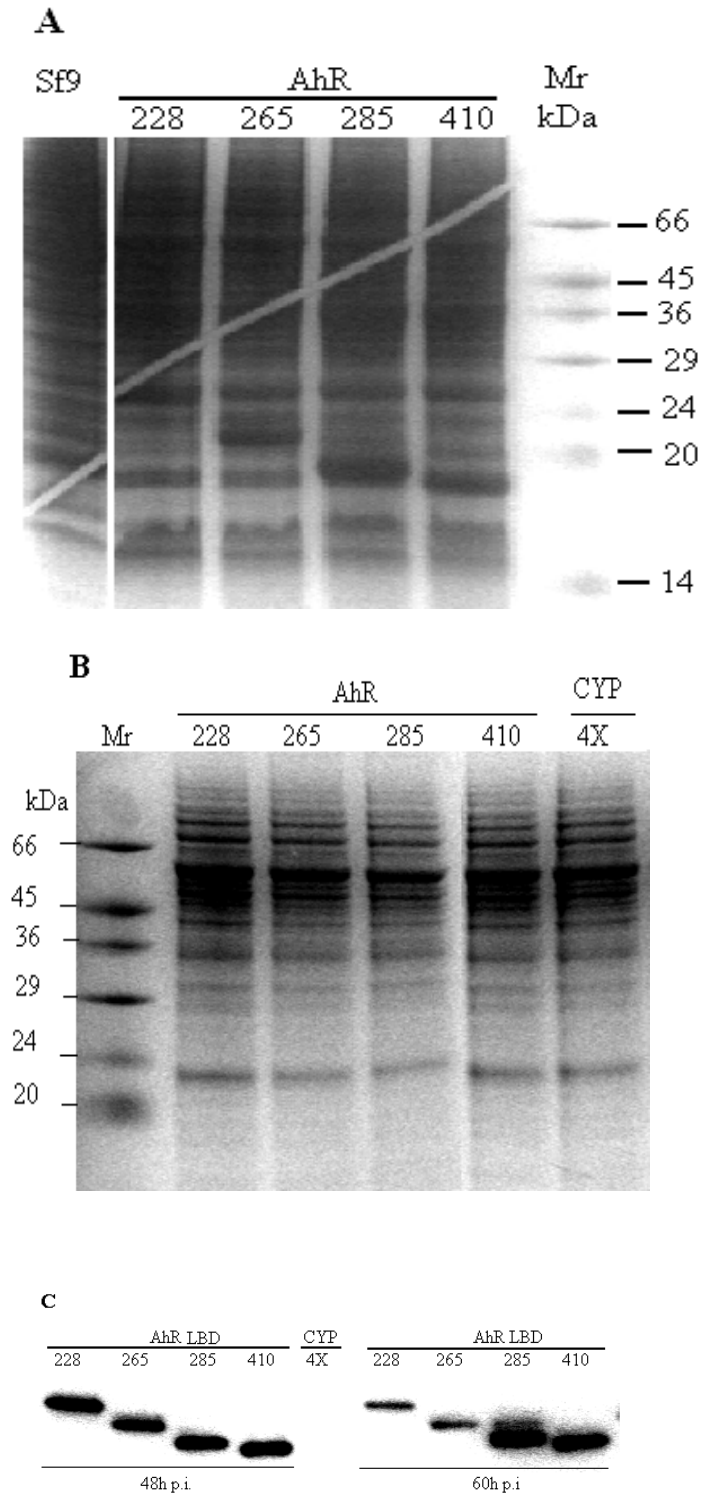

Figure 3- 23. AhR LBD expression in Sf9 cells.
A, Coomassie blue staining of total protein in crude cell extract (25µg protein/lane). **B**, Coomassie blue staining of the cytosol extract (7µg cytosol protein/lane) prepared as described (Section 2.7.1.2). Protein marker (Mr, unit=kDa) was labeled. **C**, a representative Western blot of the AhR LBDs in cytosol extract (7µg/lane).

3.3.8 Mass spectrometry analysis of AhR LBD

In order to confirm the identity of the expressed peptides, the expressed AhR constructs in Sf9 cells were analyzed by mass spectrometry. Crude cell extracts were prepared by lysis the cells with 2x SDS-PAGE loading buffer and the lysates were separated on 12% SDS-PAGE as described in Section 2.3.2. Corresponding AhR bands on the gel were excised. Three of the four expressed peptides were subjected to tryptic digestion for MS analysis and MS sequencing. The results in Table 3-3 show that the tryptic fragments with mass of bigger than 1kDa were detected on MS. The identification was based on a detected peak being within 0.1Da of the predicted size. All of the fragments were identified with two exceptions. These were the pepitide "STSLPFMFATGEAVLYEISSPFSP" in the C-terminal end, which had no charged amino acid. This may cause the fragment being poorly charged, hence not be detected on MS. The other exception was N-terminus. A protein of 92Da smaller than the theory was observed; this diminished size is consistent with loss of the N-terminal methionine, and subsequent N-terminal acetylation. These are common post-transcriptional modifications (personal communication with Dr. D R Bell). MS-based protein sequencing were further performed among several detected fragments (Table 3-3), and the identity of these fragments confirmed. Therefore, the expressed proteins are mouse AhR.

Measured (M)	Computed (M+H)	Residues	Peptide sequences Detected by TOF-MS
AhR410			
1084.5	1084.51	81-90	(K)TGESGMTVFR(L)
1236.6	1236.59	31-41	(L)DFTPIGCDAK(G)
1751.9	1751.90	42-56	**(G)QLILGYTEVELCTR**(G)
2301.2	2301.16	111-130	(R)NGRPDYIIATQRPLTDEEGR(E)
2382.2	2382.14	57-77	(G)SGYQFIHAADILHCAESHIR(M)
1570.78	1569.77	137-151	STSLPFMFATGEAVL(-)
3626.7*	3718.67	1-30	SYYH**HHHHHDYDIPTTENL**YFQGAMGIQHK(L)
AhR265			
1084.5	1084.51	81-90	(K)TGESGMTVFR(L)
1236.6	1236.59	31-41	**(L)DFTPIGCDAK**(G)
1751.9	1751.90	42-56	(G)**QLILGYTEVELCTR**(G)
2301.2	2301.16	111-130	(R)NGRPDYIIATQRPLTDEEGR(E)
2382.2	2382.14	57-77	(G)SGYQFIHAADILHCAESHIR(M)
2578.24	2577.23	156-179	STSLPFMFATGEAVLYEISSPFSP(-)
4514.0*	4606.12	1-38	SYYHHHHHHDYDIPTT**ENLYFQGAMDPLQP**PSILEIR (T)
AhR228			
1084.5	1084.51	81-90	(K)**TGESGMTVFR**(L)
1236.6	1236.59	31-41	(L)DFTPIGCDAK(G)
1751.9	1751.90	42-56	(G)QLILGYTEVELCTR(G)
2301.2	2301.16	111-130	(R)NGRPDYIIATQRPLTDEEGR(E)
2382.2	2382.14	57-77	**(G)SGYQFIHAADILHCAESHIR**(M)
2854.7	2854.64	48-74	KDGALLPPQLALFAIATPLQPPSILEIRT
2578.24	2577.23	156-179	STSLPFMFATGEAVLYEISSPFSP(-)
4242.91*	4334.83	1-36	SYYHHHHHHDYDIPTTENLYFQGAMGILAMNFQGR(L)

Table 3- 3. Summary of mass spectrometry analysis.
Three of the four of the expressed AhR constructs (AhR410, AhR285 and AhR228) subjected to tryptic digest and were analysed by TOF-MS. Tryptic fragments were identified by the molecular mass of the ion being within 0.1Da mass unit of the predicted size, whereas the fragments not identified are underlined. Fragments which were further analysed and confirmed by sequencing are in bold.
*: A diminished size of 92Da from the theory was observed caused by the post-translational modification, i.e., loss of the N-terminal methionine, and subsequent N-terminal acetylation.

3.3.9 Levels of expression AhR LBD protein

The amount of soluble AhR was further quantified. The prepared cytosol was serially diluted and proteins dissolved on SDS-PAGE followed by Western blot

analysis. It revealed in Figure 3-24 that soluble form of expressed AhR228 protein was about 1.3-1.7µg /mg (0.1-0.2%) of cytosol protein. That approximation could be translated to 150µg of soluble AhR from a 500ml of cell suspension. 150µg of soluble AhR is equivalent to what can be obtained from 150 mouse livers.

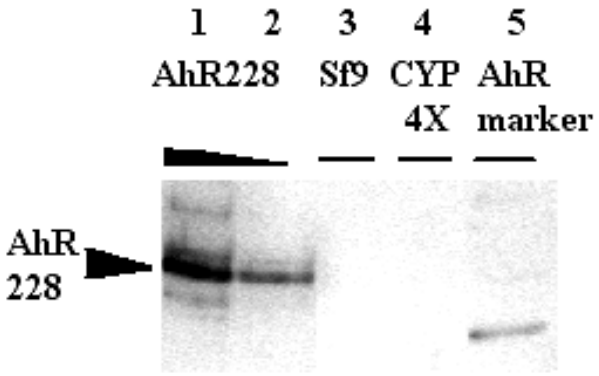

Figure 3- 24. Quantification of soluble AhR in Sf9 cell cytosol.
A representative Western blot showing level of soluble AhR expression. Cytosol was prepared from uninfected Sf9 cells or cells infected with baculovirus containing AhR228 or irrelevant CYP4x construct (2.7.1.2). Proteins were separated on 16% SDS-PAGE. The AhR was detected by Western blot. The concentrations of cytosol protein loaded were: lane 1, 18µg; lane 2, 9µg; lane 3 and 4, 18µg; lane 5 (Marker), 7.7ng.

3.3.10 Effect of glucose supplementation on AhR solubility in Sf9 cells

It was previously shown that supplementation of the Sf9 culture medium with additional glucose resulted in an increase in intracellular ATP levels, and more hsp90 in association with the overexpressed GR (Srinivasan, et al. 1997). However, it is not clear whether glucose supplementation could cause more hsp90 to interact with AhR in Sf9 cells, and so increase the soluble AhR. Therefore, baculovirus infected Sf9 cells were cultured in Ex-420 serum free medium in the

presence and absence of additional glucose (0.1%) supplementation. Given that molybdate has the ability to stabilize receptor-hsp90 heterocomplexes, in parallel cultures, molybdate at a final concentration of 10mM was added into the culture during the last 12 hours of incubation.

At 48 hours p.i., cells were harvested, and aliquot of cell pellet from each culture was used to prepare cytosol and high-salt extract. Protein preparations were subject to gel electrophoresis and Western blot analysis. One representative result is shown in Figure 3-25. There was an increased amount of overexpressed AhR in cytosol from cells grown in glucose-supplemented medium. However, there was no much difference in the quantity of the AhR in high salt extracts from cells grown in glucose-supplemented medium when compared to that from cells grown in unsupplemented medium. Molybdate supplementation showed little effect on the amount of expressed AhR both in cytosol and in high salt extract. However it remains to see its effect on AhR ligand binding capacity.

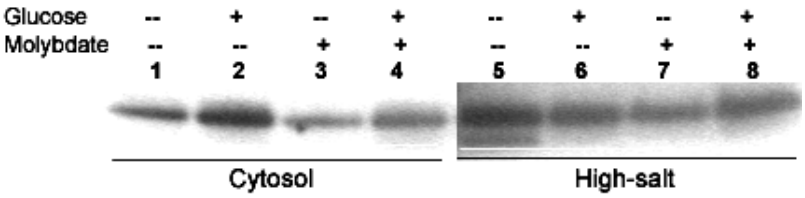

Figure 3- 25. Effect of glucose supplementation on AhR solubility.
Sf9 cells were transfected with baculovirus-AhR265 and allow to grow in Ex-420 serum free medium with or without (+/–) additional supplementation of glucose (0.1%) as indicated on the top of the blot. Molybdate at final concentration of 10mM was added into the indicated cultures at 36 hours p.i. At 48 hours p.i., cells were harvested. Cytosol was prepared from infected cells with MENG buffer (Section 2.7.1.2), and high-salt extract prepared with MENG buffer containing 400mM KCl. Proteins were separated on SDS-PAGE (20μg/lane) and analysed by Western blot. *Lane 1-4*, cytosol; *lane 5-8*, high salt extract.

3.3.11 Effect of coexpression of the AhR LBD with p23

It has been showed that the binding of cochaperone p23 to hsp90 can physically stabilize the receptor-hsp90 interaction, thereby enhancing the amount of receptor that exists in the high-affinity ligand binding conformation (Pratt 1997; Cox and Miller 2002). However, p23 was showed to be the limiting component of the multiprotein chaperone system *in vivo* in Sf9 cells, and coexpression of p23 increased GR-hsp90 heterocomplexes stability in Sf9 cells (Morishima, et al. 2003). Therefore it was of interest to investigate the effect of coexpression of p23 on the solubility of the AhR in Sf9 cells.

In this experiment, Sf9 cells were transfected with baculovirus-AhR228 with or without cotransfection of p23 at a MOI of 1. After 48 hours of transfection, cells were harvested. Total AhR in crude extract and the AhR in 100 000g pellet were prepared and analysed by Coomassie blue staining of SDS-PAGE. The results showed that cotransfection of p23 did not substantially change the subcellular localisation of the overexpressed AhR. The overexpressed AhR resided mainly in the high-speed pellet (Figure 3-26).

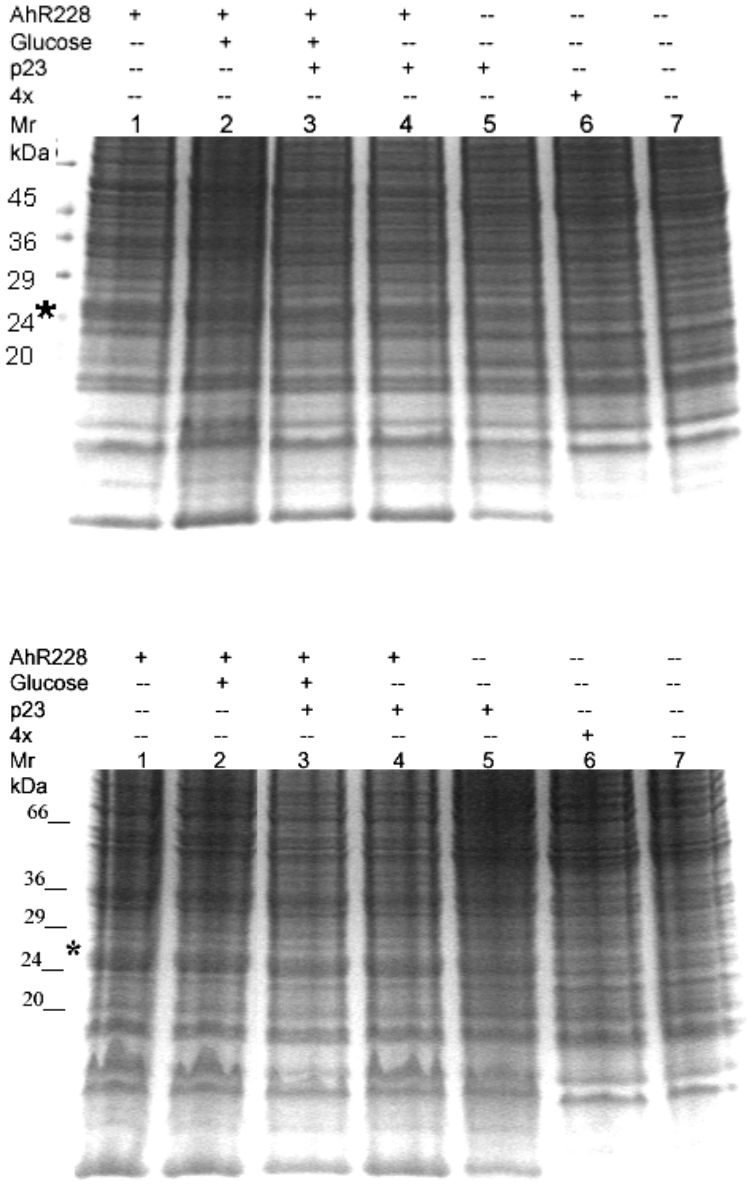

Figure 3- 26. Effect of p23 coexpression on subcellular localization of the AhR LBD in Sf9 cells.

Baculovirus-p23 was cotransfected at MOI of 1 with the baculovirus-AhR228 into Sf9 cells. Cultures were supplemented with additional glucose (0.1%) in the appropriate cultures. At 48h p.i. cells were harvested. Crude extract and cytosol were prepared as described in Section 2.7.1.2. After the cytosol extraction the resulting 100 000g pellet was re-extracted with SDS-PAGE loading buffer. The proteins from crude and pellet extracts were separated on SDS-PAGE followed by Coomassie blue stain. ***Uper Panel***, crude extract; ***lower panel***, pellet extract. Deferent treatment for each culture was indicated on the top of each gel. The position of the AhR228 is indicated by a start, and molecular marker (unit=kDa) was labelled on the left.

The amount of AhR cytosol and in high-speed pellet was further evaluated by Western blot. In Figure 3-27 the results shown that p23 cotransfection caused a decrease in the amount of AhR in high-speed pellet without substantial change in the amount of cytosolic AhR. The reduction of the AhR aggregates by coexpression of p23 is not accompanied by an increase in cytosolic AhR. It is possible that enhanced AhR degradation is taking place. It is also of interesting to see the effect of p23 coexpression on AhR binding activity.

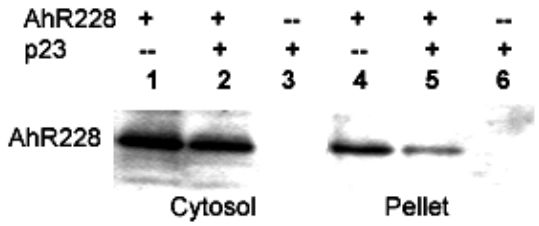

Figure 3- 27. Effect of p23 coexpression on soluble AhR LBD in Sf9 cells.
Baculovirus-p23 was cotransfected at MOI of 1 with the baculovirus-AhR228 into Sf9 cells. Cultures were supplemented with additional glucose (0.1%). At 48h p.i. cells were harvested, and cytosol and pellet extracts were prepared as described in legend to Figure 3-16. The proteins were separated by SDS-PAGE and analysed by Western blot. *Lane 1-3*, cytosol extracts; *lane 4-6*, pellet extracts. Deferent treatment for each culture is indicated on the top of each gel. The position of AhR228 is indicated.

3.4 Calibration of ligand [^{3}H]TCDD concentration

TCDD (2,3,7,8-tetrachlorodibenzo-*p*-dioxin) and its related compounds are highly insoluble in water (Poland and Glover, 1976). This is problematic for *in vitro* ligand binding assay, since there is only a very limited amount of ligand available for receptor to bind. Therefore TCDD concentrations in various aqueous solutions were investigated.

3.4.1 Effect of protein concentration on TCDD solubility

The experiments were carried out to determine TCDD solubility over a range of protein concentrations. [^{3}H]TCDD was diluted in either *p*-Dioxane or water. The resulting solution was added to different concentrations of protein solution (final concentration = 0.1% (v/v)). After 0 and 16 hours of incubation, samples were removed for scintillation counting and radioactivity quantified.

The results (Figure 3-28A) indicate that TCDD is highly insoluble in water, however its solubility increased drastically in the protein-containing solution. A much higher concentration of TCDD was found in protein-containing solution when [^{3}H]TCDD was originally dissolved in *p*-Dioxane than that it was originally dissolved in water (95% vs. 10%).

The results from another experiment (Figure 3-28B) show that TCDD solubility in protein solution was consistent over a range of protein concentrations tested, from 2mg/ml to 10mg/ml. Either BSA or cytosol protein had the same effect on TCDD solubility. Under this condition, at least 90% of the added radioligand remained in solution after 16 hours incubation at 4˚C.

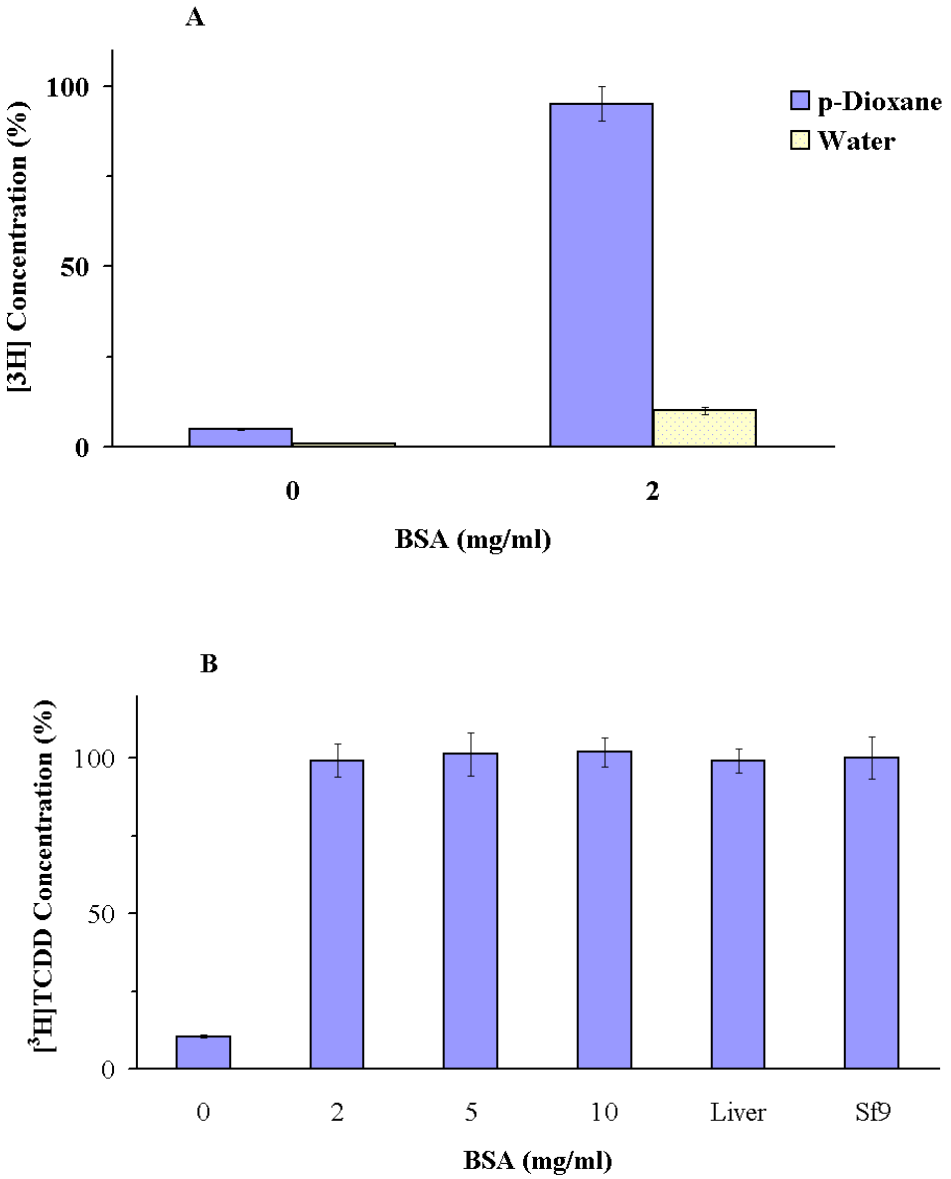

Figure 3- 28. Effect of protein on [^{3}H]TCDD solubility.
A, [^{3}H]TCDD was dissolved in p-Dioxane and water. The resulting solution was added to 0 and 2mg of BSA in MENG buffer at final concentration of 1nM (0.1%, v/v). After 0 and 16 hours incubation at 4˚C, a 100µl aliquot of sample was removed and radioactivity in solution was determined by liquid scintillation counting. The results are expressed as the percentage of the TCDD concentration in solution at 0 hour. **B**, 1nM [^{3}H]TCDD dissolved in p-Dioxane was incubated with varying concentrations of BSA (0, 2, 5 and 10mg/ml in MENG buffer), rat liver cytosol at 5mg/ml and 1mg of Sf9 cell cytosol protein plus 5mg BSA /ml. At the same condition as to A, radioactivity in solution was determined at 16 hours incubation at 4˚C. Each bar represents the mean ± S.E. of triplicate samples.

3.4.2 Solubility of TCDD in assay solution

The solubility of radioligand in assay solution was then further tested in the presence of the competitor TCAOB (3,4,3',4'-tetrachloroazoxybenzene) (Poland, *et al.,* 1976). [^{3}H]TCDD at varying concentrations ranging from 0.18 to 2.6nM plus a 200-fold excess of competitor TCAOB was added into MENG buffer containing 5mg of BSA/ml. Radioactivity was measured after 0 and 16 hours of incubation at 4˚C. The results show that the [^{3}H]TCDD concentration after 16 hours of incubation was generally lower than the concentration of radioligand originally added to the tubes. Within the originally added TCDD concentration ranging from 0.18nM to 1nM, the TCDD concentration decreased up to 10%, whereas when the added TCDD increased to 1.68nM to 2.6nM, the TCDD concentration fell by 25% after 16 hours incubation (Figure 3-29). This observation was consistent with previous report (Poland *et al*., 1976; Bradfield and Poland 1988).

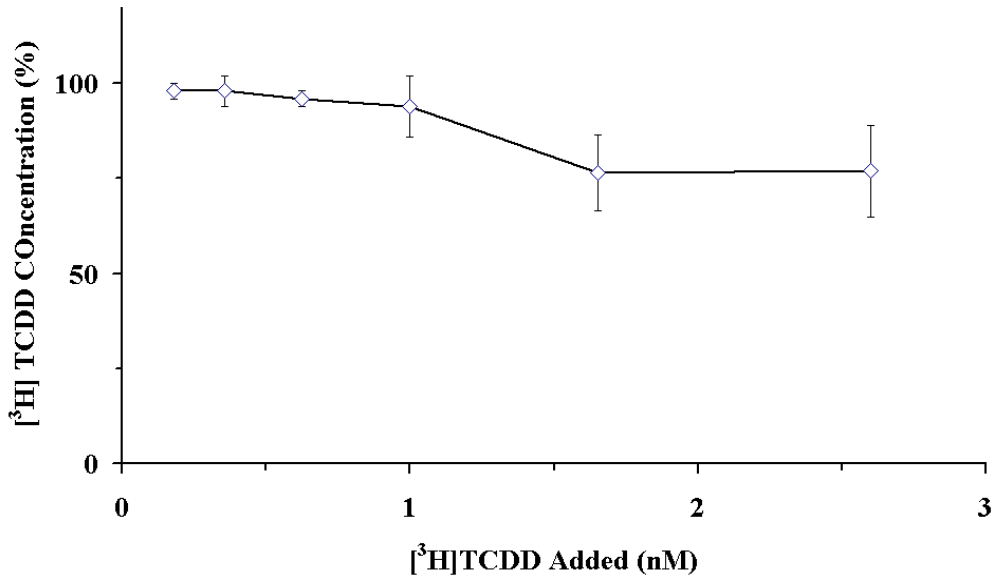

Figure 3- 29. Solubility of radioligand in assay solution.
BSA at 5mg /ml in MENG buffer was incubated at 4˚C with varying concentrations of [^{3}H]TCDD (0.18-2.6nM) in the presence of 200-fold excess of competitor TCAOB.

Samples were taken after 0 and 16 hours of incubation. The radioactivity in solution was determined by liquid scintillation counting. The results are expressed as the percentage of the TCDD concentration in solution at 0 hour. Each point represents the mean ±SD of triplicate samples.

The results show that the combination of [^{3}H]TCDD plus a 200-fold excess of TCAOB caused some [^{3}H]TCDD to come out of solution after a 16 hour incubation, which may lead to erratic results in the assay. Therefore for the subsequent experiments, the TCDD concentration was restricted to <1.5nM, where the TCDD remained soluble.

3.5 Optimization of *in vitro* ligand binding assay

As a source of the Ah receptor, mouse and rat liver cytosol was used to optimise a [^{3}H]TCDD ligand binding assay. Based on radioligand concentration of 1 nM (Section 3.4.2), other components present in the binding assay system, including liver cytosol protein and charcoal-dextran concentrations, were optimised.

3.5.1 Rationale

The assay for the binding of [^{3}H]TCDD by liver cytosol is based on the assumption that the total binding of TCDD by liver cytosol represents a small pool of high affinity sites (defined as specific binding) and a much larger pool of lesser affinity sites (defined as nonspecific binding). [^{3}H]TCDD was incubated with liver cytosol and then the unbound and loosely bound radioligand was removed by adsorption to a mixture of charcoal-dextran. The [^{3}H]TCDD remaining in the solution after adsorption represents the total binding. To distinguish specific

binding from total binding, another experiment was carried out simultaneously by incubating liver cytosol with [^{3}H]TCDD plus a large excess of an unlabelled competitor (which blocks [^{3}H]TCDD binding to the small pool of high affinity sites) and the unbound radioligand was removed by charcoal-dextran adsorption. The radioactivity remaining in the solution represents a non-saturable pool of binding, which is defined as nonspecific binding. Specific binding was the difference between total binding and nonspecific binding (Figure 3-30).

3.5.2 Effect of protein concentration on ligand binding

When a sufficient concentration of [^{3}H]TCDD (34.7 mCi/mmol) had been solubilized in solution (i.e. 1nM), it was important to optimize the amount of receptor in solution, so as to detect the specific binding. Therefore experiments were carried out to determine how much liver cytosol protein could be used in a binding experiment.

A representative result in Figure 3-30 indicates that the specific binding of [^{3}H]TCDD to mouse liver cytosol can be detected using protein concentrations ranging from 2 mg/ml to 6mg/ml. For 1nM [^{3}H]TCDD with specific activity of 34.7Ci/mmol, the determined binding capacities of AhR in mouse liver cytosol were 31.6, 22.4 and 19.2fmol/mg cytosol protein when assayed at protein concentrations of 2, 4 and 6mg protein/ml. It showed that decreasing cytosol protein concentration could increase the apparent binding sites detected.

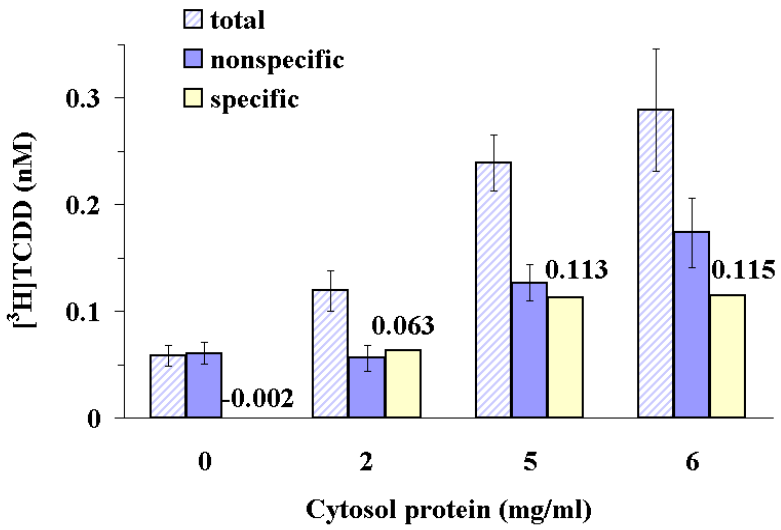

Figure 3- 30. Effect of protein concentration on binding of [^{3}H]TCDD to mouse liver cytosol

The radioligand (1nM) was incubated at 4˚C with varying concentrations of liver cytosol preparation (0, 2, 5 and 6mg/ml in MENG buffer) in the presence or absence of a 200-fold excess of competitor TCAOB (Section 2.7.1.5). To 0mg/ml preparation, BSA at 6mg/ml in assay buffer was added. After 16h incubation, free radioligand was removed by charcoal-dextran treatment. Aliquots of the resultant solution from each sample were collected for scintillation counting. Total, nonspecific and specific binding was determined (Section 2.7.1.7). Each bar represents the mean ±S.E. of triplicate samples.

3.5.3 Effect of charcoal-dextran

Dextran-coated charcoal is known to remove, by adsorption, any unbound and loosely bound radioligand in solution prior to the assay of bound radioligand in the medium (Hulme 1993). Due to the reversible nature of [^{3}H]TCDD binding it is possible that too much charcoal may remove bound TCDD in addition to unbound TCDD. Therefore, a range of charcoal-dextran concentrations (0.1-2mg/mg of cytosol protein) was tested (Manchester, et al. 1987).

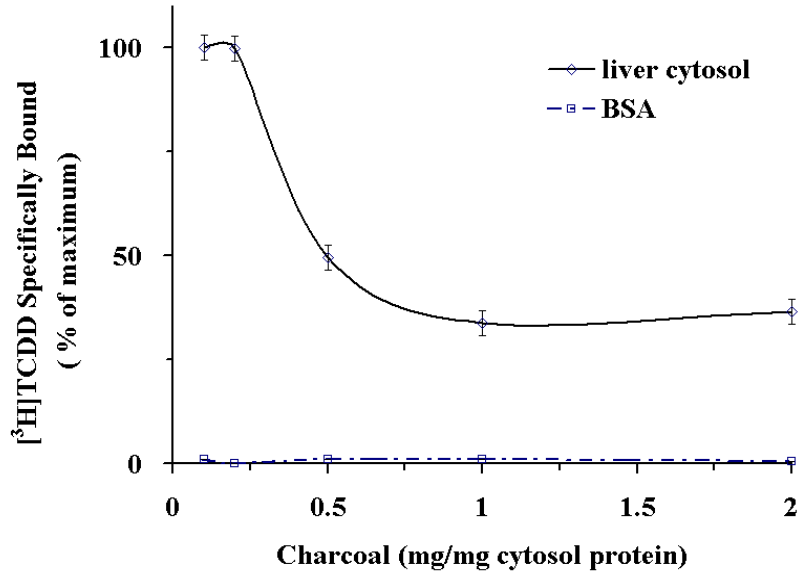

Figure 3- 31. Binding of [^{3}H]TCDD to liver ytosol at varying charcoal concentrations
[^{3}H]TCDD (1nM) with or without a 200-fold excess of TCAOB was incubated with mouse liver cytosol or BSA (5mg/ml) for 16h at 4˚C. The mixtures were then treated with varied amounts of charcoal-dextran (0.1, 0.2, 0.5, 1 and 2mg/mg of cytosol protein) dissolved in assay buffer. Charcoal-dextran was removed by centrifugation at 24000 g for 10min. Radioligand in solution was measured and specific binding was determined (Section2.7.1.7). The abscissa is [^{3}H]TCDD specifically bound, in percentage of the maximum, and the ordinate is charcoal concentration (mg/mg of protein). Each point shows mean ±SD of triplicate samples.

The critical effect of charcoal-dextran on specific binding of TCDD to liver cytosol can be seen in Figure 3-31. Within the charcoal concentrations of 0.1-0.2 mg/mg of cytosol protein, the detected specific binding was the highest. At the charcoal concentration of 0.5mg/mg protein, the specific binding fell by 50%. Further excessive charcoal (1-2mg/mg of cytosol protein) caused about 75% of specific binding loss. Therefore, a level of 0.2mg charcoal per mg protein provides a balance between an unacceptably high background radioactivity and excessive “stripping” of specific binding from the receptor. It could also be seen that under the same experimental condition, changes of charcoal concentration had no effect on [^{3}H]TCDD binding to BSA, showing BSA does not specifically bind to [^{3}H]TCDD (Figure 3-31).

3.5.4 Analysis of binding of [^{3}H]TCDD to hepatic cytosol

Based on the investigations presented above, optimal conditions for radioligand binding assay were chosen to be:

Radioligand concentration ranging from 0.1 to 2.6 nM

Cytosol protein concentration of 5mg/ml

Incubation time of 16h at 4ºC

Charcoal-dextran concentration of 0.2mg/mg of cytosol protein

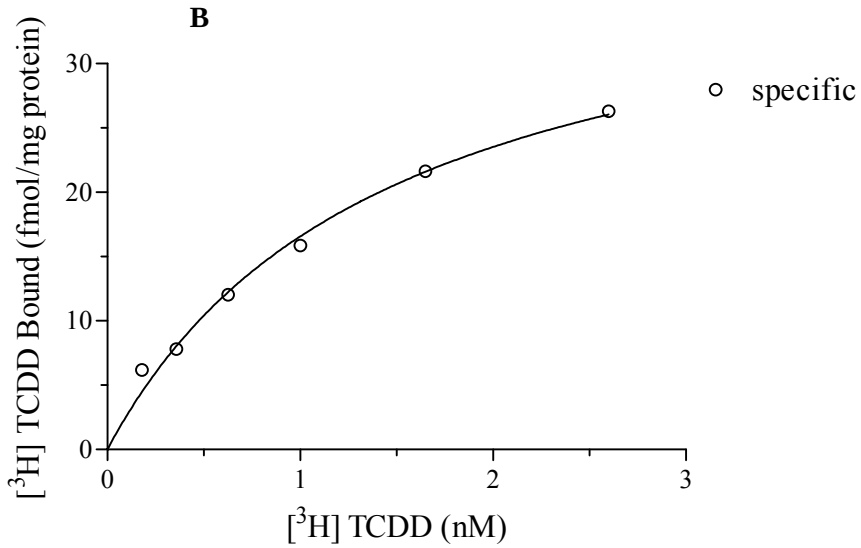

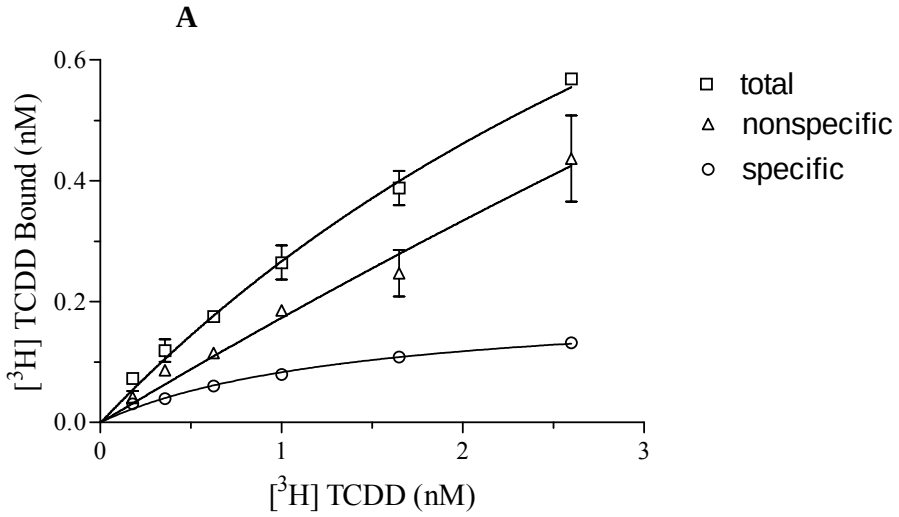

Figure 3- 32. Binding of [^{3}H]TCDD to rat liver cytosol.
A, varying concentrations of [^{3}H]TCDD, ranging from 0.179 to 2.6 nM, were incubated with 5mg/ml of rat liver cytosol with presence and absence of a 200-fold excess of competitor TCAOB. After 16h incubation at 4C, free radioligand was removed by charcoal-dextran treatment. Aliquots of the resultant solution form each sample were collected for scintillation counting. Total, nonspecific and specific binding was determined as described. Each point represents the mean ±SD of triplicate samples. **B**, specific binding data from Figure A were plotted to show specific binding capacities (fmol/mg cytosol protein) of [^{3}H]TCDD within the concentrations tested. Each point represents the average of triplicate samples. One side binding analysis was performed using GraphPad Prism version 4.00 for Windows (GraphPad Software, San Diego California USA).

A representative binding curve for [^{3}H]TCDD binding to the AhR in mouse liver cytosol determined under these conditions is shown in Figure 3-32A. In Figure 3-32B, specific binding in Figure 3-29A was plotted as the binding capacity (fmol/mg of protein) of AhR against different concentrations of [^{3}H]TCDD added. Under these conditions, the number of binding sites (B_{max}) was calculated to be 40.6±3.59 fmol/mg of cytosol protein, with an apparent affinity (K_D) of 1.45±0.25 nM; a correlation coefficient of 0.988 was calculated by Graphpad Prism version 4.00 using a one site binding equation. The results were consistent with previous reports as compared in Table 3-4. Therefore, these specially modified assay techniques could be used to detect and accurately quantitate receptor binding in

the following experiments.

[^{3}H]TCDD Ci/mmol	Cytosol Protein	K_D nM	B_{max} fmol/mg of protein	References
52.5	2mg/ml	0.27	84	Polane *et al*., 1976
55	5mg/ml	2.4	187	Manchester *et al.*, 1987
34.7	5mg/ml	1.45	40.6	Present study

Table 3- 4. Comparison of saturation binding of [^{3}H]TCDD to mouse liver cytosol
The saturation binding were performed on the AhR at various protein concentrations and the radioligand [^{3}H]TCDD with different specific activities. The binding parameters K_D and B_{max} are compared.

3.5.5 Displacement of [^{3}H]TCDD specific binding by DF203

Many drug candidates are ligands for AhR, but differ widely in their binding affinities. Binding affinity of these compounds for the AhR could be determined by a competitive binding assay. 2-(4-Amino-3-methylphenyl)benzothiazole (DF203) is an anticancer drug candidate. Its binding affinity for the AhR was measured by its capacity to compete with the specific binding of [^{3}H]TCDD. [^{3}H]TCDD at 1nM ± TCAOB was incubated with liver cytosol protein of 5mg/ml for 16h at 4ºC. Initial specific binding of [^{3}H]TCDD was determined as described in Section 2.7.1.5. The other experiment was run simultaneously with increasing concentrations of DF203 as a competitor to displace the specific binding of [^{3}H]TCDD (Section 2.7.2.1). The displacement was calculated as described in Section 2.7.2.2.

The competitive binding curve was shown in Figure 3-33. The initial total bound ligand was 1,4452 dpm, nonspecific binding was 9,770 dpm and specific binding was 4,682 dpm. The concentration of DF203, which produces a reduction in specifically, bound radioligand equal to one-half the initial value (EC_{50}) was 1.02E-7±0.20 M.

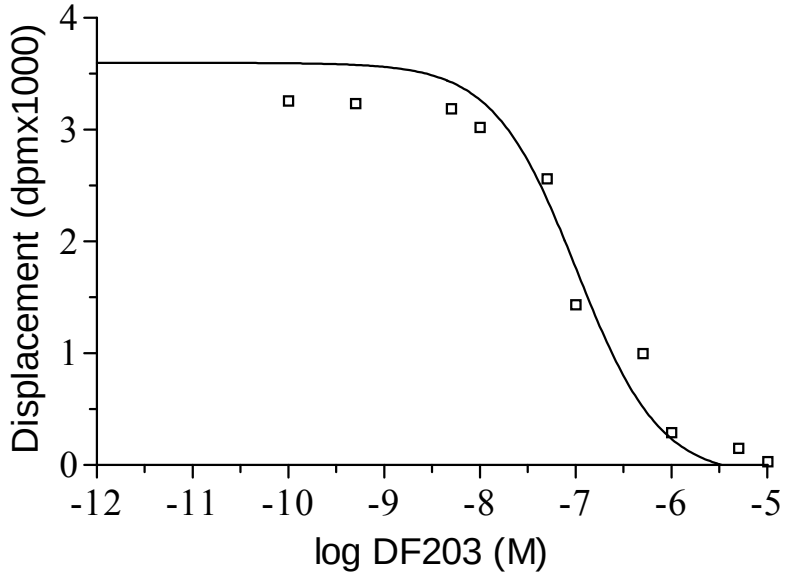

Figure 3- 33. Competitive binding of DF203 for specific binding of [^{3}H]TCDD to mouse liver cytosol.
The assay was run as described in Section 2.7.2.1, with increasing concentrations of DF203, a total radioligand concentration of 1 nM and liver cytosol protein of 5mg/ml. The competition binding curve was analyzed by using GraphPad Prism version 4.00 for Windows (GraphPad Software, San Diego California USA). Ordinate: [H3] TCDD concentration counted in dpm x1000; abscissa: log molar concentrations of DF203. Each value was the result of triplicate determinations.

3.6 Characterization of the recombinant AhR LBD

Since the AhR is highly instable in nature, it was important to determine the conditions under which Sf9 cell cytosol containing recombinant AhR could be prepared and stored without loss of specific binding capacity. Therefore under

different conditions baculovirus infected Sf9 cell cytosol was prepared and ligand-binding activity evaluated.

3.6.1 Effect of molybdate on specific binding

Molybdate has been shown to stabilize the low affinity mAhR allele (d-allele), and to have little effect on high affinity alleles (b-alleles) (Poland et al, 1990). Therefore, the stability effect of molybdate on recombinant AhR was investigated. AhR228 (residues 228-416) cytosol was prepared from infected Sf9 cells and assayed for its binding activity with MENG buffer containing varying concentrations of sodium molybdate (0, 5, 10, 20 and 30 mM), or 30mM of potassium chloride as described in Section 2.7.1.2. Figure 3-34A shows that molybdate affected AhR binding activity in a concentration dependent manner, with the maximum binding activity at a molybdate concentration of 10mM. If the AhR228 cytosol was prepared and assayed in buffer without molybdate, the binding activity was completely lost. The stabilizing effect of molybdate could not be substituted by potassium chloride. A Western blot (Figure 3-34C) shows that molybdate kept a greater amount of recombinant AhR in solution indicating that greater specific binding of TCDD is due to increased levels of soluble protein. In contrast, the effect of molybdate on binding activity of native AhR in B6 mouse liver cytosol was minor, with only 10% increase in the presence of 10mM of molybdate (Figure 3-34B). This experiment showed that inclusion of 10mM molybdate in buffer throughout cytosol extraction and binding assay was absolutely necessary to stabilize the recombinant AhR LBD.

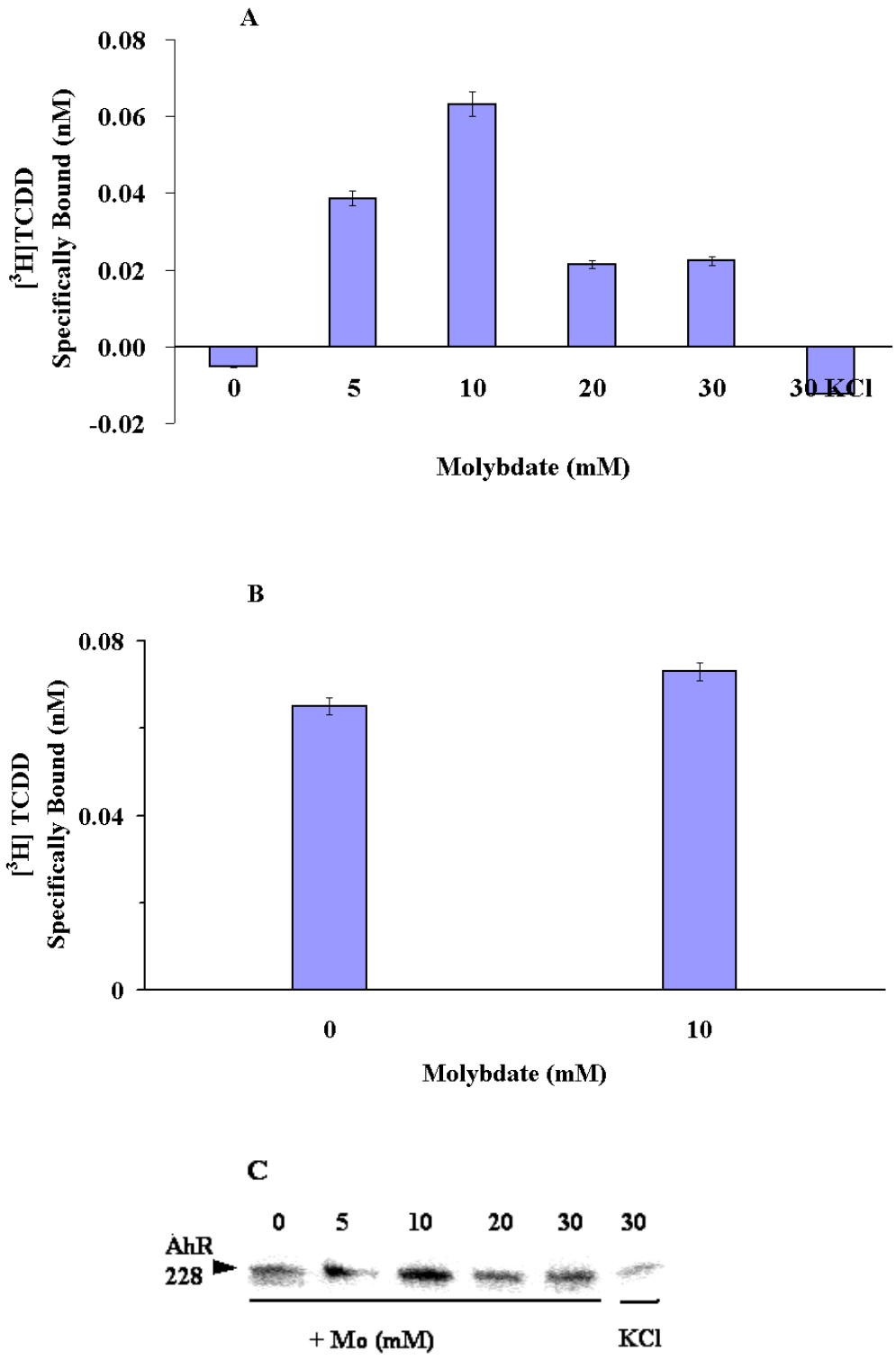

Figure 3- 34. Effect of molybdate on specific binding.
A, Specific binding of [^{3}H]TCDD to AhR228 prepared in the presence of different concentrations of molybdate. The *abscissa* showed molybdate concentration and the *ordinate* showed [^{3}H]TCDD specifically bound (nM). **B**, Specific binding of liver cytosol

in the presence and absence of 10mM of molybdate. Each bar showed the average ±SD of triplicate samples. **C**, Western blot for AhR LBD. The samples prepared in A were subjected to Western blotting, and 10µg of cytosol protein loaded per track. Numbers on the top of the blot show the concentrations of molybdate or potassium (mM). The position of the AhR228 was indicated by an arrowhead on the left of the blot.

3.6.2 Effect of Triton X-100 on specific binding

The nonionic detergent, Triton X-100, is a common component in protein extraction buffers (Meyer, 1999). Its effect on AhR binding activity was examined. Mouse liver cytosol and Sf9 cell cytosol were prepared with MENG buffer containing 0.1% of Triton X-100 as described in Sections 2.7.1.1 and 2.7.1.2. Cytosols were then further diluted with buffer in the presence and absence of Triton X-100 for binding assay. Specific binding was determined as described in Section 2.7.1.7. In the presence of Triton X-100, the specific binding of AhR in liver cytosol decreased by 57%, whereas specific binding of AhR228 was completely lost. Figure 3-35A shows that AhR expressed in Sf9 cells was more sensitive to Triton X-100 compared with AhR in mouse liver cytosol.

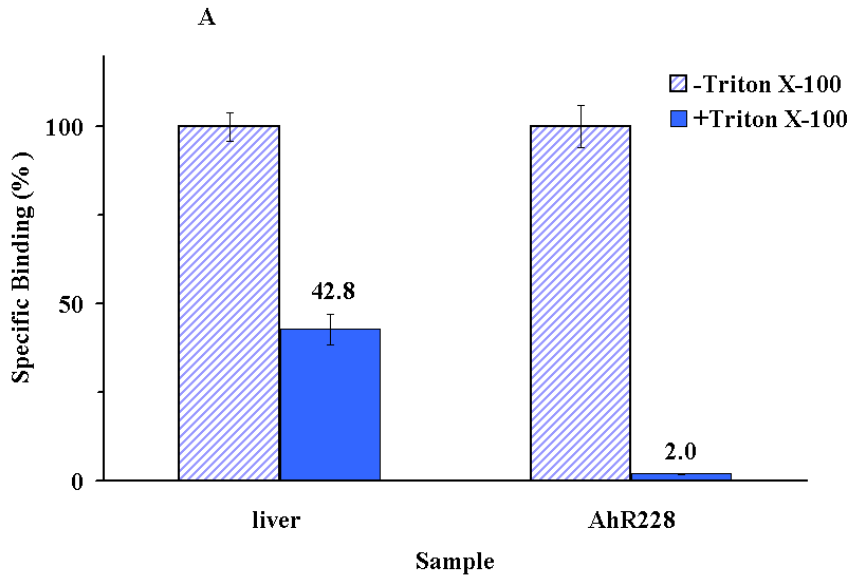

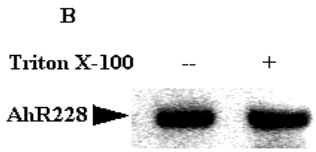

Figure 3- 35. Effect of Triton X-100 on [^{3}H]TCDD specific binding
A, loss of specific binding in Triton X-100 containing buffer. Specific binding of AhR in buffer without Triton X-100 was arbitrarily set as 100%. The *ordinate* showed specific binding of AhR to [^{3}H]TCDD in percentage of that without Triton X-100 in buffer. Each bar showed the average of triplicate samples from two independent determinations. **B**, a representative Western blot for AhR228 prepared in the presence and absence of Triton X-100 in buffer. The AhR228 was indicated by an arrowhead on the left of the gel.

Triton X-100 abolished the specific binding of TCDD to AhR228, but it increased the recovery of AhR in solution (Figure 3-35B) and is known to increase solubility of TCDD in solution (Poland 1976).

3.6.3 Thermal stability of AhR

Thermolability is a powerful tool for detection of changes in the AhR protein structure (Poland 1994). Therefore the effect of temperature on specific binding of AhR in liver cytosol and Sf9 cell cytosol was evaluated.

In the first experiment, separate aliquots of fresh cytosol from rat liver or baculovirus infected Sf9 cells were subject to indicated cycles of freeze-thaw by freezing at –80˚C and thawing on ice. Aliquots of Sf9 cell cytosol from each treatment were used for Western blot analysis of the AhR concentration in solution. The rest of the samples were then incubated overnight with radioligand TCDD at 4˚C for determination of specific binding (Section 2.7.1.5). In Figure 3-36A is a plot of specific binding (specific binding at a given time as a fraction of initial specific binding) of different cycles of freeze-thaw. It showed that the binding capacities of both liver and Sf9 cell cytosol underwent a constant decline

after increased cycles of freeze-thaw. However, the amount of the AhR in solution detected by Western blot did not show any difference after different cycles of freeze-thaw treatment (Figure 3-36B).

Through this experiment it was concluded that functional AhR should not be prepared by freeze-thaw method, and that repeated freeze-thaws should be avoided during storage of the AhR preparations.

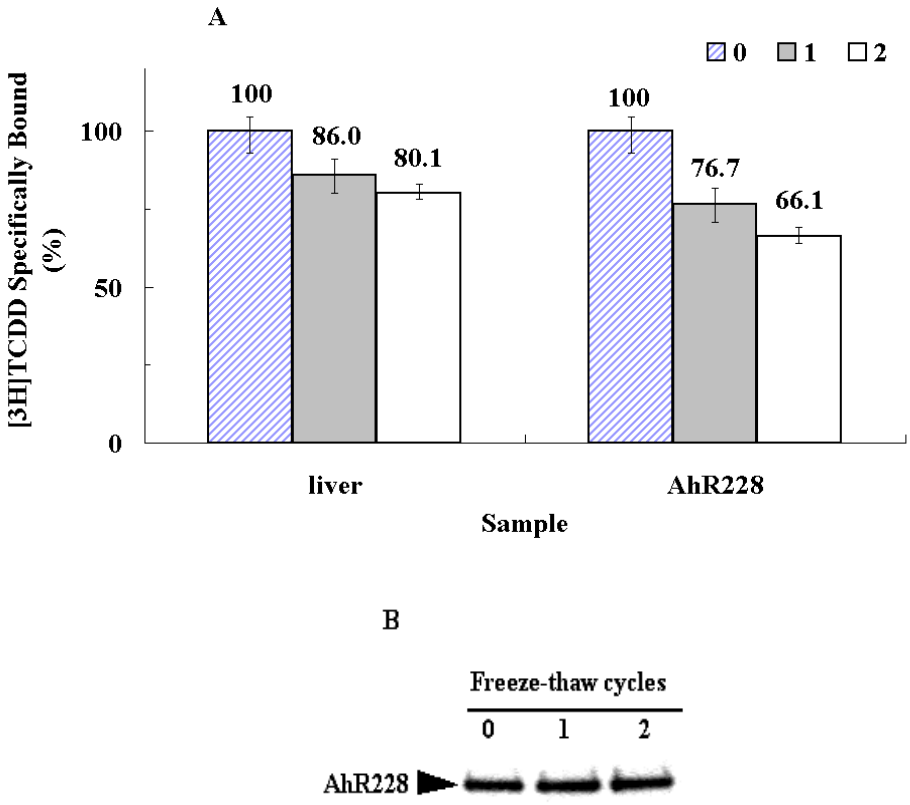

Figure 3- 36. The effect of freeze-thaw on the inactivation of the AhR from mouse liver and baculovirus infected Sf9 cells.
A, loss of specific binding after indicated cycles of freeze-thaw. Cytosols were pretreated and specific binding was determined as described in text. Each bar represented the fractional specific binding resulted from triplicate determinations: dashed bar, 0 cycle; gray bar, 1 cycle and open bar, 2 cycles. **B**, a representative Western blot of AhR228 in Sf9 cell cytosol (10μg/lane) after indicated cycles of freeze-thaw. The position of AhR228 was showed by an arrowhead.

Second experiment was carried out to determine the half-lives of the AhR in liver and Sf9 cell cytosol in response to thermal denaturation. Separate aliquots of fresh mouse liver and Sf9 cell cytosols were preincubated for various time periods at 30˚C prior to a TCDD binding assay. Specific binding was measured as in Section 2.7.1.7. In Figure 3-37A is a plot of specific binding (specific binding at a given time as a fraction of initial specific binding) versus time of incubation at 30˚C. Linear regression analysis showed that the half-life of binding site inactivation was 100 min for both AhR from mouse liver and from Sf9 cell cytosol (Figure 3-34A).

Aliquots of Sf9 cell cytosol from each preincubation at 30˚C were used for Western blot analysis of the AhR in solution. Figure 3-37B shows that the AhR228 concentration in solution did not change over a period of 200 min incubation at 30˚C. This indicates that the inactivation of the AhR binding activity was not due to gross proteolysis, and suggests that it is likely due to changes of tertiary structure during the high temperature treatment.

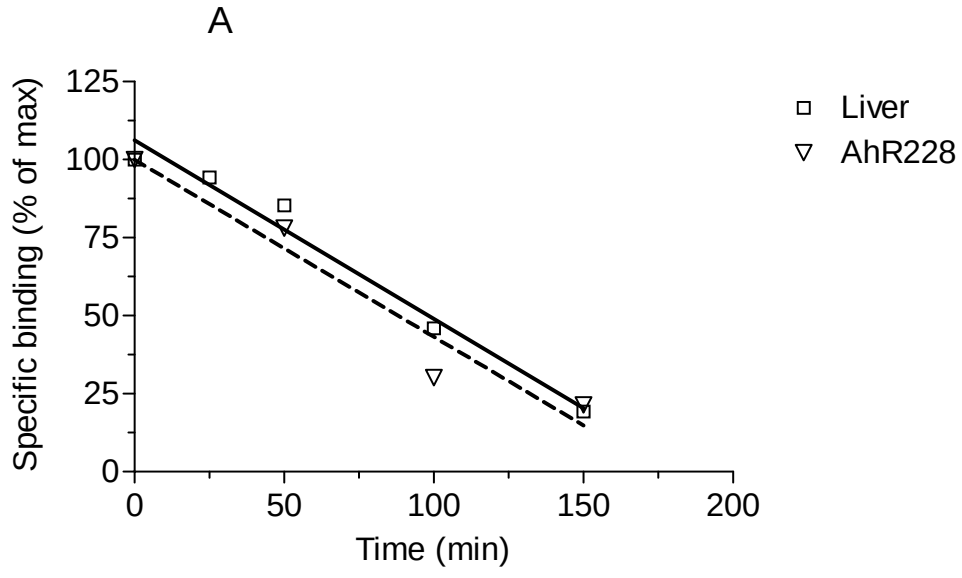

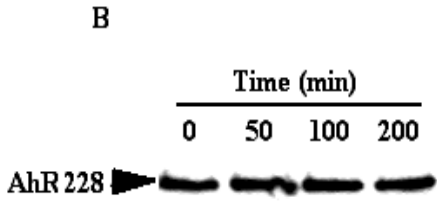

Figure 3- 37. The effect of temperature on theraml inactivation of the AhR
A, fresh rat and Sf9 cell cytosols were preincubated for various time periods at 30˚C prior to addition of TCDD ± TCAOB and overnight incubation at 4˚C, as described in text. The data points shown are the means of triplicate samples (□, AhR in rat liver and ▼, AhR228 in Sf9 cells). Linear regression analysis was done by GraphPad Prism version 4.00 for Windows (GraphPad Software, San Diego California USA): solid line for liver cytosol, r^2=0.976; and dashed line for AhR228, r^2= 0.940. **B,** Western blot analysis of AhR228 incubated at 30˚C for indicated periods of time. The incubation time was given on the top and the position of AhR228 was indicated.

3.6.4 Effect of sonication during Sf9 cell rupture

In order to recover the recombinant AhR efficiently, means to rupture the cells were evaluated. Sf9 cells resuspended in lysis buffer were broken on ice, either by homogenization as described in Section 2.7.1.2, or sonication with varying length of time, i.e. 15, 25, 30 and 45 seconds at 10% of maximum power. Cytosol was then prepared and specific binding determined as described in Se ction .7.1.7.

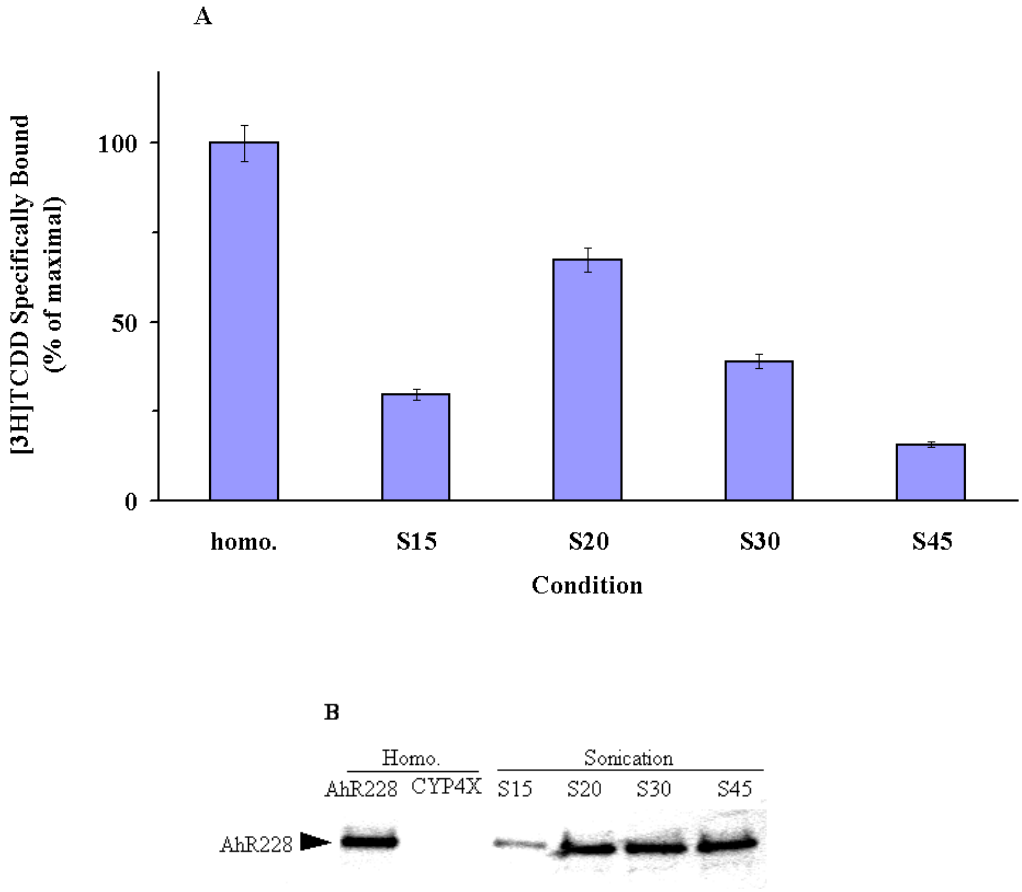

Figure 3- 38. Effect of sonication on specific binding.
A, specific binding of the AhR in Sf9 cell cytosol extracted under different conditions. Homo. represents homogenization; S15, S20, S30, and S45 represent sonication for 15, 20, 30 and 45 seconds. Each bar shows the mean ± SD of triplicate samples. **B**, Western blot of AhR228 in each cytosol preparation. The position of the AhR228 was shown by an arrowhead on the left of the gel.

The results in Figure 3-38A show that AhR recovered by homogenization retained the highest binding activity, whereas different lengths of sonication yielded the AhR with lower binding activity. Increasing sonication time (20-30 seconds) could yield increased binding activity.

Aliquots of the sample from each preparation were analyzed by Western blot for the AhR in solution (Figure 3-38B). It showed that higher concentrations of AhR

were found in homogenization and longer time sonication (>20 seconds) preparations. However, the concentration of soluble AhR was not simply related to binding activity after cell lysis by sonication. Taken production and activity into consideration, cell lysis by homogenization was a better way to recover functional recombinant AhR from infected Sf9 cells, therefore this method was adopted in the rest of the preparations.

3.7 Binding capacity of recombinant AhR LBD

Having optimised recombinant AhR LBD expression and recovery conditions, the functionality of recombinant AhR was further examined by a radioligand-binding assay. AhR228 was used as a model to determine the properties of Sf9 expressed AhR, and followed by the determination of binding property of each construct individually.

3.7.1 Titration of binding of the AhR228

It was speculated that the expressed AhR in SF9 cells might have very large pool size of binding sites. Therefore, binding capacity of the AhR228 to TCDD was titered. Freshly prepared AhR228 in Sf9 cell cytosol was serially diluted into 0.1 to 1.5 mg of cytosol protein/ml with assay buffer containing 5mg of BSA/ml prior to a TCDD binding assay. The binding results show that the specific binding of AhR228 to TCDD was protein concentration-dependent (Figure 3-39). Specific binding increased linearly with increasing protein concentration up to 1mg/ml.

Above this concentration, however, specific binding decreased. This might be because there were too much AhR in solution, which cased extensive binding of TCDD. This overwhelmed the capacity of the binding system to block nonspecific binding with limited competitor TCAOB. Should this happen, specific binding could not be determined accurately.

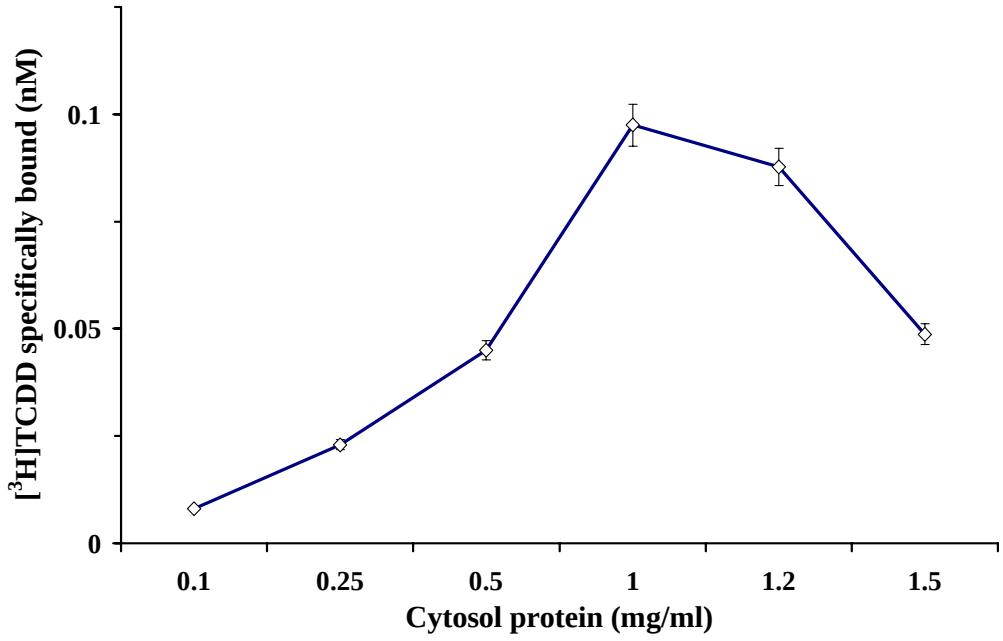

Figure 3- 39. Specific binding of [^{3}H]TCDD to AhR228 at different cytosol concentrations.
[^{3}H]TCDD at 1nM was incubated with AhR228 in Sf9 cell cytosol of varying concentrations (0.1, 0.25, 0.5, 1.0, 1.2 and 1.5 mg cytosol protein/ml). Radioligand binding assay was performed and specific binding determined (Section 2.7.1.7). The *abscissa* showed the cytosol protein concentration, and the *ordinate* showed [^{3}H]TCDD specifically bound (nM). Samples were in triplicate. Each point represented mean ± SD.

3.7.2 Titration of binding of the AhR265, AhR286 and AhR410

Determination of binding capacities of the rest of the AhR constructs were then carried out with the same profile as used for AhR228, i.e. by holding the radioligand concentration constant at 1nM, varying cytosol protein concentration. Mouse liver cytosol, BSA and CYP 4X in Sf9 cell cytosol were used as positive and negative controls, respectively. Specific binding of each construct was presented in Table 3-5 as fractional specific binding of liver cytosol. The results show that all AhR constructs expressed in Sf9 cells specifically bind to TCDD. And the binding capacity was concentration-dependent. Compared to other constructs, the AhR228 showed the highest binding capacity at protein concentration of 1mg/ml. This was true in repeated experiments.

Cytosol Protein (mg/ml)	5	1	0.5	0.25	0.1
Liver	100				
AhR228		100.41	35.35	17.35	1.98
AhR256		67.34	32.79	16.93	14.87
AhR285		82.22	57.69	10.02	
AhR410		89.44	49.67		
CYP 4X		0.01			
BSA	0.02				

Table 3- 5. Concentration-dependent of specific binding of recombinant AhR LBD constructs for radioligand TCDD.
Freshly prepared cytosol from Sf9 cells infected with corresponding AhR LBD constructs or CYP 4X were serially diluted into indicated concentrations with assay buffer plus 5mg/ml of BSA. Mouse liver cytosol was diluted into 5mg/ml. Protein dilutions were incubated with radioligand ^{3}[H] TCDD (1nM) ± 200-fold access of competitor TCAOB for 16h at 4ºC. Specific binding was determined (Section 2.7.1.7). Specific binding of liver cytosol at 5mg/ml was arbitrarily set as 100%, and specific binding of each recombinant AhR at a given concentration was expressed as a fractional specific binding. Samples were in triplicate means taken.

In conclusion, functional AhR LBD has been successfully expression in Sf9 cells using a baculovirus expression system. A minimal AhR ligand-binding domain can be down to 125 amino acids long (residuals 285-410 of the mAhR protein). This molecular size would be favourable for structural study.

Chapter 4. Discussion

4.1 Expression of recombinant cytochrome b5

Cytochrome b5 (b5) is required for the function of a number of cytochrome P450-catalyzed metabolisms of many exogenous compounds, some of which also act as P450 inducers or the AhR ligands. Among them chlorobenzene and benzo[a]pyrene are included (Waskell, Vigne et al. 1991).

4.1.1 Expression conditions

A goal of the present experiment was to produce high-level functional human version of b5. This has been achieved by using pRSET expression vector and *E. coli* strain C41(DE3). The expression vector, pRSET carries a strong T7 promoter derived from pUC expression vectors designed for high-level protein expression and purification. The host cell, C41(DE3) provides the T7 RNA polymerase from the λ-lysogen DE3 to induce the target protein. However the DE3 lysogen in C41(DE3) contains mutations, which produce either deficient or less T7 RNA polymerase (Miroux and Walker 1996)These effects are supposed to prevent uncoupling of transcription and translation leading to moderate levels of protein expression but increased cell viability and decreased plasmid loss during growth of cultures. Therefore C41(DE3) has been widely used for its reported low toxicity mediated by IPTG induction of membrane protein expression (Miroux and Walker 1996).

Prior to the present experiment, expression of b5 was investigated in our laboratory from BL21(DE3)-pRSET- and HMS174(DE3)-pRSET-b5 cells (Minqi Fan, unpublished observation). In these cells phage T7 was inhibited by the phage's lysozyme provided by the additional plasmid pLysS in the cells. However, it was reported that the pLysS did not suppress the toxicities of some target proteins when these proteins were induced by IPTG, which proved to be lethal to the host cells (Miroux and Walker 1996). As a starting point, in the present experiment a similar expression condition (i.e. cultural temperature, inducer's concentration and induction time) was used. It was found that b5 yields from pRSET-b5 in C41(DE3) were routinely 7- to 10-fold higher than the same plasmid in BL21(DE3) or HMS174(DE3). This result is in agreement with a previous report, in which mammalian b5 production using T7 expression system in C41(DE3) was 4- to 10-fold higher than the same expression vector in BL21(DE3) (Mulrooney and Waskell 2000)). Interestingly, in this experiment C41(DE3) cells were cultured at 37ºC with induction time of 10-16 hours, whereas BL21(DE3) cells were kept at room temperature and induction time was ~40 hours (Mulrooney and Waskell 2000). It is clear that the expression conditions are greatly depending upon the host cells. A higher temperature may bring about higher b5 protein production in C41(DE3), but not in BL21(DE3) cells. This is probably due to fact that the T7 promoter in C41(DE3) is less strong than that in BL21(DE3). As a result the toxicity caused by the overexpression of membrane protein b5 was effectively reduced in C41(DE3) cells, which contributed to the increased cell viability and plasmid retention (Miroux and

Walker, 1996; Mulrooney and Waskell 2000). However in BL21(DE3) cells the strong T7 promoter usually brings about high level of target protein expression in the presence of pLysS, hence increased the toxicity to the cells. Therefore moderate cell growth and expression speeds may somewhat be beneficial for protein production. However even under an optimised condition the expression levels of b5 in BL12 (DE3) was constantly lower than that in C41(DE3), indicating that *E. coli* strain of C41(DE3) is a better host for membrane protein expression. This result is consistent with other investigations (Holmans, Shet et al. 1994); Mulrooney and Waskell 2000).

In the present study, the optimal IPTG concentration for the protein induction was investigated and determined to be 100 μM, whereas reduce IPTG concentration to 5-10 did not greatly reduce protein induction. This result is in agreement with a previous report (Mulrooney and Waskell 2000). As mentioned above, in C41(DE3) the reduced level of T7 polymerase weakens T7 promoter activity. As a result, changes in IPTG concentration could not actively affect the target protein transcription level. Therefore this system is not sensitive to high concentrations of IPTG.

4.1.2 Reconstitution of apo-b5

The yield of the b5 in intact cells directly measured by spectrophotometer reached the highest level (3.5nmol/ml of culture) when grown at 28ºC in the presence of 0.1mM of IPTG, whereas higher temperature did not increase the level of spectrally measurable b5 in intact cells. Interestingly, at 30˚C a yield of wet cell

pellet per 500ml of culture was routinely higher than that at 28˚C (11.0g vs. 8.8g), indicating that the cells continued to grow to high cell densities after the induction of expression. By addition of exogenous hemin into the sonicated cell suspension from this culture, a spectrally functional b5 was reconstituted indicated by an increase in absorbance at 412 nm (Figure 3-4), characteristic of the oxidised state of b5. Thereby, a higher level of b5 production was obtained in cultures at 30˚C than that at 28˚C. This may be because of b5 protein synthesis driven by T7 promoter being seven times higher than in the *E. coli* host (Makarova, Makarov et al. 1995). Consequently, a mixture of apo and holo protein is produced since haem synthesis and incorporation of hemin cannot be maintained at comparable levels to protein expression. The accumulation of apo-b5 in high levels in C41(DE3) cells was reported previously, in which more than 90% of overexpressed b5 was in apo form and could be reconstituted by addition of exogenous heme to the lysed cells containing the apoprotein (Mulrooney and Waskell, 2000). It is also supported by the present observation that cells grown at 30˚C appeared faint hint of red colour in the cell pellet. When the growth temperature was lowered to 28˚C the cell culture was a visibly more intense colour suggesting a greater incorporation of hemin by cytochrome b5. Therefore hemin is absolutely required to reconstitute functional b5. The reconstituted b5 showed an increased stability during protein purification process.

4.1.3 Purification of b5

Incorporation of a H-tag at the N-terminal of b5 allowed the use of immobilized nickel affinity column for purification of the expressed b5, which was proved

successful in previous reports (Mulrooney and Waskell, 2000; (Begum, Newbold et al. 2000). However, in the present study b5 purified from nickel affinity chromatography was contaminated with other proteins, and then it was further purified on Uno Q ion exchange chromatography. Two-step purification procedure yielded a preparation of b5 without any detectable impurities (Figure 3-8). The purified b5 showed a characteristic spectrum peaked at 421 nm (Figure 3-9).

In summary, an *E. coli* expression system has been described that led to a high-level of human cytochrome b5 production. The yield of the b5 in intact cells reached 4000 nmol/liter of cell culture. Although majority of the expressed b5 was in apo form, it was readily reconstituted by addition of exogenous hemin. Two-step purification procedure yielded a spectrally functional b5 with total recovery rate of 19.2%.

4.2 Expression and characterization of the AhR LBD

AhR LBD was originally identified in a CNBr cleavage fragment, which bound to photoaffinity-labeled ligand (Burbach and Poland 1992), and confirmed by others in deletion experiments (Dowick and Swanson 1993; Poland et al. 1994; Fukunaga, et al. 1995; Coumailleau, et al. 1995; McGuire, et al. 2001). It has been established that a minimal LBD (residues 230-421) possesses ligand binding and hsp90 interaction activities, thereby binds to ligand with high affinity similar to that in the full-length AhR (Coumailleau, et al. 1995; McGuire et al. 2001). In the present study truncated LBDs were expressed in *Spodoptera frugiperda* (Sf9) cells using BAC-TO-BAC baculovirus expression system. Functionality analysis showed that the recombinant proteins bound radioligand TCDD with high-affinity, which is similar to their native counterpart from mouse liver cytosol.

4.2.1 Polyclonal antibody to the AhR LBD

LBD is part of a much larger protein. Commercially available antibodies to the AhR protein, produced with pepitides corresponding to amino acids outside of LBD might not react with LBD. Therefore an antibody to LBD was required for the analysis of expressed AhR LBD, and so the construct 5g (containing residues 285-416) was used to produce antigen by bacterial expression. The bacterial expression yielded only an insoluble protein; however, it was proved to be a good antigen for the generation of antisera in rabbit, because two rabbits immunised produced high titre antisera. The 5g contains 131 amino acids of the mouse AhR,

of which 29 were charged, which may contribute to its antigenicity. The antisera can specifically detect as low as 0.3ng of the recombinant AhR LBD in the cytosol of Sf9 cells, and of wild type AhR in mouse liver cytosol. It can also detect the AhR from humans (personal communication with Dr. D.R. Bell). It is not surprising that the produced antisera react with AhR LBD and the AhR from B6 mice and humans, because the antigen 5g from murine AhR has 84% identity with the human AhR, and is fairly well conserved across species. Therefore, the antisera should prove useful for further studies. Although these antisera bind denatured antigen with high specificity, sensitivity and species cross-reactivity, the capacity of the antisera to immunoprecipitation of the AhR LBD has to be defined, as it has been reported that the LBD bound to hsp90 (Perdew, et al. 1996), and so may be masked by chaperone proteins.

4.2.2 Development of a [^{3}H] TCDD ligand binding assay

A sensitive and reproducible ligand-binding assay is required for functional analysis of the expressed AhR LBD. Therefore a series of experiments were set out to develop a reversible [^{3}H] TCDD ligand binding assay by using mouse liver cytosol as a source of the AhR. The assay yielded an estimate for the apparent equilibrium dissociation constant, K_D of C57B/6 mouse liver binding at 1.4nM, comparable with reported values, e.g. 1-3nM for mouse and rat AhR binding to [^{3}H] TCDD (Manchester, Gordon et al. 1987). However, it has been recognised that higher specific activity of the radioligand can lead to an increase in sensitivity of the ligand binding assay. When a much higher specific activity radioligand [^{125}I]2-iodo-7,8-dibromodibenzo -*p*-dioxin (2176 Ci/mmol) than [^{3}H]TCDD

(34.7Ci/mmol), was used, a much lower K_D of 6.5pM was obtained (Bradfield, Kende et al. 1988).

The present optimised ligand-binding assay was sensitive and reproducible. This was further confirmed by a competitive binding assay. Competitive binding assay measures the specific binding of radioligand [^{3}H] TCDD that were displaced by different concentrations of competing ligand. The present study showed that 2-(4-amino-3-methylphenyl)benzothiazole (DF203), a novel and potent antitumour agent with selective growth inhibitory properties against human cancer cell lines (Kashiyama, Hutchinson et al. 1999), bound mouse AhR with the estimated ED_{50} of 0.102 ± 0.20 μM. Theses values were comparable to the IC_{50} (concentration causing 50% growth inhibition) of <0.1μM, which was encountered in the most sensitive breast cancer cell lines (Kashiyama, Hutchinson et al. 1999). Therefore this carefully modified ligand binding assay should prove useful not only for determination of biding capacity of the AhR, but also as a screen to detect other ligands, either exogenous or endogenous, of the AhR.

4.2.3 Expression of AhR LBD in Sf9 cells

There are no published reports of the AhR LBD expression in Sf9 cells except one paper reported expression of full-length AhR in baculovirus system, and so conditions of protein expression were optimised. Under optimal conditions, the total induced AhR accumulated over a period of six days post-infection, whereas the soluble form of the protein peaked at day two post-infection. Importantly, the expression levels of the four constructs were similar, which allowed direct

comparison of binding activity among these constructs. In the present study, a very high level of the AhR LBD was expressed; however, the majority of the LBD protein was insoluble. The soluble protein was indeed undetectable by Coomassie staining of SDS-PAGE, although it could be visualised by Western blot. In contrast to the present low concentrations of soluble AhR LBD recovered, a previous study reported that a 16% of total expressed full-length AhR protein could be recovered from Sf9 cells at 3-days post-infection by baculovirus (Chan, et al. 1994).

The reasons for the different soluble AhR protein yields are presently unclear but may reflect, in part, the different experiment conditions. First, the authors used high salt buffer (300mM KCl) and a single centrifugation of 16,000g for 15 minutes to extract soluble protein. However, in the present study, the cytosol protein was extracted with low salt buffer (MENG buffer) and two centrifugation steps (the second centrifugation was at 100,000g for 25 minutes). Second, in the previous study full-length AhR was prepared from the cells of three days post-infection by recombinant baculovirus, whilst the present study the LBD was prepared from baculovirus infected cells at day two post-infection. Given that the total protein accumulated over 6 days post-infection, the delayed harvest time coupled with lower centrifugation speed and high salt buffer for sample preparation was most likely to bring about a higher protein production. It is known that high salt concentration (0.3M KCl) in the buffer could significantly increase the amount of AhR extracted from mouse liver and cultured cells (Denison, et al. 1985; present study). Furthermore, high salt has deteriorated

effects on the receptor function (reviewed by Pratt and Toft, 1997). It has been shown that high salt disrupts the binding of the receptor to hsp90 complex, shown as converting the 9.4S receptor oligomeric complex into 4.9S receptor monomers (Denison, et al. 1986; Pohjanvirta, Viluksela et al. 1999). As a result the AhR in some strains of mouse and rat lost their ligand-binding ability (Kester and Gasiewicz 1987; Denison, et al, 1986; Pohjanvirta, Viluksela et al. 1999).

4.2.4 Aggregates of the expressed AhR LBD

In the present study, the majority of the overexpresssed LBD was insoluble. It was suggested that the overexpressed LBD tend to self-interaction than that of the full-length AhR (Chan, et al. 1994). Consistent with this notion, the DNA-binding domain of the AhR was soluble in bacteria (Chapman-Smith, Lutwyche et al. 2004; Kikuchi, Ohsawa et al. 2003), whereas LBD of the AhR was completely insoluble in bacteria (Comailleau, et al. 1995; present study). Steroid receptors are mechanistically similar to the AhR in requiring chaperone proteins for their proper folding and stabilising. Coincidentally, baculovirus expressions of the truncated glucocorticoid and minerialocorticoid receptors (GR and MR), lacking steroid binding domain were relieved of self-interaction. These truncated proteins were expressed in a soluble form (Alnemri and Litwack 1993), whereas over 90% of the overexpressed full-length GR and MR were found as insoluble aggregates in the nuclear fraction (Alnemri, Fernandes-Alnemri et al. 1993). These results suggest that expression of the full-length receptor protein aid solubility of the

AhR LBD. However, it remains to be seen whether there is any effect of the AhR N-terminus on the folding or function of the AhR LBD.

4.2.5 Coinfection of LBD with p23

The production of insoluble aggregates may relate to the lack of chaperone proteins necessary for proper receptor processing, folding and subcellular location. Among these chaperonins, hsp90 is thought as an essential component and p23 as a limiting component (Morishima, et al. 2003). It was hypothesised that increasing the levels of the chaperone proteins in the expression system might enhance the levels or the solubility of the expressed receptors. Therefore coexpression experiments were carried out in several laboratories and in the present study. Interestingly, coinfection of AhR LBD with p23 in the present study did not increase the amount of AhR LBD in cytosol, although it reduced the amount of AhR in 100 000 g pellet extract (Figure 3-27). This is in agreement with a previous study, in which coexpression of p23 with the GR did not alter the levels of GR in cytosol, although it reduced the insoluble form of the GR (Morishima, et al. 2003). In order to increase the solubility of the expressed receptors, a previous study coninfected GR and MR with hsp90 or hsp70. However, the results showed that the coinfection did not improve soluble receptor recovery or solubility (Alnemri and Litwack 1993). These results indicate that the solubility of the overexpressed receptor may controled by more complicated mechenisms rather than require some individual chaperone protein.

It has been shown that the formation of the receptor/hsp90 complex is ATP dependent (Bell and Poland 2000). Baculovirus infection of Sf9 cells resulted in the rapid depletion of glucose in the medium (Srinivasan, Post et al. 1997). The depletion of glucose from the medium could cause intracellular ATP depletion and consequently affect the formation of the receptor/hsp90 complex (Srinivasan, Post et al. 1997). In the present study, glucose supplementation of Sf9 cells infected with baculovirus-AhR led to an enhanced recovery of recombinant receptor in solution (Figure 3-25). This result is in disagreement with a previous study, in which the glucose supplementation of the Sf9 culture medium did not lead to any increased soluble receptor production (Srinivasan, Post et al. 1997). Therefore it is of great interest to see whether the enhanced soluble AhR production possesses ligand-binding activity.

The formation of the receptor/hsp90 heterocomplex is a dynamic process, which includes recruitment of a serious of factors in a well-defined order (Meyer, Petrulis et al. 2000; Murphy, Kanelakis et al. 2001; Murphy, Morishima et al. 2003). Overexpression of the receptors can overwhelm the capacity of the host cell system to properly process the receptors. As a result only a fraction of receptors expressed in the host cells are in complex with hsp90 whilst the majority of the receptors are present as in insoluble form or aggregates (Morishima, et al. 2003). Increasing intracellular ATP level or/and coexpression of the receptor with chaperone proteins may serve to enhance the heterocomplex formation, as indicated by higher levels of hsp90 associated with receptor (Alnemri and Litwack 1993). Heterocomplex formation with hsp90 may serve to inhibit

degradation of the expressed receptor, which may potentially increase the receptor recovery. However, the ubiquitin mediated protein degradation pathway may serve to balance the effects of any enhanced degradation (Pollenz 2002; McDonough and Patterson 2003; Song and Pollenz 2003; Galigniana, Harrell et al. 2004). This may explain the above observations, that there were no increased receptor levels in coexpression systems.

4.2.6 Fidelity of the recombinant LBD

The process for generating recombinant baculovirus involves homogenous recombination. It is important to confirm that the recombinational event had not affected the fidelity of the LBD protein sequence. Therefore the expressed AhR proteins, represented by proteins AhR228, AhR265 and AhR410, from whole cell lysate were subjected to tryptic digest, followed by MS analysis. Over 80% of the residues of the fragments from each protein were identified. Therefore the fidelity of the recombinant AhR peptides is confirmed. The data also reveal that there was no post-translational modification involving covalent binding; however, this information has limited utility. Because the vast majority of the protein used fro MS analysis was insoluble, and this may not reflect on the soluble and ligand binding form of the AhR. The N-terminus of each protein examined showed a mass consistent with proteolysis of the N-terminal methionine, followed by acetylation. Although this residue was not confirmed directly by MS/MS sequence, the N-terminal fragment was confirmed after the poly-histidine tag of pFASTBAC (Table 3-3). Therefore the recombinant AhR constructs were intact and verified the identity of the expressed protein. Having generated sufficient

amount of soluble form of the AhR LBD, it is both possible and of great interest to assess the ligand binding characteristics *in vitro*.

4.2.7 Binding specificity of recombinant LBD

In order to assess the binding specificity of the recombinant LBD, AhR228 (residues 228-416) was assayed for its ligand binding specificity by comparing with the wild type AhR. The results showed that the AhR228 specifically binds to radioligand TCDD, and the binding is receptor concentration dependent. The highest binding was detected at the concentration of 1mg/ml of Sf9 cell cytosol. Under this condition the specific binding sites of recombinant LBD was constantly at a level about 5-fold higher than that of the AhR in mouse cytosol (230 fmol/mg of cytosol protein from Sf9 cells vs. 40.6 fmol/mg of cytosol protein from mouse liver). It is worth noticing that based on Western blot data, the amount of the soluble AhR recovered from baculovirus infected Sf9 cell cytosol is approximately 0.15% of the cytosol protein. This discrepancy between LBD protein levels and ligand binding capacity in such cultures may reflect a limited capacity of Sf9 cell system to process the expressed LBD into a conformation with high-affinity for ligand binding.

Having established the specific binding of AhR228 to dioxin, the primary sequence requirement for ligand binding to AhR was further investigated. A series of constructs were produced, containing different lengths of the AhR. The results showed that all of the constructs showed specific binding to [^{3}H] TCDD. Thereby, minimal ligand-binding domain, residues 285-410, was redefined, which was

reduced to 125 amino acids in length. Published alignments of the mAhR with the PAS domain placed a β-sheet commencing at residue 218 (Procopio, et al. 2002). Based on a theoretical model for the LBD of the mouse AhR (residues 275-380), it was predicted that a positively charged residue Arg282 pointed to the chlorinated side of TCDD and may contribute to the binding by electrostatic interactions (Denison, et al. 2002). However, ligand-binding analysis clearly show that constructs commencing at amino acid 285 show ligand-binding functionality. It is unclear whether the alignments are in error, or whether the β-sheet is not required for folding of the PAS domain, and thus functionality. Clearly, further work to elucidate the structure of the AhR LBD is required.

4.2.8 Molybdate stabilise the recombinant AhR LBD

Molybdate has been shown to stabilise low affinity AhR (human and mouse d allele) (Manchester, Gordon et al. 1987; Okey, Vella et al. 1989) but to have little effect on high affinity AhR (mouse b alleles) (Poland and Glover 1990; Ramadoss and Perdew 2004). Consistent with this, the present study showed that the ligand binding capacity of the C57B/6 mouse AhR was not affected by addition of 10 mM molybdate in buffer. In contrast, molybdate was absolutely required for the ligand binding of the recombinant AhR LBD. In the absence of molybdate in the buffer through out the sample preparation and ligand binding assay, the specific binding of the LBD to [^{3}H]TCDD could not be detected, whereas with the addition of 10mM of molybdate, specific binding and a higher concentration of AhR LBD in solution were observed. Molybdate appeared both to enhance the ligand binding and to stabilize the recombinant protein, in agreement with the

suggestion that molybdate has an effect of reducing susceptibility to proteolysis (Poland and Glover, 1990).

In analogy to steroid hormone receptors, the LBD of the AhR must be bound to hsp90 for it to bind ligand. Molybdate ions have been shown to stabilize the interaction between hsp90 and a number of hsp90 interaction proteins (Kazlauskas, et al. 1999). The mechanism of action of molybdate was suggested by several investigators (Grenert and Jonson, et al. 1999; Kazlauskas, et al. 1998). In a mature AhR heterocmplex, molybdate binds to the hsp90 nucleotide pocket upon hydrolysis of ATP, keeping hsp90 in its ATP-bound conformation. As a result, the duration of the mature AhR/hsp90 heterocomplex was extended. It is believed that the mature complex can hold the receptors in a conformation with high affinity for ligands (Sullivan, Owen et al. 2002). In the present study LBD showed a high ligand-binding activity, however, in a molybdate dependent manner, indicating that its interaction with hsp90 is weaker than its native counterpart. It may be such that the interaction between AhR LBD and the insect hsp90 is less stable than with murine hsp90.

4.2.9 Triton X-100 affects ligand binding

Triton X-100 and Nonidet P-40 are nonionic detergents commonly used in protein assay buffers (Meyer and Perdew 1999; Lees, Peet et al. 2003). Previous reports showed that the formation of the p23/hsp90 complex was strongly promoted by molybdate and by the nonionic detergent Nonidet P-40 (Sullivan, et al. 1997; Dittmar, et al. 1998). The present study found that Triton X-100 affected

recombinant AhR function by completely abolishing its ligand binding ability, however, it did not affect the amount of the AhR in solution. In contrast, Triton X-100 reduced the specific binding of the AhR in mouse liver by 57% under the same experimental condition (Figure 3-35). It is clear that the recombinant AhR was more sensitive to Triton X-100 than that of its native counterpart. Effect of Triton X-100 on AhR ligand binding may due to perturbation of the tertiary structure of the AhR LBD. This different response of the native and recombinant AhR to Triton X-100 needs further investigation, since adverse effects of detergent on receptor function have also been reported (Poland, et al. 1976; Alnemri, et al. 1991). As demonstrated above, molybdate stabilizes the AhR whereas Triton X-100 destroys the ligand binding. It is therefore of interest to investigate if the simultaneous absence of Triton X-100 and presence of molybdate would exert an additive positive effect on these parameters.

4.2.10 Thermostability of recombinant LBD

Thermal stability is a powerful tool for differentiating between the various mouse alleles of the AhR (Poland and Glover, 1990), and knowledge of the AhR's thermostability may provide a basis for discrimination among various mechanisms of receptor dysfunction. Therefore experiments were set out to examine the relative thermolability between native and recombinant AhR. In these experiments, cytosol from mouse liver and Sf9 cells were prepared in the presence of 10 mM molybdate. The cytosols were heated at 30ºC for various times prior to incubation overnight with radioligand [^{3}H] TCDD at 4ºC for determination of specific binding. The data produced show that the rate of the heat inactivation of

specific binding to [^{3}H] TCDD is indistinguishable between native AhR and recombinant AhR LBD (Figure 3-37). Interestingly, the amount of the AhR LBD in solution remains unchanged after incubation for different length of time at 30ºC, showed no evidence of proteolytic degradation. The same phenomena were also observed when the cytosols were treated with different cycles of freeze-thaw prior to incubation with radioligand for detection of specific binding. These results are consistent with a previous investigation, which showed evidence that heat inactivated rat AhR was not due to proteases (Kester, et al. 1987).

A previous report showed significant difference of thermal stability between mouse Ah alleles (i.e. b-1, b-2, b-3 and d alleles), which indicated the differences in the primary protein structure (Poland and Glover 1990). In the present study the thermal stability of the AhR b-1 allele of C57B1/6 mouse cytosol and the recombinant LBD was indistinguishable, and Western blotting confirmed that the level of AhR LBD protein remained constant, thereby excluding proteolysis as a source of reduction in the amount of specific ligand-binding. Therefore the thermal stability of the AhR is a reflection on the LBD rather than on the interaction with chaperone proteins. The fact that the two proteins show an indistinguishable thermal lability provided the evidence for similar functionality in the ligand-binding domain.

4.2.11 Further work

A truncated AhR LBD was expressed in insect cells using a baculovirus expression system. The system yields soluble AhR LBD protein at ~0.15% of

cytosol protein and which retains its ligand binding activity. However there is a discrepancy between LBD protein levels and ligand-binding capacity in such cultures. It is known that the functionality of the AhR requires chaperone protein hsp90 and a number of cochaperones and the formation of the AhR/hsp90 complexes is an ATP dependent process. The present study showed that supplementation of the Sf9 culture medium with additional glucose resulted in an increase in the amount of soluble AhR, due to the a increased intracellular ATP level. However it is not clear whether the enhanced soluble AhR production is accompanied by a greater binding capacity of the LBD to dioxin. Furthermore, cotransfection of AhR with cochaperone p23 reduced the amount of AhR in high-speed pellet; through it did not change the level of soluble AhR. It is of interest to investigate the ligand binding capacity of the AhR LBD under further optimised expression conditions. Having established the binding activity of the recombinant LBD, the recombinant protein can also be used to screen other ligands, either exogenous or endogenous, of the AhR.

The aim of the project was to produce large amount of functional AhR LBD for crystallographic study. For this reason, a his-tag has been inserted into the N-terminal of the LBD construct for facilitating the recombinant protein purification on a Ni-NTA column. Therefore purification of the recombinant AhR LBD is necessary and can be performed based on a large-scale expression.

Chapter 5. References

Adachi, J., Y. Mori, et al. (2001). "Indirubin and indigo are potent aryl hydrocarbon receptor ligands present in human urine." J Biol Chem **276**(34): 31475-8.

Alnemri, E. S., T. Fernandes-Alnemri, et al. (1993). "Overexpression, characterization, and purification of a recombinant mouse immunophilin FKBP-52 and identification of an associated phosphoprotein." Proc Natl Acad Sci U S A **90**(14): 6839-43.

Alnemri, E. S. and G. Litwack (1993). "The steroid binding domain influences intracellular solubility of the baculovirus overexpressed glucocorticoid and mineralocorticoid receptors." Biochemistry **32**(20): 5387-93.

Alnemri, E. S., A. B. Maksymowych, et al. (1991). "Overexpression and characterization of the human mineralocorticoid receptor." J Biol Chem **266**(27): 18072-81.

Antonsson, C., M. L. Whitelaw, et al. (1995). "Distinct roles of the molecular chaperone hsp90 in modulating dioxin receptor function via the basic helix-loop-helix and PAS domains." Mol Cell Biol **15**(2): 756-65.

Ashida, H. (2000). "Suppressive effects of flavonoids on dioxin toxicity." Biofactors **12**(1-4): 201-6.

Begum, R. R., R. J. Newbold, et al. (2000). "Purification of the membrane binding domain of cytochrome b5 by immobilised nickel chelate chromatography." J Chromatogr B Biomed Sci Appl **737**(1-2): 119-30.

Bell, D. R. and A. Poland (2000). "Binding of aryl hydrocarbon receptor (AhR) to AhR-interacting protein. The role of hsp90." J Biol Chem **275**(46): 36407-14.

Berg, P. and I. Pongratz (2001). "Differential usage of nuclear export sequences regulates intracellular localization of the dioxin (aryl hydrocarbon) receptor." J Biol Chem **276**(46): 43231-8.

Berg, P. and I. Pongratz (2002). "Two parallel pathways mediate cytoplasmic localization of the dioxin (aryl hydrocarbon) receptor." J Biol Chem **277**(35): 32310-9.

Bose, S., T. Weikl, et al. (1996). "Chaperone function of Hsp90-associated proteins." Science **274**(5293): 1715-7.

Bradfield, C. A., E. Glover, et al. (1991). "Purification and N-terminal amino acid sequence of the Ah receptor from the C57BL/6J mouse." Mol Pharmacol **39**(1): 13-9.

Bradfield, C. A., A. S. Kende, et al. (1988). "Kinetic and equilibrium studies of Ah receptor-ligand binding: use of [125I]2-iodo-7,8-dibromodibenzo-p-dioxin." Mol Pharmacol **34**(2): 229-37.

Bradfield, C. A. and A. Poland (1988). "A competitive binding assay for 2,3,7,8-tetrachlorodibenzo-p-dioxin and related ligands of the Ah receptor." Mol Pharmacol **34**(5): 682-8.

Burbach, K. M., A. Poland, et al. (1992). "Cloning of the Ah-receptor cDNA reveals a distinctive ligand-activated transcription factor." Proc Natl Acad Sci U S A **89**(17): 8185-9.

Carlson, D. B. and G. H. Perdew (2002). "A dynamic role for the Ah receptor in cell signaling? Insights from a diverse group of Ah receptor interacting proteins." J Biochem Mol Toxicol **16**(6): 317-25.

Carver, L. A. and C. Bradfield (1999). Simple models of dioxin action. Molecular biology of the toxic response. A. Puga and K. B. Wallace. New York, NY, Taylor & Francis**:** 355-375.

Carver, L. A. and C. A. Bradfield (1997). "Ligand-dependent interaction of the aryl hydrocarbon receptor with a novel immunophilin homolog in vivo." J Biol Chem **272**(17): 11452-6.

Carver, L. A., J. B. Hogenesch, et al. (1994). "Tissue specific expression of the rat Ah-receptor and ARNT mRNAs." Nucleic Acids Res **22**(15): 3038-44.

Carver, L. A., V. Jackiw, et al. (1994). "The 90-kDa heat shock protein is essential for Ah receptor signaling in a yeast expression system." J Biol Chem **269**(48): 30109-12.

Carver, L. A., J. J. LaPres, et al. (1998). "Characterization of the Ah receptor-associated protein, ARA9." J Biol Chem **273**(50): 33580-7.

Chadli, A., I. Bouhouche, et al. (2000). "Dimerization and N-terminal domain proximity underlie the function of the molecular chaperone heat shock protein 90." Proc Natl Acad Sci U S A **97**(23): 12524-9.

Chan, W. K., R. Chu, et al. (1994). "Baculovirus expression of the Ah receptor and Ah receptor nuclear translocater. Evidence for additional dioxin responsive element-binding species and factors required for signaling." J Biol Chem **269**(42): 26464-71.

Chang, C. Y. and A. Puga (1998). "Constitutive activation of the aromatic hydrocarbon receptor." Mol Cell Biol **18**(1): 525-35.

Chapman-Smith, A., J. K. Lutwyche, et al. (2004). "Contribution of the Per/Arnt/Sim (PAS) domains to DNA binding by the basic helix-loop-helix PAS transcriptional regulators." J Biol Chem **279**(7): 5353-62.

Chen, H. S. and G. H. Perdew (1994). "Subunit composition of the heteromeric cytosolic aryl hydrocarbon receptor complex." J Biol Chem **269**(44): 27554-8.

Chen, H. S., S. S. Singh, et al. (1997). "The Ah receptor is a sensitive target of geldanamycin-induced protein turnover." Arch Biochem Biophys **348**(1): 190-8.

Coumailleau, P., B. Billoud, et al. (1995). "Evidence for a 90 kDa heat-shock protein gene expression in the amphibian oocyte." Dev Biol **168**(2): 247-58.

Coumailleau, P., L. Poellinger, et al. (1995). "Definition of a minimal domain of the dioxin receptor that is associated with Hsp90 and maintains wild type ligand binding affinity and specificity." J Biol Chem **270**(42): 25291-300.

Cox, M. B. and C. A. Miller, 3rd (2002). "The p23 co-chaperone facilitates dioxin receptor signaling in a yeast model system." Toxicol Lett **129**(1-2): 13-21.

Cox, M. B. and C. A. Miller, 3rd (2003). "Pharmacological and genetic analysis of 90-kDa heat shock isoprotein-aryl hydrocarbon receptor complexes." Mol Pharmacol **64**(6): 1549-56.

Crews, S. T., J. B. Thomas, et al. (1988). "The Drosophila single-minded gene encodes a nuclear protein with sequence similarity to the per gene product." Cell **52**(1): 143-51.

Denis, M., J. A. Gustafsson, et al. (1988). "Interaction of the Mr = 90,000 heat shock protein with the steroid-binding domain of the glucocorticoid receptor." J Biol Chem **263**(34): 18520-3.

Denison, M. S., P. A. Harper, et al. (1986). "Ah receptor for 2,3,7,8-tetrachlorodibenzo-p-dioxin. Codistribution of unoccupied receptor with cytosolic marker enzymes during fractionation of mouse liver, rat liver and cultured Hepa-1c1 cells." Eur J Biochem **155**(2): 223-9.

Denison, M. S. and S. R. Nagy (2003). "Activation of the aryl hydrocarbon receptor by structurally diverse exogenous and endogenous chemicals." Annu Rev Pharmacol Toxicol **43**: 309-34.

Denison, M. S., A. Pandini, et al. (2002). "Ligand binding and activation of the Ah receptor." Chem Biol Interact **141**(1-2): 3-24.

Denison, M. S., L. M. Vella, et al. (1986). "Structure and function of the Ah receptor for 2,3,7,8-tetrachlorodibenzo-p-dioxin. Species difference in molecular properties of the receptors from mouse and rat hepatic cytosols." J Biol Chem **261**(9): 3987-95.

Dittmar, K. D., M. Banach, et al. (1998). "The role of DnaJ-like proteins in glucocorticoid receptor.hsp90 heterocomplex assembly by the reconstituted hsp90.p60.hsp70 foldosome complex." J Biol Chem **273**(13): 7358-66.

Dittmar, K. D. and W. B. Pratt (1997). "Folding of the glucocorticoid receptor by the reconstituted Hsp90-based chaperone machinery. The initial

hsp90.p60.hsp70-dependent step is sufficient for creating the steroid binding conformation." J Biol Chem **272**(20): 13047-54.

Dolwick, K. M., J. V. Schmidt, et al. (1993). "Cloning and expression of a human Ah receptor cDNA." Mol Pharmacol **44**(5): 911-7.

Dolwick, K. M., H. I. Swanson, et al. (1993). "In vitro analysis of Ah receptor domains involved in ligand-activated DNA recognition." Proc Natl Acad Sci U S A **90**(18): 8566-70.

Ema, M., N. Ohe, et al. (1994). "Dioxin binding activities of polymorphic forms of mouse and human arylhydrocarbon receptors." J Biol Chem **269**(44): 27337-43.

Fang, Y., A. E. Fliss, et al. (1998). "SBA1 encodes a yeast hsp90 cochaperone that is homologous to vertebrate p23 proteins." Mol Cell Biol **18**(7): 3727-34.

Fernandez-Salguero, P., T. Pineau, et al. (1995). "Immune system impairment and hepatic fibrosis in mice lacking the dioxin-binding Ah receptor." Science **268**(5211): 722-6.

Freeman, B. C., S. J. Felts, et al. (2000). "The p23 molecular chaperones act at a late step in intracellular receptor action to differentially affect ligand efficacies." Genes Dev **14**(4): 422-34.

Freeman, B. C., D. O. Toft, et al. (1996). "Molecular chaperone machines: chaperone activities of the cyclophilin Cyp-40 and the steroid aporeceptor-associated protein p23." Science **274**(5293): 1718-20.

Fukunaga, B. N., M. R. Probst, et al. (1995). "Identification of functional domains of the aryl hydrocarbon receptor." J Biol Chem **270**(49): 29270-8.

Galigniana, M. D., J. M. Harrell, et al. (2004). "Retrograde transport of the glucocorticoid receptor in neurites requires dynamic assembly of complexes with the protein chaperone hsp90 and is linked to the CHIP component of the machinery for proteasomal degradation." Brain Res Mol Brain Res **123**(1-2): 27-36.

Gasiewicz, T. A. and P. A. Bauman (1987). "Heterogeneity of the rat hepatic Ah receptor and evidence for transformation in vitro and in vivo." J Biol Chem **262**(5): 2116-20.

Gasiewicz, T. A., C. J. Elferink, et al. (1991). "Characterization of multiple forms of the Ah receptor: recognition of a dioxin-responsive enhancer involves heteromer formation." Biochemistry **30**(11): 2909-16.

Geiger, L. E. and R. A. Neal (1981). "Mutagenicity testing of 2,3,7,8-tetrachlordibenzo-p-dioxin in histidine auxotrophs of Salmonella typhimurium." Toxicol Appl Pharmacol **59**(1): 125-9.

Grenert, J. P., B. D. Johnson, et al. (1999). "The importance of ATP binding and hydrolysis by hsp90 in formation and function of protein heterocomplexes." J Biol Chem **274**(25): 17525-33.

Grenert, J. P., W. P. Sullivan, et al. (1997). "The amino-terminal domain of heat shock protein 90 (hsp90) that binds geldanamycin is an ATP/ADP switch domain that regulates hsp90 conformation." J Biol Chem **272**(38): 23843-50.

Gu, Y. Z., J. B. Hogenesch, et al. (2000). "The PAS superfamily: sensors of environmental and developmental signals." Annu Rev Pharmacol Toxicol **40**: 519-61.

Hankinson, O. (1995). "The aryl hydrocarbon receptor complex." Annu Rev Pharmacol Toxicol **35**: 307-40.

Harper, P. A., J. Y. Wong, et al. (2002). "Polymorphisms in the human AH receptor." Chem Biol Interact **141**(1-2): 161-87.

Heath-Pagliuso, S., W. J. Rogers, et al. (1998). "Activation of the Ah receptor by tryptophan and tryptophan metabolites." Biochemistry **37**(33): 11508-15.

Heid, S. E., R. S. Pollenz, et al. (2000). "Role of heat shock protein 90 dissociation in mediating agonist-induced activation of the aryl hydrocarbon receptor." Mol Pharmacol **57**(1): 82-92.

Hogenesch, J. B., W. K. Chan, et al. (1997). "Characterization of a subset of the basic-helix-loop-helix-PAS superfamily that interacts with components of the dioxin signaling pathway." J Biol Chem **272**(13): 8581-93.

Holmans, P. L., M. S. Shet, et al. (1994). "The high-level expression in Escherichia coli of the membrane-bound form of human and rat cytochrome b5 and studies on their mechanism of function." Arch Biochem Biophys **312**(2): 554-65.

Huang, Z. J., I. Edery, et al. (1993). "PAS is a dimerization domain common to Drosophila period and several transcription factors." Nature **364**(6434): 259-62.

Hulme, E. C. and N. J. M. Birdsall (1993). Receptor-ligand interactons, a practical approach.

Ikuta, T., H. Eguchi, et al. (1998). "Nuclear localization and export signals of the human aryl hydrocarbon receptor." J Biol Chem **273**(5): 2895-904.

Jain, S., K. M. Dolwick, et al. (1994). "Potent transactivation domains of the Ah receptor and the Ah receptor nuclear translocator map to their carboxyl termini." J Biol Chem **269**(50): 31518-24.

Johnson, B. D., A. Chadli, et al. (2000). "Hsp90 chaperone activity requires the full-length protein and interaction among its multiple domains." J Biol Chem **275**(42): 32499-507.

Josephy, P. D. (1997). The Ah receptor and the toxicity of chlorinated aromatic compounds. Molecular Toxicology. P. D. Josephy. NY, Oxford University Press**:** 253-260.

Kashiyama, E., I. Hutchinson, et al. (1999). "Antitumor benzothiazoles. 8. Synthesis, metabolic formation, and biological properties of the C- and N-oxidation products of antitumor 2-(4-aminophenyl)benzothiazoles." J Med Chem **42**(20): 4172-84.

Kay, J. M. (1997). "Hypoxia, obstructive sleep apnea syndrome, and pulmonary hypertension." Hum Pathol **28**(3): 261-3.

Kay, S. A. (1997). "PAS, present, and future: clues to the origins of circadian clocks." Science **276**(5313): 753-4.

Kazlauskas, A., L. Poellinger, et al. (1999). "Evidence that the co-chaperone p23 regulates ligand responsiveness of the dioxin (Aryl hydrocarbon) receptor." J Biol Chem **274**(19): 13519-24.

Kazlauskas, A., L. Poellinger, et al. (2000). "The immunophilin-like protein XAP2 regulates ubiquitination and subcellular localization of the dioxin receptor." J Biol Chem **275**(52): 41317-24.

Kazlauskas, A., S. Sundstrom, et al. (2001). "The hsp90 chaperone complex regulates intracellular localization of the dioxin receptor." Mol Cell Biol **21**(7): 2594-607.

Kester, J. E. and T. A. Gasiewicz (1987). "Characterization of the in vitro stability of the rat hepatic receptor for 2,3,7,8-tetrachlorodibenzo-p-dioxin (TCDD)." Arch Biochem Biophys **252**(2): 606-25.

Kikuchi, Y., S. Ohsawa, et al. (2003). "Heterodimers of bHLH-PAS protein fragments derived from AhR, AhRR, and Arnt prepared by co-expression in Escherichia coli: characterization of their DNA binding activity and preparation of a DNA complex." J Biochem (Tokyo) **134**(1): 83-90.

King, G. A., A. J. Daugulis, et al. (1992). "Recombinant beta-galactosidase production in serum-free medium by insect cells in a 14-L airlift bioreactor." Biotechnol Prog **8**(6): 567-71.

Kuzhandaivelu, N., Y. S. Cong, et al. (1996). "XAP2, a novel hepatitis B virus X-associated protein that inhibits X transactivation." Nucleic Acids Res **24**(23): 4741-50.

Lahvis, G. P., S. L. Lindell, et al. (2000). "Portosystemic shunting and persistent fetal vascular structures in aryl hydrocarbon receptor-deficient mice." Proc Natl Acad Sci U S A **97**(19): 10442-7.

Landers, J. P. and N. J. Bunce (1991). "The Ah receptor and the mechanism of dioxin toxicity." Biochem J **276 (Pt 2)**: 273-87.

LaPres, J. J., E. Glover, et al. (2000). "ARA9 modifies agonist signaling through an increase in cytosolic aryl hydrocarbon receptor." J Biol Chem **275**(9): 6153-9.

Lees, M. J., D. J. Peet, et al. (2003). "Defining the role for XAP2 in stabilization of the dioxin receptor." J Biol Chem **278**(38): 35878-88.

Lees, M. J. and M. L. Whitelaw (2002). "Effect of ARA9 on dioxin receptor mediated transcription." Toxicology **181-182**: 143-6.

Lin, T. M., K. Ko, et al. (2002). "Effects of aryl hydrocarbon receptor null mutation and in utero and lactational 2,3,7,8-tetrachlorodibenzo-p-dioxin exposure on prostate and seminal vesicle development in C57BL/6 mice." Toxicol Sci **68**(2): 479-87.

Luckow, V. A. (1993). "Baculovirus systems for the expression of human gene products." Curr Opin Biotechnol **4**(5): 564-72.

Ma, Q. and K. T. Baldwin (2000). "2,3,7,8-tetrachlorodibenzo-p-dioxin-induced degradation of aryl hydrocarbon receptor (AhR) by the ubiquitin-proteasome pathway. Role of the transcription activaton and DNA binding of AhR." J Biol Chem **275**(12): 8432-8.

Ma, Q. and J. P. Whitlock, Jr. (1996). "The aromatic hydrocarbon receptor modulates the Hepa 1c1c7 cell cycle and differentiated state independently of dioxin." Mol Cell Biol **16**(5): 2144-50.

Ma, Q. and J. P. Whitlock, Jr. (1997). "A novel cytoplasmic protein that interacts with the Ah receptor, contains tetratricopeptide repeat motifs, and augments the transcriptional response to 2,3,7,8-tetrachlorodibenzo-p-dioxin." J Biol Chem **272**(14): 8878-84.

Makarova, O. V., E. M. Makarov, et al. (1995). "Transcribing of Escherichia coli genes with mutant T7 RNA polymerases: stability of lacZ mRNA inversely correlates with polymerase speed." Proc Natl Acad Sci U S A **92**(26): 12250-4.

Manchester, D. K., S. K. Gordon, et al. (1987). "Ah receptor in human placenta: stabilization by molybdate and characterization of binding of 2,3,7,8-tetrachlorodibenzo-p-dioxin, 3-methylcholanthrene, and benzo(a)pyrene." Cancer Res **47**(18): 4861-8.

McDonough, H. and C. Patterson (2003). "CHIP: a link between the chaperone and proteasome systems." Cell Stress Chaperones **8**(4): 303-8.

McGuire, J., P. Coumailleau, et al. (1995). "The basic helix-loop-helix/PAS factor Sim is associated with hsp90. Implications for regulation by interaction with partner factors." J Biol Chem **270**(52): 31353-7.

McGuire, J., K. Okamoto, et al. (2001). "Definition of a dioxin receptor mutant that is a constitutive activator of transcription: delineation of overlapping repression and ligand binding functions within the PAS domain." J Biol Chem **276**(45): 41841-9.

McGuire, J., M. L. Whitelaw, et al. (1994). "A cellular factor stimulates ligand-dependent release of hsp90 from the basic helix-loop-helix dioxin receptor." Mol Cell Biol **14**(4): 2438-46.

Meyer, B. K. and G. H. Perdew (1999). "Characterization of the AhR-hsp90-XAP2 core complex and the role of the immunophilin-related protein XAP2 in AhR stabilization." Biochemistry **38**(28): 8907-17.

Meyer, B. K., J. R. Petrulis, et al. (2000). "Aryl hydrocarbon (Ah) receptor levels are selectively modulated by hsp90-associated immunophilin homolog XAP2." Cell Stress Chaperones **5**(3): 243-54.

Meyer, B. K., M. G. Pray-Grant, et al. (1998). "Hepatitis B virus X-associated protein 2 is a subunit of the unliganded aryl hydrocarbon receptor core

complex and exhibits transcriptional enhancer activity." Mol Cell Biol **18**(2): 978-88.

Meyer, P. (2004). "Structural basis for recruitment of the ATPase activator Aha1 to the Hsp90 chaperone machinery." Embo J **23**(6): 1402-10.

Meyer, P., C. Prodromou, et al. (2003). "Structural and functional analysis of the middle segment of hsp90: implications for ATP hydrolysis and client protein and cochaperone interactions." Mol Cell **11**(3): 647-58.

Meyer, P., C. Prodromou, et al. (2004). "Structural basis for recruitment of the ATPase activator Aha1 to the Hsp90 chaperone machinery." Embo J **23**(3): 511-9.

Mhin, B. J., J. Choi, et al. (2001). "A simple rule for classification of polychlorinated dibenzo-p-dioxin congeners on the basis of IR frequency patterns." J Am Chem Soc **123**(15): 3584-7.

Mimura, J., M. Ema, et al. (1999). "Identification of a novel mechanism of regulation of Ah (dioxin) receptor function." Genes Dev **13**(1): 20-5.

Mimura, J. and Y. Fujii-Kuriyama (2003). "Functional role of AhR in the expression of toxic effects by TCDD." Biochim Biophys Acta **1619**(3): 263-8.

Mimura, J., K. Yamashita, et al. (1997). "Loss of teratogenic response to 2,3,7,8-tetrachlorodibenzo-p-dioxin (TCDD) in mice lacking the Ah (dioxin) receptor." Genes Cells **2**(10): 645-54.

Miroux, B. and J. E. Walker (1996). "Over-production of proteins in Escherichia coli: mutant hosts that allow synthesis of some membrane proteins and globular proteins at high levels." J Mol Biol **260**(3): 289-98.

Monson, E. K., M. Weinstein, et al. (1992). "The FixL protein of Rhizobium meliloti can be separated into a heme-binding oxygen-sensing domain and a functional C-terminal kinase domain." Proc Natl Acad Sci U S A **89**(10): 4280-4.

Morishima, Y., K. C. Kanelakis, et al. (2001). "Evidence for iterative ratcheting of receptor-bound hsp70 between its ATP and ADP conformations during assembly of glucocorticoid receptor.hsp90 heterocomplexes." Biochemistry **40**(4): 1109-16.

Mulrooney, S. B. and L. Waskell (2000). "High-level expression in Escherichia coli and purification of the membrane-bound form of cytochrome b(5)." Protein Expr Purif **19**(1): 173-8.

Murphy, P. J., K. C. Kanelakis, et al. (2001). "Stoichiometry, abundance, and functional significance of the hsp90/hsp70-based multiprotein chaperone machinery in reticulocyte lysate." J Biol Chem **276**(32): 30092-8.

Murphy, P. J., Y. Morishima, et al. (2003). "Visualization and mechanism of assembly of a glucocorticoid receptor.Hsp70 complex that is primed for subsequent Hsp90-dependent opening of the steroid binding cleft." J Biol Chem **278**(37): 34764-73.

Nair, S. C., E. J. Toran, et al. (1996). "A pathway of multi-chaperone interactions common to diverse regulatory proteins: estrogen receptor, Fes tyrosine kinase, heat shock transcription factor Hsf1, and the aryl hydrocarbon receptor." Cell Stress Chaperones **1**(4): 237-50.

Nambu, J. R. (1991). Cell **67**: 1157-1167.

Obermann, W. M., H. Sondermann, et al. (1998). "In vivo function of Hsp90 is dependent on ATP binding and ATP hydrolysis." J Cell Biol **143**(4): 901-10.

Okey, A. B., L. M. Vella, et al. (1989). "Detection and characterization of a low affinity form of cytosolic Ah receptor in livers of mice nonresponsive to induction of cytochrome P1-450 by 3-methylcholanthrene." Mol Pharmacol **35**(6): 823-30.

Omura, T. and R. Sato (1964). "The Carbon Monoxide-Binding Pigment of Liver Microsomes. I. Evidence for Its Hemoprotein Nature." J Biol Chem **239**: 2370-8.

Panaretou, B., C. Prodromou, et al. (1998). "ATP binding and hydrolysis are essential to the function of the Hsp90 molecular chaperone in vivo." Embo J **17**(16): 4829-36.

Panaretou, B., G. Siligardi, et al. (2002). "Activation of the ATPase activity of hsp90 by the stress-regulated cochaperone aha1." Mol Cell **10**(6): 1307-18.

Pearl, L. H. and C. Prodromou (2001). "Structure, function, and mechanism of the Hsp90 molecular chaperone." Adv Protein Chem **59**: 157-86.

Pellequer, J. L., K. A. Wager-Smith, et al. (1998). "Photoactive yellow protein: a structural prototype for the three-dimensional fold of the PAS domain superfamily." Proc Natl Acad Sci U S A **95**(11): 5884-90.

Perdew, G. H. (1994). "Production of murine anti-peptide polyclonal antibodies utilizing a nonantigenic adjuvant." Anal Biochem **220**(1): 214-6.

Perdew, G. H. and C. F. Babbs (1991). "Production of Ah receptor ligands in rat fecal suspensions containing tryptophan or indole-3-carbinol." Nutr Cancer **16**(3-4): 209-18.

Perdew, G. H. and C. A. Bradfield (1996). "Mapping the 90 kDa heat shock protein binding region of the Ah receptor." Biochem Mol Biol Int **39**(3): 589-93.

Perdew, G. H. and A. Poland (1988). "Purification of the Ah receptor from C57BL/6J mouse liver." J Biol Chem **263**(20): 9848-52.

Peters, J. M. and L. M. Wiley (1995). "Evidence that murine preimplantation embryos express aryl hydrocarbon receptor." Toxicol Appl Pharmacol **134**(2): 214-21.

Pitot, H. C., T. Goldsworthy, et al. (1980). "Quantitative evaluation of the promotion by 2,3,7,8-tetrachlorodibenzo-p-dioxin of hepatocarcinogenesis from diethylnitrosamine." Cancer Res **40**(10): 3616-20.

Pohjanvirta, R., M. Viluksela, et al. (1999). "Physicochemical differences in the AH receptors of the most TCDD-susceptible and the most TCDD-resistant rat strains." Toxicol Appl Pharmacol **155**(1): 82-95.

Poland, A. and E. Glover (1979). "An estimate of the maximum in vivo covalent binding of 2,3,7,8-tetrachlorodibenzo-p-dioxin to rat liver protein, ribosomal RNA, and DNA." Cancer Res **39**(9): 3341-4.

Poland, A. and E. Glover (1990). "Characterization and strain distribution pattern of the murine Ah receptor specified by the Ahd and Ahb-3 alleles." Mol Pharmacol **38**(3): 306-12.

Poland, A. and A. Kende (1976). "2,3,7,8-Tetrachlorodibenzo-p-dioxin: environmental contaminant and molecular probe." Fed Proc **35**(12): 2404-11.

Poland, A. and J. C. Knutson (1982). "2,3,7,8-tetrachlorodibenzo-p-dioxin and related halogenated aromatic hydrocarbons: examination of the mechanism of toxicity." Annu Rev Pharmacol Toxicol **22**: 517-54.

Poland, A., D. Palen, et al. (1994). "Analysis of the four alleles of the murine aryl hydrocarbon receptor." Mol Pharmacol **46**(5): 915-21.

Pollenz, R. S. (2002). "The mechanism of AH receptor protein down-regulation (degradation) and its impact on AH receptor-mediated gene regulation." Chem Biol Interact **141**(1-2): 41-61.

Pollenz, R. S., C. A. Sattler, et al. (1994). "The aryl hydrocarbon receptor and aryl hydrocarbon receptor nuclear translocator protein show distinct subcellular localizations in Hepa 1c1c7 cells by immunofluorescence microscopy." Mol Pharmacol **45**(3): 428-38.

Pratt, W. B. (1997). "The role of the hsp90-based chaperone system in signal transduction by nuclear receptors and receptors signaling via MAP kinase." Annu Rev Pharmacol Toxicol **37**: 297-326.

Pratt, W. B., M. D. Galigniana, et al. (2004). "Role of hsp90 and the hsp90-binding immunophilins in signalling protein movement." Cell Signal **16**(8): 857-72.

Pratt, W. B., M. D. Galigniana, et al. (2004). "Role of molecular chaperones in steroid receptor action." Essays Biochem **40**: 41-58.

Pratt, W. B. and D. O. Toft (2003). "Regulation of signaling protein function and trafficking by the hsp90/hsp70-based chaperone machinery." Exp Biol Med (Maywood) **228**(2): 111-33.

Procopio, M., A. Lahm, et al. (2002). "A model for recognition of polychlorinated dibenzo-p-dioxins by the aryl hydrocarbon receptor." Eur J Biochem **269**(1): 13-8.

Prodromou, C., B. Panaretou, et al. (2000). "The ATPase cycle of Hsp90 drives a molecular 'clamp' via transient dimerization of the N-terminal domains." Embo J **19**(16): 4383-92.

Ramadoss, P. and G. H. Perdew (2004). "Use of 2-azido-3-[125I]iodo-7,8-dibromodibenzo-p-dioxin as a probe to determine the relative ligand affinity of human versus mouse aryl hydrocarbon receptor in cultured cells." Mol Pharmacol **66**(1): 129-36.

Richter, K. and J. Buchner (2001). "Hsp90: chaperoning signal transduction." J Cell Physiol **188**(3): 281-90.

Sabatini, D. M., M. M. Lai, et al. (1997). "Neural roles of immunophilins and their ligands." Mol Neurobiol **15**(2): 223-39.

Safe, S. (1990). "Polychlorinated biphenyls (PCBs), dibenzo-p-dioxins (PCDDs), dibenzofurans (PCDFs), and related compounds: environmental and mechanistic considerations which support the development of toxic equivalency factors (TEFs)." Crit Rev Toxicol **21**(1): 51-88.

Savouret, J. F., M. Antenos, et al. (2001). "7-ketocholesterol is an endogenous modulator for the arylhydrocarbon receptor." J Biol Chem **276**(5): 3054-9.

Schmidt, J. V. and C. A. Bradfield (1996). "Ah receptor signaling pathways." Annu Rev Cell Dev Biol **12**: 55-89.

Schmidt, J. V., G. H. Su, et al. (1996). "Characterization of a murine Ahr null allele: involvement of the Ah receptor in hepatic growth and development." Proc Natl Acad Sci U S A **93**(13): 6731-6.

Seed, B. and J. Y. Sheen (1988). "A simple phase-extraction assay for chloraphenicol activity." Gene **67**: 271-277.

Shu, H. P., D. J. Paustenbach, et al. (1987). "A critical evaluation of the use of mutagenesis, carcinogenesis, and tumor promotion data in a cancer risk assessment of 2,3,7,8-tetrachlorodibenzo-p-dioxin." Regul Toxicol Pharmacol **7**(1): 57-88.

Song, Z. and R. S. Pollenz (2003). "Functional analysis of murine aryl hydrocarbon (AH) receptors defective in nuclear import: impact on AH receptor degradation and gene regulation." Mol Pharmacol **63**(3): 597-606.

Srinivasan, G., J. F. Post, et al. (1997). "Optimal ligand binding by the recombinant human glucocorticoid receptor and assembly of the receptor complex with heat shock protein 90 correlate with high intracellular ATP levels in Spodoptera frugiperda cells." J Steroid Biochem Mol Biol **60**(1-2): 1-9.

Sullivan, W., B. Stensgard, et al. (1997). "Nucleotides and two functional states of hsp90." J Biol Chem **272**(12): 8007-12.

Sullivan, W. P., B. A. Owen, et al. (2002). "The influence of ATP and p23 on the conformation of hsp90." J Biol Chem **277**(48): 45942-8.

Swanson, H. I. and G. H. Perdew (1993). "Half-life of aryl hydrocarbon receptor in Hepa 1 cells: evidence for ligand-dependent alterations in cytosolic receptor levels." Arch Biochem Biophys **302**(1): 167-74.

Swanson, H. I., K. Tullis, et al. (1993). "Binding of transformed Ah receptor complex to a dioxin responsive transcriptional enhancer: evidence for two distinct heteromeric DNA-binding forms." Biochemistry **32**(47): 12841-9.

Walker, C. H. (2001). Major organic pollutants. Organic pollutants, an ecotoxicological perspective. New York, NY, Taylor & Francis**:** 121-176.

Waskell, L. A., J. L. Vigne, et al. (1991). "Site of action of substrates requiring cytochrome b5 for oxidation by cytochrome P450." Methods Enzymol **206**: 523-9.

Wei, Y. D., L. Bergander, et al. (2000). "Regulation of CYP1A1 transcription via the metabolism of the tryptophan-derived 6-formylindolo[3,2-b]carbazole." Arch Biochem Biophys **383**(1): 99-107.

Whitelaw, M. L., J. A. Gustafsson, et al. (1994). "Identification of transactivation and repression functions of the dioxin receptor and its basic helix-loop-helix/PAS partner factor Arnt: inducible versus constitutive modes of regulation." Mol Cell Biol **14**(12): 8343-55.

Whitlock, J. P., Jr. (1999). "Induction of cytochrome P4501A1." Annu Rev Pharmacol Toxicol **39**: 103-25.

Wilhelmsson, A., S. Cuthill, et al. (1990). "The specific DNA binding activity of the dioxin receptor is modulated by the 90 kd heat shock protein." Embo J **9**(1): 69-76.

Yao, G., M. Craven, et al. (2004). "Interaction networks in yeast define and enumerate the signaling steps of the vertebrate aryl hydrocarbon receptor." PLoS Biol **2**(3): E65.

Young, J. C. and F. U. Hartl (2000). "Polypeptide release by Hsp90 involves ATP hydrolysis and is enhanced by the co-chaperone p23." Embo J **19**(21): 5930-40.

Zhulin, I. B., B. L. Taylor, et al. (1997). "PAS domain S-boxes in Archaea, Bacteria and sensors for oxygen and redox." Trends Biochem Sci **22**(9): 331-3.